Texas A&M University at Galveston
1001 Texas Clipper Road
Galveston, TX 77554

FINAL REPORT

JANUARY 31ST, 2025

Project Title: The Fate and Toxicity of Microplastics and Persistent Pollutants in the Shellfish and Fish of Matagorda Bay

Submitted To:

Matagorda Bay Mitigation Trust

Performing Laboratory:

Texas A&M University on behalf of Texas A&M University at Galveston

Texas A&M University at Galveston
1001 Texas Clipper Road
Galveston, TX 77554

Authors:

Dr. David Hala, Ph.D.

Dr. Karl Kaiser, Ph.D.

Dr. Robert Wells, Ph.D.

Dr. Lene H. Petersen, Ph.D.

Dr. Antonietta Quigg, Ph.D.

Dr. Emily Meese, Ph. D.

Mr. Asif Mortuza (Ph.D. candidate)

Mr. Marcus Wharton (Master's student)

Personnel

Principal Investigators:

Drs. David Hala, Karl Kaiser, Robert (David) Wells, Lene H. Petersen, Antonietta Quigg

Consulting MBMT Project Coordinator:

Mr. Steven J. Raabe

Location:

Texas A&M University at Galveston

Project Duration:

01 June 2021 – 31 December 2024

Texas A&M University at Galveston
1001 Texas Clipper Road
Galveston, TX 77554

CONTENTS

Texas A&M University at Galveston
1001 Texas Clipper Road
Galveston, TX 77554

SUMMARY OF KEY FINDINGS

Objective 1: *Quantify microplastics in the surface waters of Matagorda Bay*.

- A novel pyrolysis gas chromatography and triple quadrupole mass spectrometry (Py-GCMS/MS) method was developed to quantify up to 12 nano(micro)plastics (NMPs, ≥700 nm particle size) in surface waters or biota sampled from Matagorda Bay.
- The sum of total NMPs measured in the surface waters of Matagorda Bay ranged from 0.1 – 3.91 μg L^{-1}, with the highest level reported at Port O'Connor. Given its location near the entrance to Matagorda Bay, the high NMP levels measured may be a consequence of the bay's hydrodynamic properties towards concentrating microplastics at this location.
- The top three most prominently detected plastics were polycarbonate (PC) > polyethylene (PE) > polyvinyl chloride (PVC). The prominence of PC, PE, and PVC highlights the presence of general plastics degradation products, including those from plastic pellets such as nurdles.

Objective 2: *Quantify persistent and microplastics pollutants in the biota (shellfish and fish) of Matagorda Bay*.

- We report the concentrations of 12 nano(micro)plastics (NMPs, >700 nm particle size), 14 polycyclic aromatic hydrocarbons (PAHs), and 28 polychlorinated biphenyls (PCBs, including 11 dioxin-like PCBs) in the gill/mantle tissue of eastern oysters (*Crassostria virginica*) and; muscle and liver tissues of gafftopsail catfish (*Bagre marinus*), red drum (*Sciaenops ocellatus*), and spotted seatrout (*Cynoscion nebulosus*) from Matagorda Bay.
- Py-GCMS/MS was used to quantify the NMPs, and GCMS was used for PAHs and PCBs

Texas A&M University at Galveston
1001 Texas Clipper Road
Galveston, TX 77554

quantifications.

- Analysis of the total contaminant concentrations across all the biota showed NMPs to exhibit the highest body-burdens (~2,000x - 60,000x) relative to PAHs and PCBs. Amongst the biota, oysters exhibited the highest contaminant body-burdens versus fish. For PAHs and PCBs, the gill/mantle of oysters exhibited ~2 - 11x higher body-burdens than the muscle tissue of fish. And for NMPs, 5 - 25x higher body-burdens than in fish muscle.
- Source ratio analysis for PAHs indicated the presence of mainly petrogenic (oil-derived) hydrocarbons.
- Toxic equivalents (TEQ) based risk assessment for dioxin-like PCBs indicated the likelihood for adverse health effects in catfish only.
- Finally, the calculation of human average yearly NMPs consumption through seafood indicated the ingestion of 0.01 – 0.2 grams of plastics per year.
- A key finding of our work is that the body-burdens of NMPs (emerging pollutants) were several orders of magnitude higher than those for PAHs and PCBs (persistent pollutants).

Objective 3: *Assess the toxicity of bioaccumulated persistent pollutants and microplastics using embryo-larval life stages of zebrafish (Danio rerio).*

- In this study we showed that exposures to mixtures of PAHs or PCBs strongly induced a CYP450 biotransformation response (i.e., EROD activity), which also corresponded with an elevated metabolic rate (i.e., MO_2).
- The elevated metabolic rate likely reflects the increased metabolic demand for molecular oxygen (O_2), which in turn satisfies the increased catalytic mono-oxygenation reactions as

Texas A&M University at Galveston
1001 Texas Clipper Road
Galveston, TX 77554

catalyzed by CYP450s.

- Exposure of fish to only polystyrene (PS) microplastics particles in suspension (10 µg L^{-1} final concentration) caused no statistically significant effects on any of the biomarkers measured. However, co-exposure of the fish to PHE + PS or PCB 81 + PS induced MO_2 activity by 70% and 57% respectively relative to their respective solvent control group (0.1% DMSO). Although these increases were not statistically significant.
- Finally, we observed a statistically significant decrease in cardiac blood flow activity in fish co-exposed to PCB 18 + PS, PCB 81 + PS, and PCB 105 + PS. We postulate this effect to be more reflective of exposure to PCBs than the PS microplastics.
- Our studies show the utility of using *in vivo* EROD activity as a likely proxy for MO_2 measurements for exposure assessments to PAHs and PCBs. And the importance of including cardiac function biomarkers in the toxicity assessments of persistent (PAHs, PCBs) and/or emerging (microplastics) pollutants.

Objective 4: *Promote educational outreach to local high school students on the science of ecosystem health monitoring*.

- Public educational outreach demonstrating key issues related to plastics pollution in coastal and marine environments was performed through four summer camp modules/activities, that were integrated into the annual TAMUG Sea Camp (over the summer of 2022). These activities were led by the P.I.'s Hala and Kaiser, and involved graduate students who were either fully or partially funded by this MBMT award (Mortuza, Wharton, Summers, Miller).

Texas A&M University at Galveston
1001 Texas Clipper Road
Galveston, TX 77554

- Funding from this MBMT award has, either directly or indirectly, supported the graduate research activities of four graduate students: Mrs. Asif Mortuza and Marcus Wharton; and Ms. Emily Summers and Katie Miller. And supported the public presentations of 6 platform (oral) and 3 poster presentations at various scientific conferences or meetings.
- Funding from this MBMT award has, either directly or indirectly, supported the research activities of 11 undergraduate students from TAMUG.
- A collection of photographs taken on Matagorda Bay with Dr. Kaiser and the two graduate students directly funded by this MBMT award, Mr. Asif Mortuza and Mr. Marcus Wharton, are shown below:

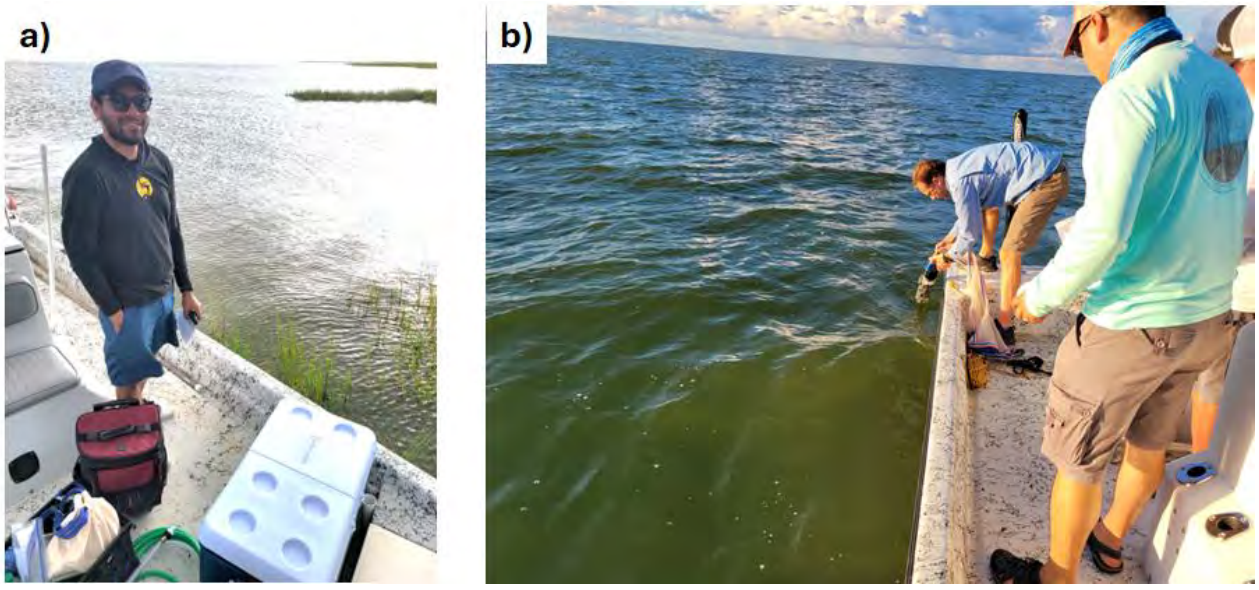

Image: a) Asif Mortuza (graduate student), and **b)** Dr. Karl Kaiser (collecting a water sample) and Mr. Marcus Wharton (graduate student, standing) while sampling on Matagorda Bay (August 17th, 2021).

Texas A&M University at Galveston
1001 Texas Clipper Road
Galveston, TX 77554

1. OVERALL BACKGROUND

Matagorda Bay is located along the upper mid coast of Texas and is the second largest estuary along the Gulf coast of Texas (TSHA, 2023). The natural wildlife of Matagorda Bay serves the local birding and fishing tourism industry, with commercial fishing generating ~$7 million dollars in revenue annually (Fisher, 2016). The bay is also home to major chemical industries such as the Aluminum Company of America, Union Carbide, Du Pont, and Formosa Plastics (TSHA, 2023). More recently, the Formosa Plastics company was litigated against and found liable for the release of up to 121 tons of plastics nurdles (i.e., plastic pellets) into the Bay (Conkle, 2018; Anchondo, 2019). However, the overall extent of plastic pellets and powder release into Matagorda Bay is considered to be much more extensive with accounts of observable pollution spanning for almost a decade (starting in 2010) (Wilson, 2018). The case was settled for a fine $50 million dollars to Formosa Plastics (Conkle, 2018; Moore-Eissenberg, 2019).

The current project, funded by the Matagorda Bay Mitigation Trust (MBMT), aimed to study the overall environmental distribution (or fate) of microplastics pollution in the surface waters and biota (shellfish and fish) of Matagorda Bay. In addition, and taking the opportunity of the biota sampling efforts, we also studied the extent of persistent pollutant exposure of the biota sampled from Matagorda. Finally, we addressed an important knowledge gap in the assessment of likely toxicity effects due to exposure to mixtures of persistent pollutants and microplastics. Using embryo-larval life stages zebrafish (*Danio rerio*) as a model organism, we exposed the fish to pollutant concentrations spanning the levels measured in the body-burdens of biota from

Texas A&M University at Galveston
1001 Texas Clipper Road
Galveston, TX 77554

Matagorda Bay. Taken together, the results of this project provided new data on the fate and toxicity of persistent and microplastics pollutants in the Matagorda Bay system.

1.1. Pollution concerns along the Gulf of Mexico

The U.S. coastline along the Gulf of Mexico (GoM) is a heavily developed coastal zone with an extent of urbanization and industrialization ~10% higher than the U.S. national average (census.gov, 2019; comptroller.texas.gov, 2020). Furthermore, its offshore zone hosts ~3,200 active oil and gas structures (NOAA, 2024). Such a high level of development has led to concerns for aquatic pollution from persistent pollutants, such as oil or combustion derived polycyclic aromatic hydrocarbons (PAHs) and 'legacy' pollutants such as polychlorinated biphenyls (PCBs) (Frank et al., 2001; Kennicutt, 2017; Oziolor et al., 2018; Pulster et al., 2020; Rowe et al., 2020). However, there is recent concern for the presence of so-called 'emerging' pollutants, such as pharmaceuticals, per/poly-fluoroalkyl substances (PFAS), and microplastics in nearshore coastal environments (Deblonde et al., 2011; Gavrilescu et al., 2015; Geissen et al., 2015; Arman et al., 2021). Given these concerns, there is an overall paucity of information on the presence of emerging pollutants (especially microplastics) in the aquatic environment (Horton et al., 2017; Burns and Boxall, 2018; Mintenig et al., 2018; Bhattacharya and Khare, 2022).

1.2. Legacy or persistent pollutants in the Gulf of Mexico

PAHs in aquatic environments are mainly derived from pyrogenic sources (i.e., combustion of petroleum derived hydrocarbons) or from petrogenic sources (i.e., petroleum or derived from oil spills) (Hylland, 2006). These hydrocarbons contain various alkyl (short or long chain), cyclic

Texas A&M University at Galveston
1001 Texas Clipper Road
Galveston, TX 77554

(naphthenes or cycloalkanes) and aryl (polycyclic aromatic ≥ 2 aromatic rings) hydrocarbons. Some hydrocarbons also contain sulfur (ethanethiol) and nitrogen atoms (carbazole) (Eneh, 2011). Among the PAHs, the low molecular weight hydrocarbons (LMWs, ≤3 aromatic rings) are volatile and easily degraded in the environment. Whereas high molecular weight hydrocarbons (HMW, ≥4 aromatic rings) tend to persist in the environment longer and have higher toxic effects. Increasing the number of aromatic rings and thus molecular weights of these hydrocarbons have been correlated with their bioaccumulation potential as well as toxicity (Southworth et al., 1978; Black et al., 1983). PAHs have been shown to cause metabolic (loss of energy), hemolytic (anemia), endocrine, osmoregulatory and teratogenic effects in organisms (Vandermeulen, 1987).

PCBs comprise a diverse group of chlorinated hydrocarbons that contain 1-10 chlorine atoms distributed across two benzene rings (Safe et al., 1985). PCBs were originally used as dielectrics and coolants in electronics prior to getting banned in the late 1970s due to environmental concerns (Boyle and Highland, 1979) and thus are considered to be “legacy” pollutants. However, PCBs are still detected in aquatic systems and biota due to their persistence, long half-lives and low degradation rate (Porta and Zumeta, 2002). PCBs have been shown to interfere with the immune system, nervous system, endocrine systems and cause cancer in humans (Carpenter, 1998). Metabolites of PCB have been shown to exhibit carcinogenicity, reproductive impairment, developmental neurotoxicity due to the efficient transfer of the metabolites to the brain across the placenta from mother to fetus in comparison to the parent PCBs (Quinete et al., 2014). Thus, these chemicals can pollute the environment, bioaccumulate in biota and cause health damage to

Texas A&M University at Galveston
1001 Texas Clipper Road
Galveston, TX 77554

not only the biota but also negatively affect the health and economy of human population that rely on them for food and livelihood.

1.3. Emerging pollutants in the Gulf of Mexico

Plastics were first invented in the 1940s and have been widely used due to their nature as a flexible, lightweight, durable, inexpensive and low thermo-conductive material (Andrady, 2011). Since its conception, the global production of plastics has increased from 15 million tons to 335 million tons in the last 70 years (Gall and Thompson, 2015; Dawson et al., 2018). Plastics are made of synthetic polymers such as lipophilic polyethylene, polypropylene, polystyrene, polyolefin, polyethylene terephthalate, polyvinyl chloride. Their polymeric nature makes them durable and can survive in nature as microplastics and nanoplastics when degraded. Plastics are introduced into the environment from two sources. Primary plastics are produced for industrial and domestic use. Examples include pellets, fibers, films, microbeads etc. that can be made into consumer or industrial products (Andrady, 2011; Cole et al., 2011; Duis and Coors, 2016). Secondary plastics are produced over time due to physical, chemical and biological degradation processes from primary plastics (Browne et al., 2008; Ryan et al., 2009). Once degraded, plastics can form microplastics of various shapes such as disk, circular, fragment, fiber and particle (Qiao et al., 2019). Due to their varying sizes, different sized plastic particles have been found in different tissues.

Plastics can physically block the intestine of organisms and lead to death through starvation. However, smaller particles can penetrate various tissue and affect enzymatic activity and cell

Texas A&M University at Galveston
1001 Texas Clipper Road
Galveston, TX 77554

metabolism (Deng et al., 2017). Furthermore, microplastics can act as a vector in introducing chemical additives such as flame retardants, persistent organic pollutants, pesticides, heavy metals etc. (Brennecke et al., 2016; Wang et al., 2016) to organisms, which can pose threat to biota health. Some of the health hazards of microplastics include induction of oxidative stress (Barboza et al., 2018; Pitt et al., 2018; Liu et al., 2019), altered gene expressions (Sleight et al., 2017; Qu et al., 2018), induced genotoxicity (Brandts et al., 2018), changes in cellular metabolic pathways (LeMoine et al., 2018), disrupted endocrine system (Rochman et al., 2014), induced neurotoxicity (Barboza et al., 2018), reproductive abnormalities, imbalance of energy reserves (Bour et al., 2018), activation of antioxidant enzymes (Tang et al., 2018). Bioaccumulation and biomagnification of microplastics and sorbed chemicals can reach organisms in higher trophic levels and ultimately pose hazard to human health (Wright et al., 2013; Yang et al., 2015).

1.4. Key Objectives

The key objectives of the project were as follows:

Objective 1: *Quantify microplastics in the surface waters of Matagorda Bay*.

Objective 2: *Quantify persistent and microplastics pollutants in the biota (shellfish and fish) of Matagorda Bay*.

Objective 3: *Assess the toxicity of bioaccumulated persistent pollutants and microplastics using embryo-larval life stages of zebrafish (Danio rerio)*.

Objective 4: *Promote educational outreach to local high school students on the science of ecosystem health monitoring*.

Texas A&M University at Galveston
1001 Texas Clipper Road
Galveston, TX 77554

Objective 1: Microplastics Pollution in the Surface Waters of Matagorda Bay

Texas A&M University at Galveston
1001 Texas Clipper Road
Galveston, TX 77554

1. Introduction

Plastic pollution has grown to a global environmental crisis, affecting marine ecosystems, and posing significant risks to marine life and human health (Sharma and Chatterjee, 2017). Plastic is versatile, lightweight, and robust, making it a preferred material in various industries and consumer products (Andrady and Neal, 2009). However, its durability also means that once disposed, plastic can endure in the environment for hundreds of years. With the popularization and wide application of plastics in the 20th century, the global production of plastics has increased from 1.5 million tons in 1950s to 359 million tons in 2018 (Markic et al., 2020). Annually, an estimated 4 to 23 million metric tons of plastic pollution are discharged into the ocean, contributing to the Global Plastic Cycle (Zhu et al., 2024). This influx of plastic waste has resulted in the formation of massive floating debris patches, the most infamous being the Great Pacific Garbage Patch (Lebreton et al., 2018). These patches consist of millions of tons of plastic debris and are concentrated in ocean gyres, where ocean currents converge, trapping and accumulating plastic waste. Due to this cycle, billions of tons of plastic waste have accumulated in natural habitats, from the highest mountains to the deepest ocean trenches, significantly impacting wildlife and ecosystems (Lebreton et al., 2018; Lebreton et al., 2019).

Statistical data from 2018-2019 gives the amount of plastic shipping in American dollars in **Figure 1**. Texas plastic shipping is double that of the nearest state of Ohio. All of Texas ship ports reside along the coast of the Gulf of Mexico making investigation of plastic concentrations and transport of tantamount importance. Much of the plastic shipping can be attributed to the Port of Houston where it is the nation's top gateway for preproduction plastic where it currently holds

Texas A&M University at Galveston
1001 Texas Clipper Road
Galveston, TX 77554

a market share of 60% nationally (Statista, 2025). A deeper dive into industry, urbanization, population density, and mitigation practices in this region will give a better idea of where these strategies fail or are less than sufficient.

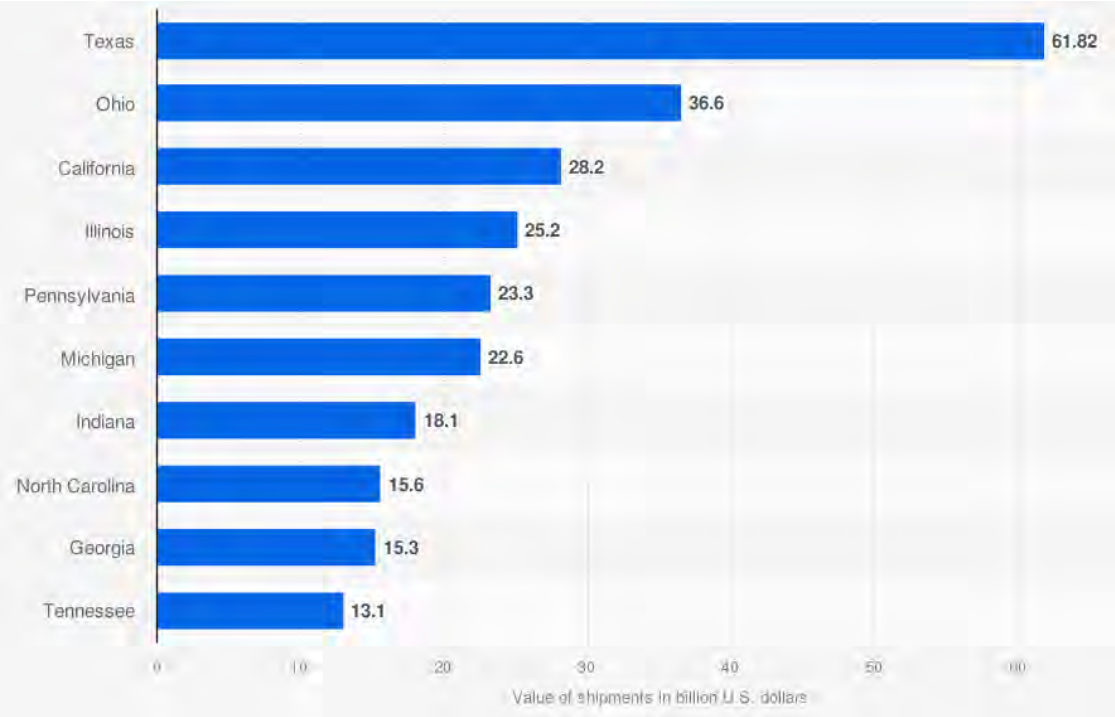

Figure 1. Value in plastic industry shipment in the US by state (2021) in billion US $ (Statista, 2025).

Mitigating plastic pollution in marine environments is an intricate challenge that demands concerted efforts from governments, industries, communities, and individuals (Alpizar et al., 2020). Plastic pollution is a global problem that transcends national boundaries. Coordinating international efforts and policies to address plastic pollution effectively requires collaboration among countries. Raising public awareness about the consequences of plastic pollution and promoting responsible consumption and waste disposal behaviors is crucial to reducing plastic

Texas A&M University at Galveston
1001 Texas Clipper Road
Galveston, TX 77554

waste. Despite advancements in research, there are still knowledge gaps concerning the long-term effects of plastic pollution on marine ecosystems and human health.

Towards this end, chemical analysis tools are fundamental to driving research on the effects of plastic pollution on natural ecosystems. For example, a significant challenge lies in comprehensively assessing the distribution of nano and microplastics ($\leq$ 5 mm size), that can easily enter aquatic ecosystems and potentially pose risks to organisms where nanoplastics can cross the intestinal barrier (Mattsson et al., 2015; Ugwu et al., 2021). The development of analytical methodologies is crucial for assessing the long-term consequences of plastic contamination, providing a greater understanding of the ecological effects, physical transport, and guiding policy decisions for environmental protection.

In this Objective, pyrolysis gas chromatography and triple quadrupole mass spectrometry (Py-GCMS/MS) was used to analyze nano- and microplastics (NMPs) pollution in the surface waters of Matagorda Bay. Py-GCMS/MS is a powerful analytical technique used to analyze plastics in various sample matrices (Santos et al., 2023). In Py-GCMS/MS, a small sample of plastic is heated to high temperatures in the presence of an inert gas. This process breaks down the polymer chains, producing a mixture of volatile compounds. The released compounds are then separated based on their chemical properties using a GC column, which separates them according to their boiling points and polarities.

Texas A&M University at Galveston
1001 Texas Clipper Road
Galveston, TX 77554

2. Materials and Methods

2.1. Materials used for calibration curve set-up, sample collection, and processing

A microplastic calibration standard kit containing polymethyl methacrylate (PMMA), polypropylene (PP), polyvinyl chloride (PVC), polyamide (PA), polycarbonate (PC), nylon-66 (N-66), polyethylene (PE), polyethylene terephthalate (PET), styrene butadiene (SBR), polyurethane (PUR), acrylonitrile butadiene styrene (ABS), and polystyrene (PS) was purchased from Frontier Labs (USA) along with 80µL Frontier Labs eco cups. Polyfluorinated styrene (PFS) was purchased from PSS (Germany). A pump was obtained from Jabsco (USA). Critical process (USA) supplied a filter housing and stainless-steel filter with 5 µm mesh. 0.7 and 2.8 µm glass fiber filters (GF/F) supplied by CYTIVIA Whatman. Toluene (HPLC grade), methanol, acetone, and Calcium carbonate (CaCO3) were obtained from J.T. Baker (USA). A vacuum aspirator was purchased from Brinkmann (USA). Glass microvolume syringe was attained from SGE (Australia). Quartz wool was purchased through ThermoScientific (USA). Milli-QTM water was utilized from a Milli-Q EQ 7000 Ultrapure Water Purification System acquired from Merck KGaA (Germany).

2.2. Collection of water samples

Surface water samples were collected at various locations within Matagorda Bay (**Figure 2**). Prior to collecting water samples, the stainless-steel filter was sonicated in deionized water and then rinsed with deionized water to remove any extraneous contaminants. One hundred liters of surface water for each sample was collected into a Pentair Pentek 150072 standard filter housing manufactured from Styrene-Acrylonitrile using a pump filtration system capturing particles 5µm

Texas A&M University at Galveston
1001 Texas Clipper Road
Galveston, TX 77554

and larger. The pump assembly consisted of a 5 mm prefilter placed in the top 20 cm of the water column at the collection site. The water was then pumped using a pump into a housing containing the stainless-steel filter with 5µm mesh. A flow meter was placed on the discharge line to measure surface water filtered with a target volume of one hundred liters. Upon completion, the filter was transported to the laboratory in the housing, where it was sonicated and washed with Millipore water to dislodge all particles. The sample was then vacuum filtered using all glass containers onto a 47 mm diameter GF/F with a pore size 0.7 µm, which was subsequently placed in an oven in a glass Petrie dish covered with aluminum for 24 hours at 35° C to remove water.

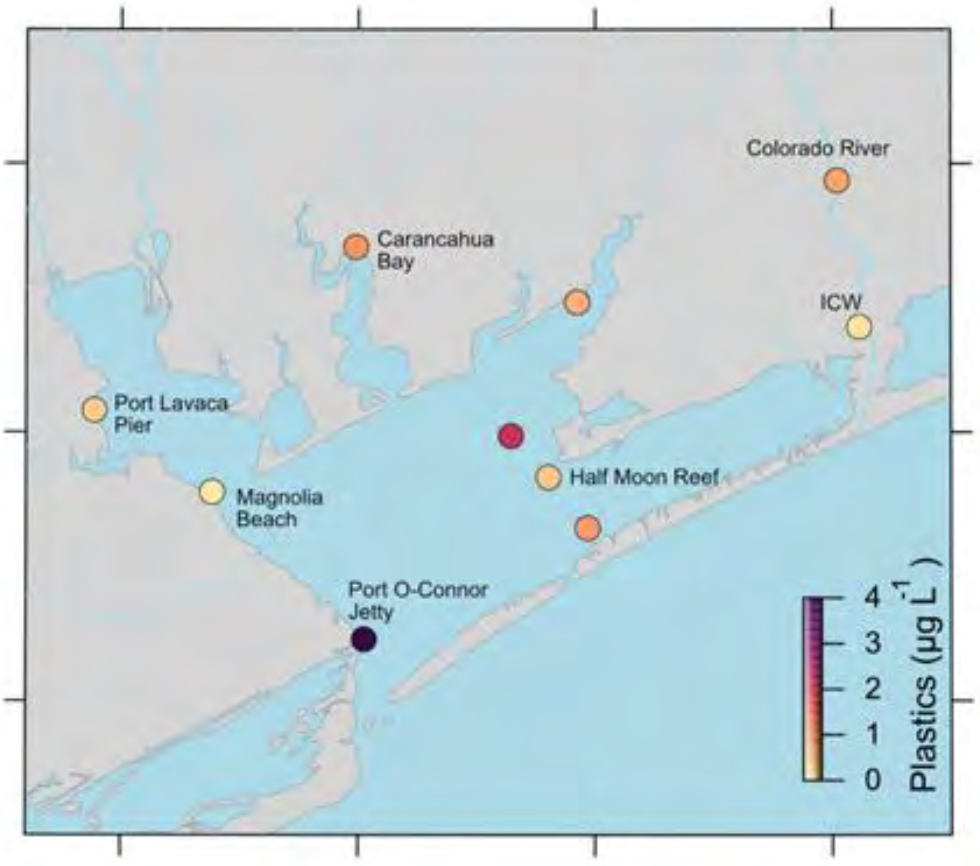

Figure 2. Average concentrations of microplastics in the surface waters of Matagorda Bay as shown at the various sampling locations. ICW, Intracoastal Waterway.

Texas A&M University at Galveston
1001 Texas Clipper Road
Galveston, TX 77554

2.3. Pyrolysis GC-MS/MS analysis

Pyrolysis gas chromatography was carried out with a Frontier Auto-Shot AS-2020E sampler and an EGA/PY-3030D multi-shot pyrolyzer connected to an Agilent 8890 GC and 7010B triple quadrupole MS (Py-GCMS/MS). Pyrolysis temperature was 600 °C. Prior to pyrolysis, GFF filters with particulates from water samples were spiked with PFS serving as an internal standard, transferred to Frontier Eco Cups and topped with 5 mg of $CaCO_3$ and quartz wool to ensure proper packing. The injector split was set to 50:1 with a column flow of 0.8 mL/min of helium as the carrier gas. The injector inlet temperature was set to 300°C. The septum purge flow was 20 mL min^{-1}. Straight liners packed with non-deactivated glass wool were used. Separation was achieved on a Frontier Ultra Alloy 5 (UA5-30M-0.25F) column with the following temperature program: start temperature 35°C, hold for 0.25 minutes, ramp at 20°C min^{-1} to 310°C, hold for 3 minutes, totaling runtime at 17 minutes.

The MS detector settings were source temperature 230 °C, quadrupole temperature 150 °C, and auxiliary temperature 280 °C with a 5 min solvent delay. Helium at 2.25 mL min^{-1} was used as the quench, and nitrogen at 1.5 mL min^{-1} was used as the collision gas. The detector was regularly autotuned using routines provided with the Agilent ChemStation software. The quantification of major plastic types was based on selected reaction monitoring (SRM) using characteristic product ions listed in **Table 1**. Qualifier ions monitored parallel to the quantifier ions provided additional identification of plastic analytes. Both quantifier and qualifier ions were selected by analyzing pure plastic standards and considering background ions from the organic matter matrix observed in biological particulates in full scan mode (50 - 650 $^{m}/_{z}$). Quantification was based on an internal

Texas A&M University at Galveston
1001 Texas Clipper Road
Galveston, TX 77554

standard calibration with PFS as the internal standard. Calibration standards were a homogenous mixture of plastics with the inert filler $CaCO_3$ to enable calibration at µg and ng amounts.

Table 1. List of plastics and their acronyms that were measured in the surface waters of Matagorda Bay using Py-GCMS/MS. Symbols, relative retention times (RRT), characteristic mass fragments and limit of detection (LOD) for plastics.

Plastic type	Abbreviation	RRT[a] (min)	Precursor ($^m/_z$)	Product ions[b] ($^m/_z$)	LOD[c] (ng)
Polymethylmethacrylate	PMMA	0.519	100	*41*, 39	295
Polypropylene	PP	0.591	126	*55*, 41	31
Polyvinyl chloride	PVC	0.677	128	*102*, 76	37
Polyamide	PA	0.731	113	*56*, 30	1
Polycarbonate	PC	0.787	134	119, *91*	1
Nylon-66	N-66	0.796	84	55, *41*, 39	7
Polyethylene	PE	0.857	82	*67*, 41	605
Polyethylene	PET	0.955	182	*105*, 77	49
Polyurethane	PUR	1.206	198	*93*, 77	2
Acrylonitrile butadiene	ABS	1.215	170	143, 128	5
Styrene butadiene	SBR	1.248	212	*170*, 119	1654
Polystyrene	PS	1.324	312	129, *91*	9
Polyfluorinated styrene*	PFS	10.80	122	*96*, 101	N/A

[a]Retention times (minutes) are relative to PFS on a Frontier Ultra Alloy 5 column. [b]Product ions are used for SRM quantification, italicized ions are used for quantification, and other ions were used as qualifier ions. [c]LOD was calculated using Signal/Noise $\geq$ 3. *Internal Standard.

3. Results and Discussion

Results from Matagorda Bay showed average concentrations of plastics in the surface waters of Matagorda Bay to range from 0.10 – 3.91 µg L^{-1} (**Figure 2**).

Texas A&M University at Galveston
1001 Texas Clipper Road
Galveston, TX 77554

Table 2. Table listing the proportional concentrations (as a percent of total concentration) of each microplastic particle type. The average concentration of microplastics quantified at each sampling site is given in µg L^{-1} (as mean ± standard error).

Sampling Locations	PE (%)	N66 (%)	PMMA (%)	PA (%)	PP (%)	PVC (%)	PC (%)	ABS (%)	PET (%)	PUR (%)	SBR (%)	PS (%)	Average (µg L^{-1})
Magnolia Beach (n=2)	0.51 ± 0.00	0.15 ± 0.00	0.00 ± 0.00	0.01 ± 0.01	0.06 ± 0.01	0.15 ± 0.00	0.03 ± 0.00	0.00 ± 0.00	0.09 ± 0.01	0.00 ± 0.00	0.00 ± 0.00	0.03 ± 0.00	**0.10 ± 0.06**
Carancahua Bay (n=2)	0.21 ± 0.00	0.04 ± 0.00	0.00 ± 0.00	0.01 ± 0.00	0.18 ± 0.00	0.13 ± 0.00	0.30 ± 0.00	0.11 ± 0.00	0.01 ± 0.00	0.00 ± 0.00	0.00 ± 0.00	0.01 ± 0.00	**0.98 ± 0.19**
Palacios Center Pier (n=4)	0.08 ± 0.03	0.03 ± 0.01	0.01 ± 0.01	0.00 ± 0.00	0.05 ± 0.02	0.09 ± 0.02	0.41 ± 0.20	0.10 ± 0.04	0.02 ± 0.01	0.00 ± 0.00	0.21 ± 0.12	0.01 ± 0.00	**0.69 ± 0.19**
Port Lavaca Pier (n=4)	0.21 ± 0.02	0.05 ± 0.01	0.02 ± 0.01	0.01 ± 0.01	0.13 ± 0.01	0.19 ± 0.05	0.14 ± 0.07	0.12 ± 0.05	0.03 ± 0.01	0.00 ± 0.00	0.10 ± 0.06	0.01 ± 0.00	**0.37 ± 0.10**
Port O'Connor (n=7)	0.15 ± 0.01	0.10 ± 0.03	0.01 ± 0.01	0.01 ± 0.00	0.11 ± 0.03	0.22 ± 0.05	0.12 ± 0.10	0.06 ± 0.05	0.05 ± 0.01	0.00 ± 0.00	0.07 ± 0.02	0.01 ± 0.00	**3.91 ± 0.91**

Texas A&M University at Galveston
1001 Texas Clipper Road
Galveston, TX 77554

Colorado River (n=3)	0.18 ± 0.10	0.10 ± 0.07	0.01 ± 0.00	0.01 ± 0.00	0.06 ± 0.02	0.11 ± 0.07	0.48 ± 0.24	0.04 ± 0.02	0.01 ± 0.00	0.00 ± 0.00	0.00 ± 0.00	0.01 ± 0.00	**0.81 ± 0.49**
Σ Plastics	**1.33 ± 0.06**	**0.46 ± 0.02**	**0.06 ± 0.00**	**0.05 ± 0.00**	**0.58 + 0.02**	**0.90 ± 0.02**	**1.48 ± 0.07**	**0.43 ± 0.02**	**0.20 ± 0.01**	**0.00 ± 0.00**	**0.37 ± 0.03**	**0.06 ± 0.00**	**6.85 ± 0.57**

Texas A&M University at Galveston
1001 Texas Clipper Road
Galveston, TX 77554

The results shown in **Figure 2** and **Table 2** indicate that by concentration, the top three most prominently detected plastics were PC>PE>PVC. The prominence of PC, PE, and PVC highlights the presence of general plastics degradation products, including those from plastic pellets such as nurdles (specifically for the presence of PE) (OSPAR, 2018). Interestingly, we also see the prominence of the tire-derived microplastic, SBR, at the most urbanized sampling points, namely: the Palacios Center Pier, Port Lavaca Pier, and Port O'Connor (**Figure 2** and **Table 2**). SBR indicates a major source of tire-derived microplastics, which accumulate on road surfaces through daily vehicular activity. SBR is a synthetic rubber and is a major source of microplastics pollution into the environment (Hägg et al., 2023). For example, rainfall events can facilitate the transport of this debris into aquatic systems, transferring it to estuarine environments. This pathway underscores the significance of urban runoff as a vector for the introduction of tire-derived materials into marine ecosystems, highlighting the interconnectedness of terrestrial and aquatic pollutant sources.

Finally, a comparison of surface water samples between the various sampling sites shows urbanized sites to have higher microplastic concentrations vs. more rural sites. For example, the mean microplastics levels at Port O'Connor (3.91 ± 0.91 μg L^{-1}) were 41x higher than those quantified at Magnolia Beach (0.10 ± 0.06 μg L^{-1}). Port O'Connor also exhibited the highest levels of mean microplastics quantified (**Figure 2** and **Table 2**). Given its location near the entrance to Matagorda Bay, we may be seeing a consequence of the bay's hydrodynamic properties towards concentrating microplastics at this location (**Figure 2**).

Texas A&M University at Galveston
1001 Texas Clipper Road
Galveston, TX 77554

Objective 2: Persistent and Microplastics Body-burdens in the Biota from Matagorda Bay

Texas A&M University at Galveston
1001 Texas Clipper Road
Galveston, TX 77554

1. Introduction

For this objective, we used gas chromatography and mass spectrometry (GCMS) to measure the levels of 14 PAHs and 28 PCBs (including 11 dioxin-like PCBs or DL-PCBs) in shellfish (gill/mantle from oysters) and fish (liver and muscle) from Matagorda Bay. We also used pyrolysis gas chromatography and tandem mass spectrometry (Py-GCMS/MS) to quantify 12 NMPs in the biota. We hypothesized that the legacy and lipophilic nature of PAHs and PCBs will result in greater body-burdens in biota relative to NMPs. In addition to measuring the body-burdens of pollutants, the likely sources of PAHs in the bay was also assessed by comparing the ratios of diagnostic low vs. high molecular weight (LMW vs. HMW) PAHs (Budzinski et al., 1997; Yunker et al., 2002). The cancer risk of PAHs to the human consumers of seafood was also calculated, and a toxic equivalents (TEQs) risk assessment was performed to determine likely adverse health effects of the dioxin-like PCBs in fish (Van den Berg et al., 1998; Barron et al., 2004). Lastly, the adult human average yearly intake of plastics was evaluated using the NMPs levels measured in the muscle tissue of fish and estimated amounts of seafood consumption (Nolen et al., 2022).

2. Methods

2.1. Sample collection and preparation

The following biota species were sampled from Matagorda Bay: eastern oysters (*Crassostria virginica*), gafftopsail catfish (*Bagre marinus*), red drum (*Sciaenops ocellatus*), and spotted seatrout (*Cynoscion nebulosus*). All oysters and fish were weighed, and their total and fork (fish only) lengths measured. A skin-free muscle fillet and liver was excised from each fish, and gill/mantle tissue was collected from each oyster. All tissue samples were stored at -20 °C until

Texas A&M University at Galveston
1001 Texas Clipper Road
Galveston, TX 77554

analysis. Prior to analysis, ~0.5 g of the previously frozen tissue samples was lyophilized for 24 hours at 0.20 mBar vacuum and -87 ºC using a LABCONCO freeze dryer. The resulting freeze-dried tissue was pulverized into a fine powder using a pestle and mortar.

2.2 PAH and PCB quantification

2.2.1. Accelerated solvent extraction: An accelerated solvent extraction (ASE) system (Dionex ASE 350) was used to extract persistent pollutants (i.e., PAHs and PCBs). Approximately 0.5 g of previously freeze-dried, pulverized, and re-weighed (to obtain dry weight) muscle or liver tissue was packed into a 34 mL stainless steel ASE cell, with the remainder volume packed with Ottawa sand (standard 20-30 mesh, Cat# S1010, Spectrum Chemical) above and below the sample in the cell. The sample was spiked with 10 µL of 50 µg mL^{-1} internal standards B[a]P-d_{12} and PCB65-d_5. Control or blank cells (comprising Ottawa sand only) were also spiked with internal standards to account for any background contamination. The solvent extraction was conducted at 100 ºC and 1500 psi pressure with a heating time of 5 min, preheat 5 min and a static phase of 4 min in the ASE. The flush rate was 60 % with a purge time of 300 sec. Two static cycles were completed per sample. The resulting solvent extracts were collected in 50 mL amber glass bottles and dried under a gentle stream of nitrogen (N_2). The resulting residue was reconstituted in 1 mL dichloromethane (DCM) (CAS# 75-09-2, ThermoFisher) and transferred to a smaller 5 mL test tube. The resultant solution was then subjected to solid phase extraction (SPE) through a Captiva lipid filter cartridge (Agilent Captiva EMR- Lipid, 1 mL, 40 mg) using a vacuum manifold to remove lipids from the sample. Each SPE cartridge was conditioned with 1 mL DCM, followed by the entire sample volume passing through the cartridge at a steady rate of ~1 drop sec^{-1}. The recovered solution was dried under a gentle stream of N_2, with the resulting

Texas A&M University at Galveston
1001 Texas Clipper Road
Galveston, TX 77554

residue reconstituted into 0.2 mL acetonitrile. The resuspended solution was transferred to a small volume glass insert and frozen at -20 ºC to promote the precipitation of any remainder lipids and tissue debris (Hong et al., 2004). Subsequently, 0.1 mL of the solvent supernatant was removed and dried under N_2, with the final residue reconstituted into 0.1 mL DCM, pipetted into a small volume insert and analyzed via GCMS.

2.2.2. PAH and PCB quantification using GCMS: The concentrations of 14 PAHs and 28 PCB congeners were quantified using GCMS. The 14 PAHs include: acenaphthene (ACE), fluorene (FLU), anthracene (ANT), phenanthrene (PHE), fluoranthene (FLT), chrysene (CHR), pyrene (PYR), benzo[a]anthracene (BaA), benzo[b]fluoranthene (BbF), benzo[k]fluoranthene (BkF), benzo[a]pyrene (BaP), dibenz[a,h]anthracene (DahA), benzo[g,h,i]perylene (BghiP), and indeno[1,2,3-cd]pyrene (IcdP). The 28 PCB congeners include PCBs 1, 18, 33, 52, 77, 81, 95, 101, 105, 114, 118, 123, 126, 128, 138, 149, 153, 156, 157, 167, 169, 170, 171, 177, 180, 183, 187, and 189. All PCBs are identified according to the IUPAC numbering system. The GCMS analysis was performed using a Hewlett Packard HP 6890 Series GC System coupled with Agilent Technologies 5973 Mass Selective Detector (GCMS). Samples were injected in splitless mode (2 µL) onto a DB-5MS (J&W Scientific) capillary column (30 m x 0.25 mm i.d.: 0.25 µm film thickness). Helium was used as the carrier gas at a flow rate of 1.0 mL min^{-1}. Temperatures at the front inlet and the MS interface were set to 250 ºC and 280 °C, respectively. Following injection of the sample, the GC oven initiated at 40 °C for 1 min, then ramped up to 180 °C at 20 °C min^{-1}, and then to 300 °C at 5 °C min^{-1}, for a hold of 10 min. The total runtime of the method was 40 min. The MS was operated in electron impact (EI) mode at an electron energy of 70 eV, while the MS source temperature was maintained at 230 °C. Selected ion monitoring (SIM)

Texas A&M University at Galveston
1001 Texas Clipper Road
Galveston, TX 77554

mode was used to identify and quantify all 42 analytes. The respective retention times for the PAHs and associated $^{m}/_{z}$ ions selected for quantification are reported in Hernout et al., (2020). The quantification of each PAH and PCB was performed against a linear 11-point calibration curve using serially diluted standards from 10 to 0.01 µg mL^{-1}. The limit of detection (LOD) for each compound was determined as the lowest standard that yielded a signal-to-noise ratio ≥5:1. All body-burden concentrations are reported as ng $gram^{-1}$ tissue dry weight (or ng g^{-1} DW).

2.2.3. Quality assurance of PAH and PCB quantification: Sample quality assurance included the preparation of sample blanks comprising Ottawa sand spiked with internal standards. Blanks yielding values for a compound greater than the respective LOD was used for background correction by subtracting its averaged value from all samples. Standard addition samples were also spiked with select PAHs (BaA and PYR) and PCBs (PCB 18 and 101) into muscle and liver from fish to measure recovery. For every batch of 10 muscle or liver samples analyzed, two additional replicates comprised blanks as well as standard addition samples for quality assurance. All samples were ASE extracted and analyzed via GCMS. The average recovery of selected PAHs and PCBs was (mean ± s.e.m), 74.07 ± 0.44% for BaA, 46.01 ± 9.24% for PYR, 69.07 ± 3.88% for PCB 18, and 68.5 ± 5.83% for PCB 101.

2.2.4. Source assessment of PAHs: To identify the predominant sources of PAHs, a source ratio graph was constructed. High molecular weight (HMW) PAHs (i.e., comprising ≥ 4 aromatic rings) are typically products of combustion at higher temperatures (400 – 700 °C) and are therefore mainly pyrogenic in origin. Whereas low molecular weight (LMW) PAHs (i.e., comprising < 4 aromatic rings) are products of combustion at lower temperatures (i.e., 100 – 300

Texas A&M University at Galveston
1001 Texas Clipper Road
Galveston, TX 77554

°C), and are therefore considered to be mainly petrogenic in origin (Budzinski et al., 1997; Wolska et al., 2012). Specifically, the ratios of ANT/(ANT+ PHE) and FLT/(FLT+ PYR) were used to indicate petrogenic/pyrogenic sources of PAHs.

2.2.5. Cancer risk Assessment of PAHs: To evaluate cancer risk via sea food consumption, a BaP equivalent (BaPE) concentration for fish body-burdens was calculated and compared against the Level of Concern (LOC) concentration calculated by the FDA risk assessment for exposure risk from the consumption of fish (0.035 μg g^{-1} BaPE) or oysters (0.142 μg g^{-1} BaPE) (FDA, 2010). In addition to considering the BaP body-burdens to calculate the BaPE, the individual toxicity equivalent factors (or TEFs) for PAHs whose toxicity have been standardized to that of BaP (i.e., BaA, CHR, BbF, IcdP, and DahA) were also summed to that of the BaPE value to generate an overall concentration for comparison with the FDA reference values for fish and oysters. The BaPE concentration was reported in μg g^{-1} of wet weight (WW) BaPE. Only muscle tissue body-burden was used in the calculation as it is consumed by humans and is therefore relevant for the risk assessment. The formula used is as follows:

$$BaPE\ concentration = BaP\ cocentration + \sum(equivalent\ PAHs\ concentration\ x\ respective\ TEFs)$$

2.2.6. Toxicity equivalents (TEQs) assessment of dioxin-like PCBs (or DL-PCBs): To assess the potential toxicity of DL-PCBs to fish, toxic equivalents (TEQs) were calculated using toxic

Texas A&M University at Galveston
1001 Texas Clipper Road
Galveston, TX 77554

equivalent factors (TEFs) proposed by Van den Berg et al. (1998). This approach takes into account the additive effects of DL- PCBs (i.e., non-ortho and mono-ortho PCBs) congeners in hepatic tissue. The toxicity potential was assessed for eleven DL-PCBs quantified in fish livers, namely PCBs 77, 81, 105, 114, 118, 123, 126, 156, 167, 169, and 189. The remainder PCBs were non-dioxin-like or NDL-PCBs. The lipid-normalized hepatic body-burden of each congener was multipied with its respective TEF, and then summed to calculate the TEQ value (Van den Berg et al., 1998). The summed TEQ values for each fish species were reported as $\log_{10}$ pg g^{-1} lipid weight (LW) and compared against reported upper and lower limit values shown to be toxic in aquatic mammals (1400 - 160 pg g^{-1} LW) and fish (600 - 57 pg g^{-1} LW) (Kannan et al., 2000; Steevens et al., 2005). Steevens et al. (2005) determined the TEQ upper and lower limits that were protective (survival) of 90% and 99% of fish respectively, whereas Kannan et al. (2000) determined high TEQ values that are associative with immunosuppression and endocrine disruption in marine mammals.

2.3 Microplastics quantification

2.3.1. Enzymatic digestion for isolation of plastics particles: An enzyme solution was prepared to digest the freeze dried tissue samples for microplastics extraction using a protocol adapted from von Friesen et al. (2019). Briefly, 6 g of porcine pancreatic enzyme (Pez, Millipore-Sigma, CAS# 8049-47-6) was dissolved into 100 mL of tris (tris(hydroxymethyl) aminomethane)/tris hydrochloride solution (Tris solution) (Sigma-Aldrich, Cat# T3038). Pez contains protease, amylase, and lipase enzymes, which help break down proteins and lipids in the tissue to release microplastics particles from the tissue matrix. To further remove any plastics contamination from the pancreatic enzyme, the Pez/Tris solution was placed in an oven at 40 ^{o}C for 3 hours and then

Texas A&M University at Galveston
1001 Texas Clipper Road
Galveston, TX 77554

vacuum filtered through 2.8 µm and 0.7 µm glass fiber filters (CYTIVIA Whatman GF/F and GF/D, VWR) using a Brinkmann Model B-169 vacuum aspirator. Approximately 0.02 g of dried fish and oyster tissue was placed in round bottom glass vials to be treated with 1 mL of Pez/Tris solution (0.06 g Pez/mL buffer) while maintaining an optimal pH 8 for pancreatic enzymes (Berdutina et al., 2000). The vials were then shaken for 24 hours at 40 ^{o}C on a shaker tray. The samples were then filtered through cleaned and furnaced 0.7 µm x 24 mm glass fiber filters using a vacuum filter and rinsed with Milli-Q water (Milli-Q EQ 7000 Ultrapure Water Purification System, Merck KGaA, Darmstadt, Germany). The utilized portion of each filter was then cut out using a cork borer, separated and placed in a glass Petri dish where it was dried for 24 hours at 38 °C. The filters were folded after drying and placed in separate stainless-steel Pyrolysis cups (Eco-Cup LF, Frontier Labs, Japan) that had been treated with 20 µg of polyfluorinated styrene (PFS) as internal standard. Finally, the sample cups were topped with 5 mg of calcium carbonate and quartz wool to pack the sample and placed in a Frontier Laboratories Ltd. Auto-Shot Sampler: AS-1020E Pyrolizer for pyrolysis analysis.

2.3.2. Microplastics quantification using Py-GCMS/MS: A Frontier Laboratories Auto-shot sampler pyrolyzer in conjunction with an Agilent 8890 GC System coupled with an Agilent 7010B triple quadrupole mass spectrometer (Py-GCMS/MS), was used to identify and quantify plastics polymers. The microplastics quantified included: polymethyl methacrylate (PMMA), polypropylene (PP), polyvinyl chloride (PVC), polyamide (PA), polycarbonate (PC), nylon 66 (N66), polyethylene (PE), polyethylene terephthalate (PET), acrylonitrile butadiene styrene (ABS), polyurethane (PUR), styrene-butadiene rubber (SBR), and polystyrene (PS). The pyrolysis or combustion of tissue samples at 600 ^{o}C allowed for the complete oxidation of

Texas A&M University at Galveston
1001 Texas Clipper Road
Galveston, TX 77554

organics, while the microparticles were volatilized and fragmented to smaller and more stable particles (pyrolyzates). These pyrolyzates were chromatographically separated using an Ultra Alloy^{+}-5 Capillary Column (30 m length x 0.25 mm I.D. x 0.25 µm Film) (Frontier Labs, Japan) in an Agilent 8890 GC System with an increasing temperature gradient before being introduced to an Agilent 7010B GCMS/MS Triple Quadrupole for precise mass analysis. The injector was set to a split ratio of 50:1, with a split flow of 40 mL min^{-1}. The injector temperature was set to 300 ºC. The septum purge flow was 20 mL min^{-1}. Straight liners packed with non-deactivated glass wool were used. Helium at a flow rate of 2.25 mL min^{-1} was used as the carrier gas and nitrogen at 1.5 mL min^{-1} was used as the collision gas. Chromatographic separation was achieved with the following temperature program: starting temperature 35 ºC, hold for 0.25 min, ramp at 20 º C min^{-1} to 310 º C, hold for 3 min, a total runtime of 17 min. The mass detector settings were: source temperature 230 ºC, quad temperature 150 ºC, and auxiliary temperature 280 ºC, with a 5 min solvent delay. MassHunter acquisition and associated data analysis software were used for accurate mass analysis. The quantification of individual plastic polymers was based on individual distinctive mass ions (which were blank subtracted) (as shown in **Table 1** for ***Objective 1***). The quantification of each polymer was performed against a linear five-point calibration curve spanning from 1500 – 150 µg, with 40 µg of Internal standard (Polyfluorinated styrene). All standards were placed onto a GF/F (0.7 µm pore size, 25 mm diameter) Whatman filter, transferred into Eco-cups (Frontier Labs, Japan), packed with 5 mg of $CaCO_3$, and finally sealed with a plug of quartz wool.

To correct for the interference of lipids on Polyethylene quantification as described by Rauert et al. (2022), we used a lipid triglyceride mixture from Sigma (CAS# 17810) as control. We found

Texas A&M University at Galveston
1001 Texas Clipper Road
Galveston, TX 77554

sample lipids to mainly interfere with the quantification of PE, PP, N66, PMMA, and PVC. To account for lipid contamination, a 5-point lipid calibration curve was constructed from 0.25 mg to 1.25 mg using the weights of lipids against the concentration for each of the plastics. Assuming, there were no plastics in the lipid standard from Sigma, this calibration curve showed the relation between lipid concentrations and lipid content, therefore yielding a correction factor which was subtracted from the plastic quantification in each sample.

2.3.3. Quality assurance of microplastics quantification: For each batch of 10 samples, two blank controls, two recovery controls, and a replicate were also analyzed. Each blank control pyrolysis cup contained 40 µg of Internal standard (Polyfluorinated styrene), GF/F (0.7 µm pore, 25 mm diameter) Whatman filter (after filtering 1 mL of Pez/Tris), 5 mg of $CaCO_3$, and quartz wool to measure background contamination to be subtracted from sample quantification. The standard addition/recovery control contained 40 µg of Internal Standard (Polyfluorinated styrene), GF/F Whatman filter (0.7 µm) containing a known amount of the Frontier plastics standard (Frontier labs, Lot# 21101501), 0.02 g of dry weight tissue (digested with 1 mL of Pez/Tris), 5 mg of $CaCO_3$, and quartz wool to measure the percentage recovery of plastic standards. The replicate pyrolysis cups also contained a replicate of a sample (muscle matrix) to confirm reproducibility of data. The percent recovery of notable plastics in the muscle matrix was 115 $\pm$ 0.15% for PP, 93 $\pm$ 0.08% for N66, and 113 $\pm$ 0.05% for PE.

2.3.4. Estimated Average Daily Intake of plastics: Seafood Daily Intake (DI) and NMPs Average Daily Intake (ADI) rates were calculated as follows:

Texas A&M University at Galveston
1001 Texas Clipper Road
Galveston, TX 77554

$$DI = \frac{DC_{shellfish\ or\ fish}}{BW} \quad (1)$$

$$ADI = C_{Plastics} * DI \quad (2)$$

First, a seafood daily intake (DI) in g Kg^{-1} human body weight day^{-1} was determined (Eq. (1)) by dividing the estimated daily consumption ($DC_{shellfish/fish}$) of shellfish or fish (in g day^{-1}) by the body weight (BW) of an average adult human (Kg). The Texas Department of State Health Services' (DSHS) Seafood and Aquatic Life Group's (SALG) standard adult weight of 70 kg and consumption of 30 g of shellfish or fish per day were used to calculate the DI (DSHS, 2011). Subsequently, an Average Daily Intake (ADI) rate of plastics consumption (in mg Kg^{-1} human body weight day^{-1}) was calculated by multiplying the average plastics concentration in muscle of fish or gill/mantle of oysters in µg $gram^{-1}$ wet weight (WW) ($C_{plastics}$) by the DI (Eq. (2)). While the $C_{plastics}$ were initially quantified as µg $gram^{-1}$ dry weigh (DW) (and then converted to mg $gram^{-1}$ DW), the DW values were converted to their respective wet weight (WW) basis by using an average correction factor (for each species) that accounted for the proportion of tissue weight change after freeze-drying, i.e., indicating the loss of tissue water content (as described in section *2.1. Sample collection and preparation*). Finally, the ADI in mg Kg^{-1} human body weight day^{-1} was converted to an annual or yearly plastics intake by multiplying the ADI's for each species by 365 days.

2.4 Statistical analysis

Statistical analysis was conducted using R (v4.1.3) and associated packages, tidyr and ggplot2 (for visualization) with significance at $\alpha \leq 0.05$. The normality of data was tested using Shapiro-

Texas A&M University at Galveston
1001 Texas Clipper Road
Galveston, TX 77554

Wilk's test followed by Levene's test for homogeneity of variance. For pairwise comparisons, either a parametric t-test or non-parametric Mann-Whitney U test was conducted. The statistical analysis of data comprising a main effects variable was performed using either one-way ANOVA (parametric) or the Kruskal-Wallis test (non-parametric). With post hoc testing comprising either Tukey's or Dunn's test respectively.

3. Results

3.1. Morphometric parameters of biota

Among the fish, only reddrum exhibited a significantly higher (2x) body weight compared to the spotted seatrout (**Table 1**). There were no significant differences between the fish for total or fork lengths. Oyster total lengths or weights were not compared to fish as they comprised the only shellfish species monitored in our study.

Table 1. Average weight (g), fork length (cm), and total length (cm) of fish and oysters collected from Matagorda Bay reported as mean ± standard error. Among the finfish, significant differences ($p \leq 0.05$) in weight are noted by different letters.

Common name	Number of samples	Weight (g)	Fork length (cm)	Total length (cm)
Gafftopsail catfish	10	415.80 ± 73.92[a,b]	30.30 ± 2.43	35.20 ± 2.48
Red drum	7	620.71 ± 138.90[a]	31.57 ± 2.83	37.00 ± 3.17
Spotted seatrout	9	297.78 ± 53.53[b]	29.30 ± 1.83	33.46 ± 2.24
Eastern oyster	10	41.60 ± 6.52	-	-

Texas A&M University at Galveston
1001 Texas Clipper Road
Galveston, TX 77554

3.2. Contaminant body-burdens in biota

3.2.1. PAH body-burdens: **Tables 2** and **3** list PAHs body-burdens in muscle and liver respectively. The sum of total PAH levels in muscle showed no significant differences across the biota (**Table 2(a)**). However, oysters exhibited the highest (not significant) concentrations at levels 2x higher than those in catfish, and 1.2x of seatrout and red drum respectively (**Table 2(a)**). The livers exhibited sum of total PAH levels 5x - 14x higher than those measured in the muscle tissue (**Table 3(a)**), with a statistically significant difference only between red drum vs. catfish being evident (levels 4x higher in red drum).

A comparison of PAH congener profiles showed a broad representation of LMW and HMW PAHs in muscle vs. liver (**Figure 1** and **2**). In the muscle of fish (and gill/mantle of oysters), PHE levels equivalently dominated in all species with levels ~2x higher than the other LMW PAHs (**Table 2(a)**). Whereas BaA was the most prominent HMW PAH in oysters, red drum and seatrout, with levels respectively 70x, 65x, and 26x higher than the remainder HMW PAHs (**Table 2(a)**). In catfish muscle, FLT and PYR were the most prominent HMW PAHs at 43x and 47x higher than the remaining HMW PAHs (**Table 2(a)**). While the seatrout muscle exhibited a near equivalent abundance for PYR and IcdP (19% and 17% respectively of the total HMW PAHs) (**Table 2(a)**).

In contrast to muscle, the liver tissue for all fish exhibited a predominance of LMW PAHs with the overall proportion of LMW PAHs constituting 69%, 93%, and 98% to the sum of total PAHs in catfish, red drum, and seatrout respectively (**Table 3(a)**). Of the LMW PAHs, FLU and ACE accounted for the most prominent congeners. While FLU accounted for 45%, 70%, and 81% to

Texas A&M University at Galveston
1001 Texas Clipper Road
Galveston, TX 77554

the sum of total PAHs in catfish, red drum, and seatrout respectively; ACE contributed 14%, 21%, and 15% to the sum of total PAHs in catfish, red drum, and seatrout respectively (**Table 3(a)**). For the HMW congeners, catfish exhibited high contributions of FLT (8%), PYR (6%), CHR (5%), and BaA (4%) to the sum of total PAHs (**Table 3(a)**). In red drum and seatrout, only BaA (4%) and PYR (1%) contributed sufficiently to the sum of total PAHs respectively (**Table 3(a)**).

3.2.2. PCB body-burdens: PCBs body-burdens in the muscle and liver tissue of biota are detailed in **Tables 2** and **3** respectively. The analysis of PCB congeners in muscle of fish (or gill/mantle of oysters) indicated a prominent representation of DL-PCBs, with ≥75% DL-PCBs congeners detected vs. ≥24% of NDL-PCBs. The DL-PCBs comprised 44%, 85%, 28%, and 33% of sum of total PCBs in oysters, catfish, red drum, and seatrout respectively (**Table 2(b)**). Overall, sum of total PCBs in the gill/mantle tissue of oysters exhibited higher levels relative to those measured in muscle from catfish (11x higher, statistically significant), red drum (2x higher, not significant), and seatrout (5x higher, not significant) (**Table 2(b)**). Amongst the fish species, red drum exhibited the highest sum of total PCB levels (not statistically significant) in muscle relative to catfish (6x higher) and seatrout (3x higher) (**Table 2(b)**).

The livers of fish exhibited the highest sum of total levels of PCBs relative to the muscle, ranging from 11x – 15x higher in liver vs. muscle (**Tables 2** and **3**). The normalized PCB congeners in the livers of fish also indicated a prominent representation of DL-PCBs, with ≥75% DL-PCBs congeners detected vs. ≥59% of NDL-PCBs. The DL-PCBs comprised 67%, 26%, and 51% of sum of total PCBs in catfish, red drum, and seatrout respectively (**Table 3(b)**). The

Texas A&M University at Galveston
1001 Texas Clipper Road
Galveston, TX 77554

analysis of sum of total PCBs in the livers of fish showed red drum to exhibit the highest levels (not statistically significant) vs. catfish (5x higher) or seatrout (3x higher) (**Table 3(b)**).

3.2.3. NMPs body-burdens: The sum of total NMPs in the gill/mantle tissue of oysters exhibited statistically significantly higher body-burdens relative to muscle in fish, at levels 5x higher than catfish, 9x higher than seatrout, and 25x higher than red drum (**Table 2(c)**). In oysters, PP was the most prominent NMP comprising 60% of the sum of total NMPs (**Figure 3(a)**). In catfish, PE dominated at 64% of the sum of total NMPs. And in red drum and seatrout muscle, N66 predominated at ≥97% of the sum of total NMPs (**Table 2(c)**). The sum of total NMP levels in the livers of red drum and seatrout were 51x and 7x higher than in their respective muscle tissues (**Table 2(c)** and **Table 3(c)**) (**Figure 3(b)**). Despite red drum exhibiting a mean level 3x that of seatrout, there were no statistically significant differences between them (**Table 3(c)**). The analysis of NMPs in the livers of catfish were precluded from analysis due to a lack of sufficient tissue biomass remaining after the persistent pollutant (PAHs and PCBs) analysis.

Texas A&M University at Galveston
1001 Texas Clipper Road
Galveston, TX 77554

Table 2. Muscle concentrations of **a)** PAHs, **b)** PCBs, and **c)** NMPs in oysters (gill/mantle tissue) and fish from Matagorda Bay. Levels are reported in ng g^{-1} DW for PAHs and PCBs, and µg g^{-1} DW for NMPs (mean ± standard error). Levels below the limit of detection are represented by '- '. Different letters for sum of total show significant differences ($p \leq 0.05$) between species.

a) PAHs (ng g^{-1} DW)	**Oysters (n=10)**	**Catfish (n=10)**	**Red drum (n=7)**	**Seatrout (n=9)**
Low Molecular Weight (LMW)				
Acenaphthene (ACE)	17.79 ± 5.73	12.27 ± 2.46	6.47 ± 0.71	15.80 ± 3.01
Fluorene (FLU)	19.53 ± 11.17	8.97 ± 1.43	1.83 ± 1.25	8.30 ± 4.01
Phenanthrene (PHE)	28.50 ± 8.32	23.10 ± 5.24	11.55 ± 1.07	44.91 ± 20.74
Anthracene (ANT)	1.31 ± 0.50	14.36 ± 3.23	3.83 ± 1.41	8.12 ± 3.13
High Molecular Weight (HMW)				
Fluoranthene (FLT)	4.48 ± 2.54	28.02 ± 5.14	2.22 ± 2.22	9.59 ± 5.75
Pyrene (PYR)	8.47 ± 2.60	31.13 ± 5.18	6.57 ± 1.73	22.71 ± 3.62
Benzo[a]anthracene (BaA)	114.48 ± 40.45	2.80 ± 1.87	114.71 ± 59.47	30.95 ± 16.33
Chrysene (CHR)	15.72 ± 3.15	0.91 ± 0.61	19.06 ± 15.24	13.06 ± 9.44
Benzo[b]fluoranthene (BbF)	-	-	3.44 ± 1.27	7.30 ± 1.83

Benzo[k]fluoranthene (BkF)	1.13 ± 0.95	0.25 ± 0.25	1.80 ± 1.21	8.90 ± 1.71
Benzo[a]pyrene (BaP)	4.62 ± 2.37	-	1.43 ± 0.93	2.82 ± 2.12
Indeno[1,2,3-cd]pyrene (IcdP)	2.96 ± 1.29	-	22.72 ± 1.89	20.23 ± 2.28
Dibenzo[a,h]anthracene (DahA)	6.21 ± 2.20	2.59 ± 0.80	2.48 ± 0.88	2.60 ± 1.48
Benzo[g,h,i]perylene (BghiP)	5.31 ± 1.25	-	0.80 ± 0.80	1.12 ± 0.75
ΣPAHs	**230.50 ± 82.53[a]**	**124.40 ± 26.21[a]**	**198.91 ± 90.08[a]**	**196.40 ± 76.18[a]**
b) PCBs (ng g^{-1} DW)	**Oysters (n=10)**	**Catfish (n=10)**	**Red drum (n=7)**	**Seatrout (n=9)**
Non-ortho (dioxin like)				
PCB 77	62.08 ± 33.90	1.00 ± 1.00	4.09 ± 3.19	-
PCB 81	17.07 ± 9.83	1.30 ± 0.67	7.30 ± 4.11	-
PCB 126	1.01 ± 1.01	12.84 ± 8.87	2.76 ± 2.23	0.57 ± 0.38
PCB 169	-	0.99 ± 0.32	0.68 ± 0.68	2.21 ± 1.14
Mono-ortho (dioxin like)				
PCB 105	3.16 ± 1.44	3.50 ± 1.92	6.02 ± 1.98	7.41 ± 4.29

PCB 114	26.83 ± 12.80	1.17 ± 0.82	3.82 ± 2.08	1.97 ± 1.00
PCB 118	4.71 ± 1.89	0.70 ± 0.70	5.74 ± 4.02	1.66 ± 0.85
PCB 123	3.60 ± 1.22	0.84 ± 0.84	2.40 ± 1.84	1.61 ± 0.82
PCB 156	5.92 ± 2.01	-	11.54 ± 7.48	1.11 ± 1.11
PCB 167	2.70 ± 1.50	-	-	4.62 ± 4.62
PCB 189	0.29 ± 0.29	-	-	-
Non-dioxin like				
PCB 1	4.70 ± 1.78	-	-	-
PCB 18	109.24 ± 29.54	2.34 ± 1.45	86.44 ± 54.78	31.12 ± 14.61
PCB 33	36.62 ± 12.17	0.48 ± 0.48	6.58 ± 3.83	0.79 ± 0.79
PCB 52	0.31 ± 0.31	-	1.25 ± 0.59	0.21 ± 0.17
PCB 95	1.22 ± 0.82	-	1.33 ± 0.86	-
PCB 101	2.99 ± 1.21	-	1.99 ± 1.99	-
PCB 128	1.89 ± 1.25	1.09 ± 0.73	0.57 ± 0.57	7.94 ± 7.94
PCB 138	0.93 ± 0.49	-	-	0.45 ± 0.45
PCB 149	0.87 ± 0.46	-	4.42 ± 3.12	-

PCB 153	0.32 ± 0.22	-	0.65 ± 0.65	0.77 ± 0.77
PCB 157	0.85 ± 0.46	-	2.49 ± 1.63	-
PCB 170	0.30 ± 0.30	-	1.32 ± 1.32	0.60 ± 0.60
PCB 171	0.76 ± 0.76	-	3.69 ± 1.95	-
PCB 177	-	-	3.44 ± 2.23	0.49 ± 0.49
PCB 180	1.00 ± 0.52	-	-	-
PCB 183	0.37 ± 0.37	-	-	-
PCB 187	0.55 ± 0.55	-	-	0.51 ± 0.51
ΣPCBs	**290.29 ± 117.10[a]**	**26.25 ± 17.80[b]**	**158.53 ± 101.14[ab]**	**64.04 ± 40.53[ab]**

c) NMPs (µg g^{-1} DW)	**Oysters (n=10)**	**Catfish (n=10)**	**Red drum (n=7)**	**Seatrout (n=9)**
Polymethyl Methacrylate (PMMA)	-	-	-	-
Polypropylene (PP)	5,320.77 ± 2442.74	-	-	-
Polyvinyl Chloride (PVC)	-	-	-	-

Texas A&M University at Galveston
1001 Texas Clipper Road
Galveston, TX 77554

c) NMPs (µg g^{-1} DW)	Oysters (n=10)	Catfish (n=10)	Red drum (n=7)	Seatrout (n=9)
Polyamide (PA)	-	-	-	33.66 ± 18.05
Polycarbonate (PC)	-	-	-	-
Nylon 66 (N66)	1,815.61 ± 452.94	577.19 ± 259.06	355.42 ± 183.75	933.06 ± 192.51
Polyethylene (PE)	1,789.33 ± 733.87	1,055.82 ± 535.54	-	-
Polyethylene Terephthalate (PET)	-	-	-	-
Acrylonitrile Butadiene Styrene (ABS)	-	3.96 ± 2.13	-	-
Polyurethane (PUR)	-	-	-	-
Styrene-Butadiene Rubber (SBR)	-	-	-	-
Polystyrene (PS)	-	-	-	-
ΣNMPs	**8,925.72 ± 2,590.50[a]**	**1,636.97 ± 594.91[b]**	**355.42 ± 183.75[b]**	**966.71 ± 193.35[b]**

Texas A&M University at Galveston
1001 Texas Clipper Road
Galveston, TX 77554

Table 3. Liver concentrations of **a)** PAHs **b)** PCBs, and **c)** NMPs in fish collected from Matagorda Bay. Levels are reported in ng g^{-1} DW for PAHs and PCBs, and µg g^{-1} DW for NMPs (mean ± standard error). Levels below the limit of detection are represented by '-'. Different letters show significant differences ($p \leq 0.05$) between species.

a) PAHs (ng g^{-1} DW)	**Catfish (n=10)**	**Red drum (n=7)**	**Seatrout (n=3)**
Low Molecular Weight (LMW)			
Acenaphthene (ACE)	94.99 ± 16.46	592.43 ± 194.09	431.40 ± 135.46
Fluorene (FLU)	307.02 ± 108.20	1,969.08 ± 872.06	2,287.88 ± 1498.61
Phenanthrene (PHE)	23.57 ± 9.34	47.20 ± 13.51	47.32 ± 23.96
Anthracene (ANT)	43.57 ± 4.04	24.24 ± 10.33	3.51 ± 1.82
High Molecular Weight (HMW)			
Fluoranthene (FLT)	52.87 ± 12.50	2.69 ± 1.35	0.84 ± 0.84
Pyrene (PYR)	41.69 ± 10.10	15.07 ± 4.27	19.61 ± 5.65
Benzo[a]anthracene (BaA)	29.71 ± 12.90	111.88 ± 79.47	3.98 ± 3.98
Chrysene (CHR)	34.44 ± 14.02	30.58 ± 16.55	2.43 ± 2.43
Benzo[b]fluoranthene (BbF)	1.60 ± 0.84	-	-

Benzo[k]fluoranthene (BkF)	2.22 ± 0.93	-	-
Benzo[a]pyrene (BaP)	6.80 ± 4.53	2.46 ± 1.45	4.09 ± 3.64
Indeno[1,2,3-cd]pyrene (IcdP)	21.94 ± 7.81	7.96 ± 1.81	11.62 ± 7.49
Dibenzo[a,h]anthracene (DahA)	15.62 ± 6.12	1.35 ± 0.95	-
Benzo[g,h,i]perylene (BghiP)	4.05 ± 1.28	12.85 ± 4.84	-
ΣPAHs	**680.08 ± 209.07[b]**	**2,817.79 ± 1,200.68[a]**	**2,812.69 ± 1,683.88[ab]**

b) PCBs (ng g^{-1} DW)	**Catfish (n=10)**	**Red drum (n=7)**	**Seatrout (n=3)**
Non-ortho (dioxin like)			
PCB 77	26.38 ± 12.34	42.66 ± 22.42	16.18 ± 11.80
PCB 81	7.61 ± 4.50	40.54 ± 26.05	3.00 ± 1.52
PCB 126	173.47 ± 63.13	3.09 ± 2.00	-
PCB 169	1.50 ± 1.01	-	-
Mono-ortho (dioxin like)			
PCB 105	22.95 ± 5.18	78.03 ± 26.82	17.50 ± 17.50

PCB 114	8.88 ± 4.53	191.38 ± 52.33	176.66 ± 84.50
PCB 118	7.95 ± 3.84	59.48 ± 29.65	19.52 ± 6.16
PCB 123	7.18 ± 3.15	45.13 ± 28.78	26.27 ± 21.98
PCB 156	0.47 ± 0.47	9.71 ± 3.89	1.56 ± 1.56
PCB 167	8.18 ± 5.66	50.70 ± 21.25	102.21 ± 22.51
PCB 189	0.40 ± 0.40	7.33 ± 5.45	-
Non-dioxin like			
PCB 1	40.01 ± 15.94	39.53 ± 11.21	44.64 ± 5.56
PCB 18	38.79 ± 11.65	1,251.44 ± 654.69	65.06 ± 32.96
PCB 33	7.35 ± 2.81	26.66 ± 7.16	5.63 ± 0.73
PCB 52	-	-	-
PCB 95	17.04 ± 16.37	21.42 ± 13.44	-
PCB 101	4.07 ± 2.01	55.30 ± 19.29	17.00 ± 9.89
PCB 128	12.10 ± 10.19	87.85 ± 41.07	195.97 ± 39.44
PCB 138	-	0.87 ± 0.87	9.81 ± 3.97
PCB 149	-	7.69 ± 3.22	-

PCB 153	-	0.54 ± 0.54	0.33 ± 0.33
PCB 157	0.99 ± 0.66	5.46 ± 4.73	3.36 ± 1.71
PCB 170	-	2.62 ± 1.24	2.38 ± 2.38
PCB 171	-	1.87 ± 1.87	-
PCB 177	-	0.68 ± 0.68	-
PCB 180	1.76 ± 1.28	1.42 ± 0.94	2.22 ± 2.22
PCB 183	2.33 ± 1.65	0.61 ± 0.61	-
PCB 187	3.35 ± 2.00	-	-
ΣPCBs	**392.76 ± 168.77[a]**	**2,032.03 ± 980.20[a]**	**709.30± 266.72[a]**

c) NMPs (µg g^{-1} DW)	**Red drum (n=5)**	**Seatrout (n=5)**
Polymethyl Methacrylate (PMMA)	-	-
Polypropylene (PP)	-	-
Polyvinyl Chloride (PVC)	-	-
Polyamide (PA)	-	-

Texas A&M University at Galveston
1001 Texas Clipper Road
Galveston, TX 77554

c) NMPs (µg g^{-1} DW)	Red drum (n=5)	Seatrout (n=5)
Polycarbonate (PC)	-	-
Nylon 66 (N66)	16,082.04 ± 6,524.91	6,536.69 ± 5,176.33
Polyethylene (PE)	-	-
Polyethylene Terephthalate (PET)	-	-
Acrylonitrile Butadiene Styrene (ABS)	-	-
Polyurethane (PUR)	-	-
Styrene-Butadiene Rubber (SBR)	2,084.06 ± 1,150.49	-
Polystyrene (PS)	-	-
ΣNMPs	**18,166.10 ± 6,625.56[a]**	**6,536.69 ± 5,176.33[a]**

Texas A&M University at Galveston
1001 Texas Clipper Road
Galveston, TX 77554

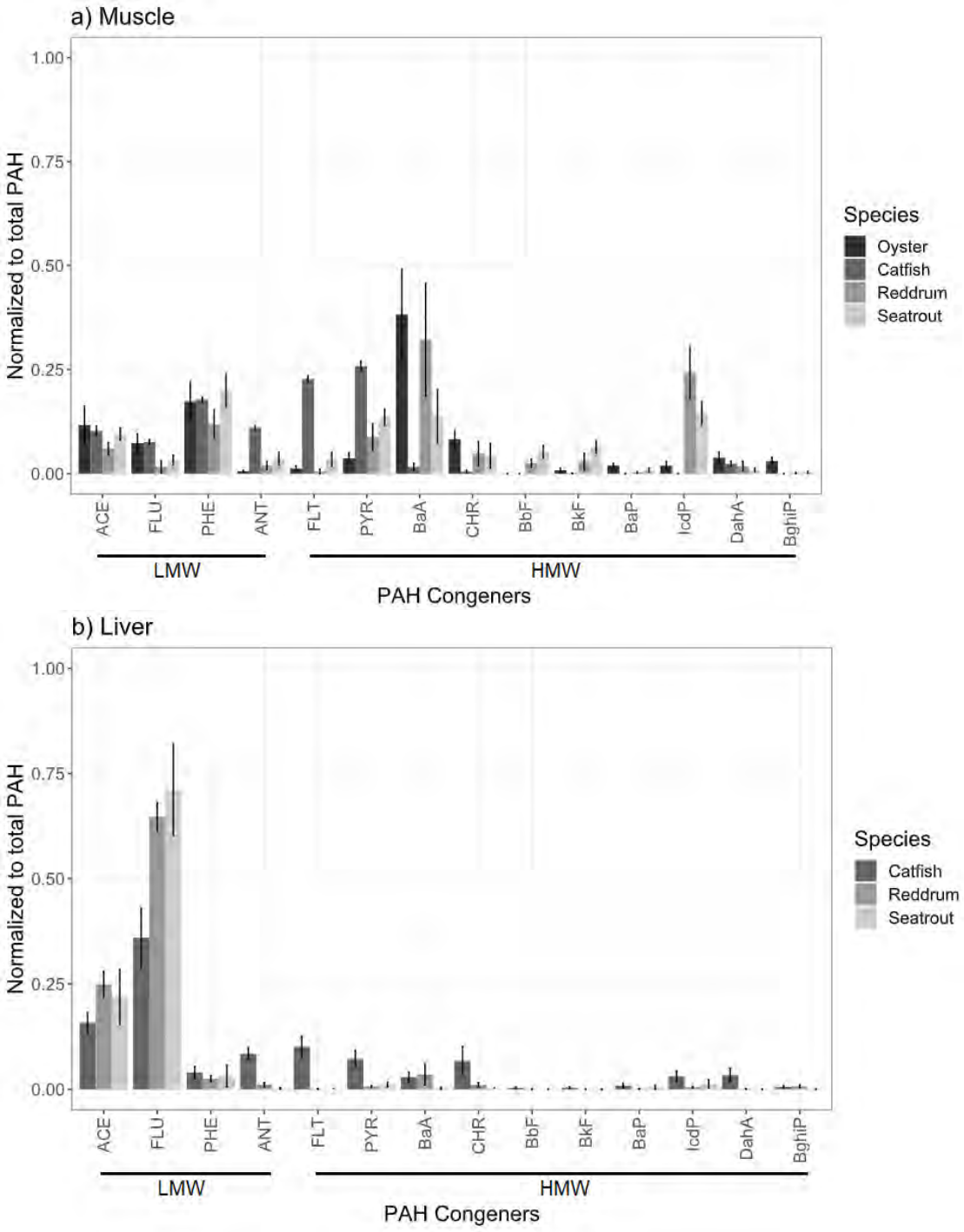

Figure 1. Normalized PAHs congener profiles in the **a)** gill/mantle of oysters and muscle from fish; and **b)** in the livers of fish collected from Matagorda Bay. All the mean values are normalized to total PAH to show relative abundance.

Texas A&M University at Galveston
1001 Texas Clipper Road
Galveston, TX 77554

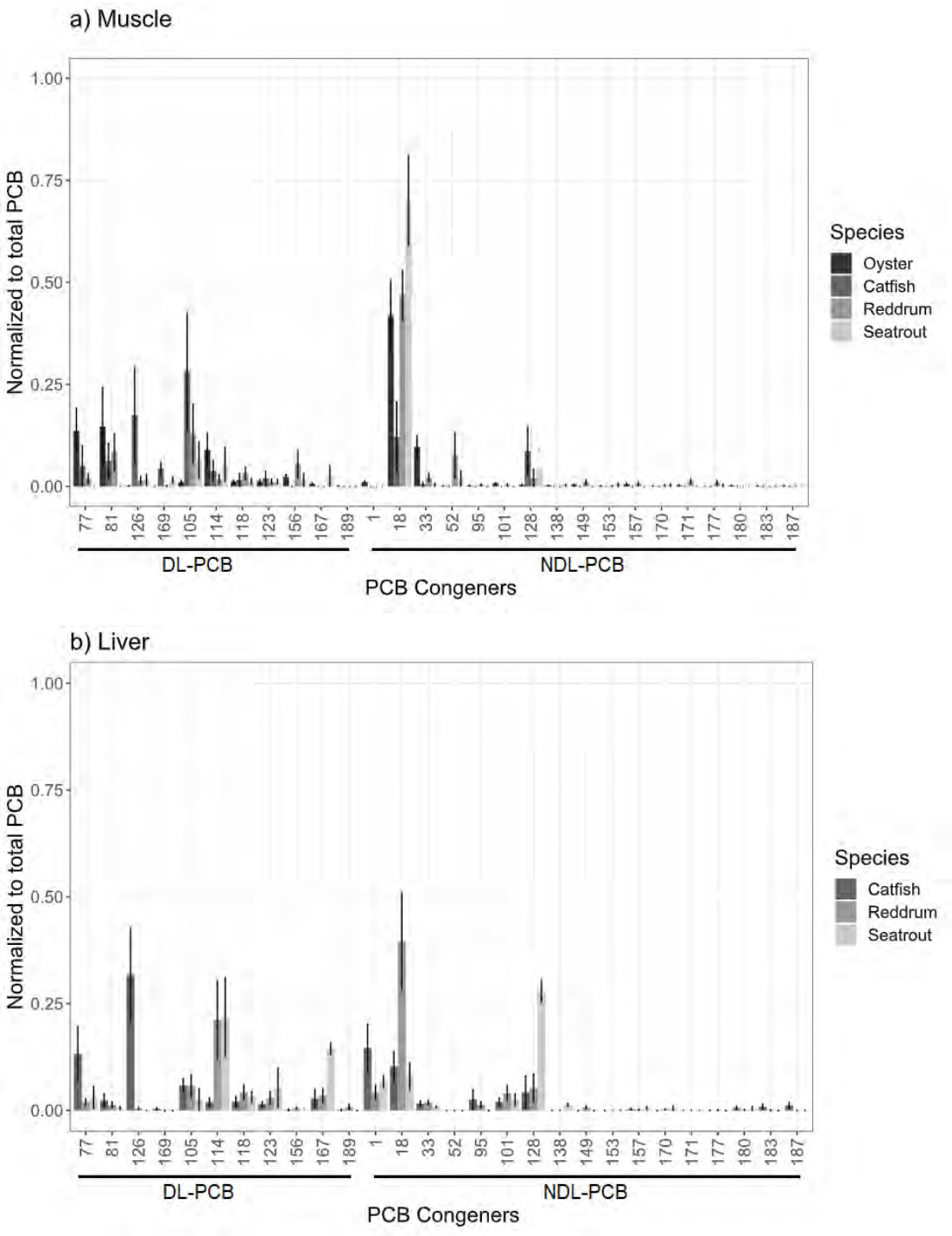

Figure 2. Normalized PCBs congener profiles in the **a)** gill/mantle of oysters and muscle from fish; and **b)** in the livers from fish collected from Matagorda Bay. All the mean values are normalized to total PCB to show relative abundance.

Texas A&M University at Galveston
1001 Texas Clipper Road
Galveston, TX 77554

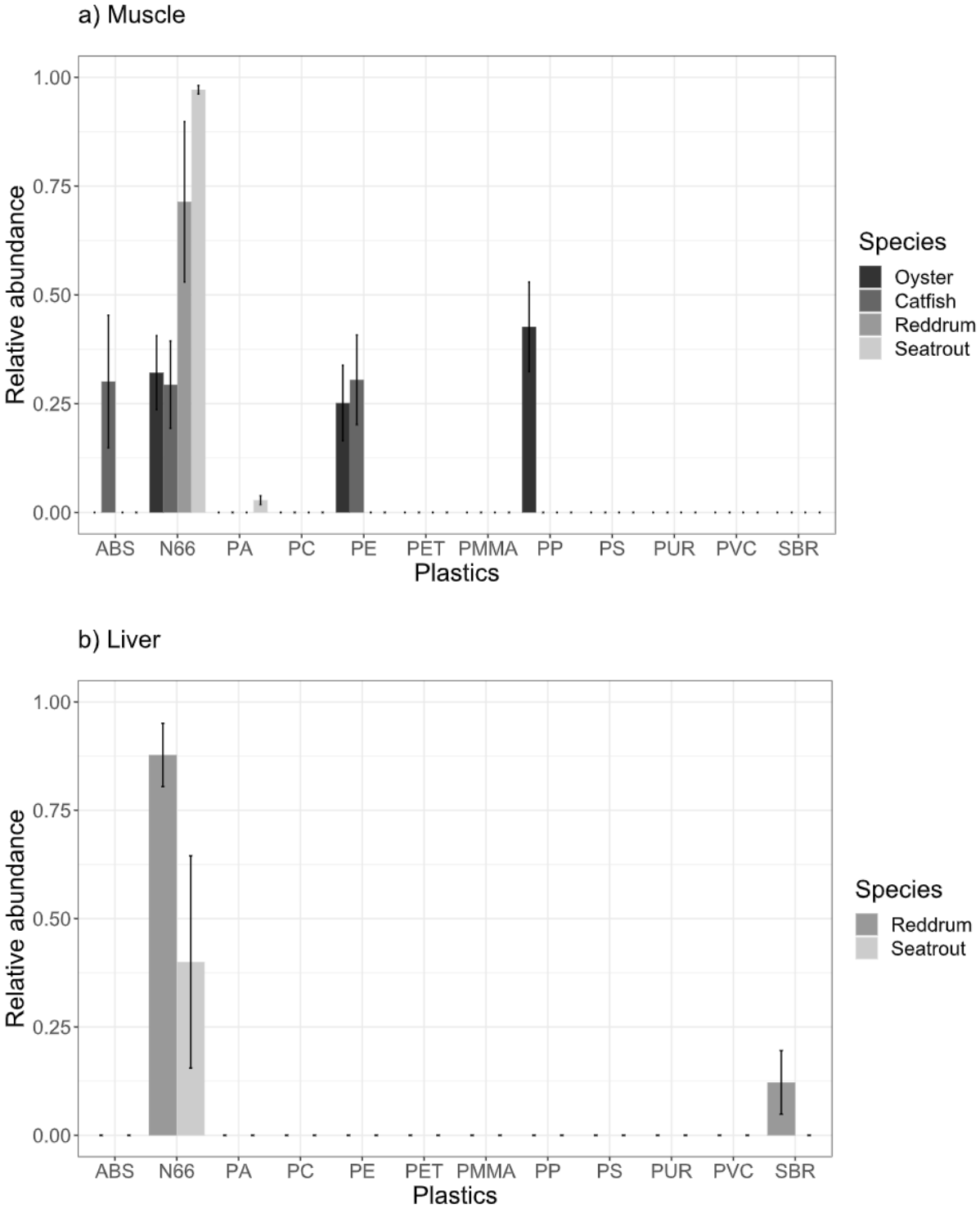

Figure 3. Normalized NMP levels in **a)** oyster gill/mantle and fish muscle; and **b)** fish liver. All concentrations are normalized to total to show relative abundance.

Texas A&M University at Galveston
1001 Texas Clipper Road
Galveston, TX 77554

3.3. Source and Toxicity assessments

3.3.1. Source assessment of PAHs: The source ratio analysis for muscle tissues showed 55% of the ratios to indicate petrogenic sources for the PAHs, 29% indicated petrogenic combustion sources, and 16% indicated pyrogenic sources (**Figure 4**). Similarly, analysis of the livers showed 72% of ratios to indicate petrogenic sources, 7% from petrogenic combustion, and 21% were pyrogenic sources. Overall, the analysis of both tissues (muscle and liver) indicated the predominance of mainly LMW petrogenic PAHs (**Figure 4**).

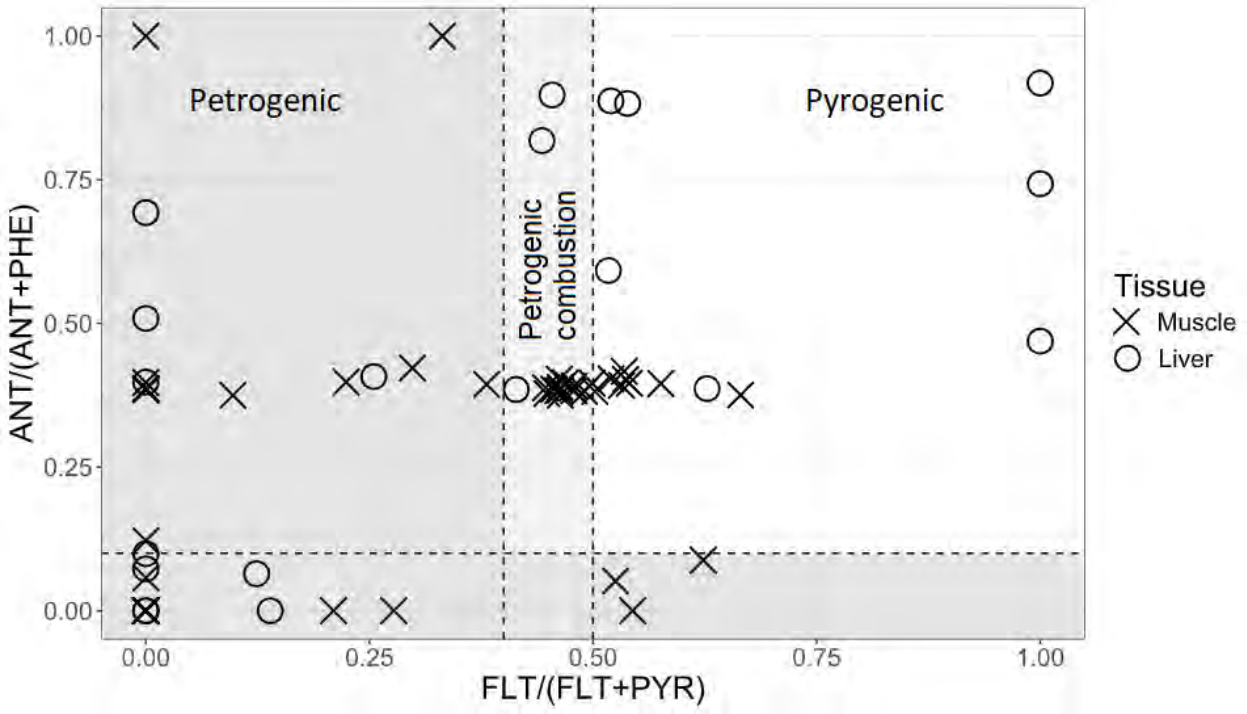

Figure 4. Source ratios analysis of PAHs in muscle (X) and liver (O) using ratios of HMW to LMW PAHs. ANT = anthracene, PHE= phenanthrene, FLT = fluoranthene, PYR = pyrene. The darker gray zones represent petrogenic dominant sources, the white zone represents pyrogenic dominant source, and the overlapping light gray zone represents petroleum combustion as a source of PAHs.

Texas A&M University at Galveston
1001 Texas Clipper Road
Galveston, TX 77554

3.3.2. Cancer risk Assessment of PAHs: The biota BaPE concentrations were significantly lower than the FDA Level of concern (LOC) for finfish (0.035 µg g^{-1} BaPE) and oysters (0.142 µg g^{-1} BaPE). For finfish, the BaPE was 19 - 93x lower for seatrout (0.0018 µg g^{-1} BaPE) and catfish (0.00038 µg g^{-1} BaPE) respectively. Whereas for oysters, the BaPE was 48x lower than the FDA LOC for oysters of 0.142 µg g^{-1} BaPE (**Figure 5**).

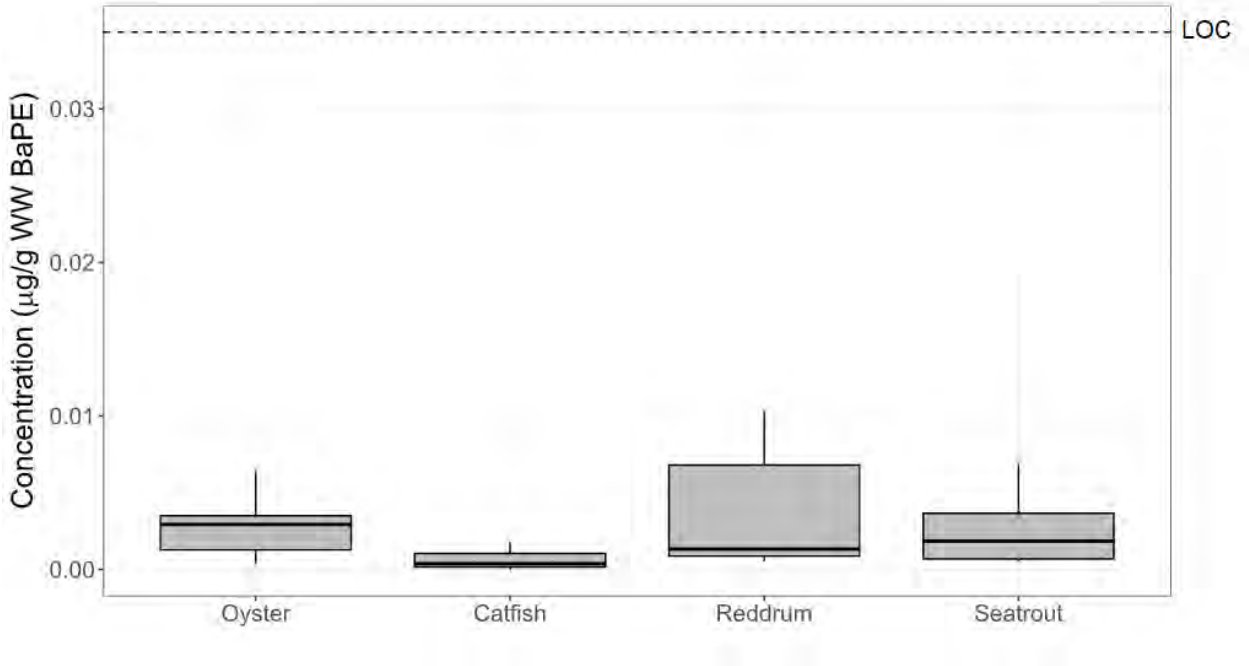

Figure 5. Cancer risk Level of Concern (LOC) set by the FDA for finfish (0.035 µg g^{-1} BaPE) is shown as a horizontal dotted line and is compared to the Benzo[a]pyrene equivalent toxicity (BaPE) concentrations of finfish and oysters collected from Matagorda Bay. The FDA LOC level for oysters (0.142 µg g^{-1} BaPE) is not shown on the graph.

Texas A&M University at Galveston
1001 Texas Clipper Road
Galveston, TX 77554

3.3.3. TEQ assessment of DL-PCBs: The TEQ analysis of fish livers indicated the median concentration in catfish to be near equivalent (1.1x) to the upper limit for adverse effects for finfish as determined by Steevens et al. (2005) (**Figure 6**). The catfish TEQs were also within range of the upper limit set for immunosuppression effects in marine mammals (Kannan et al., 2000). The TEQs for red drum were within the range of the upper and lower limits for adverse effects on finfish (Steevens et al., 2005). In contrast, seatrout TEQs were 1.4x lower than the lower limit for adverse effects for finfish (Kannan et al., 2000) (**Figure 6**).

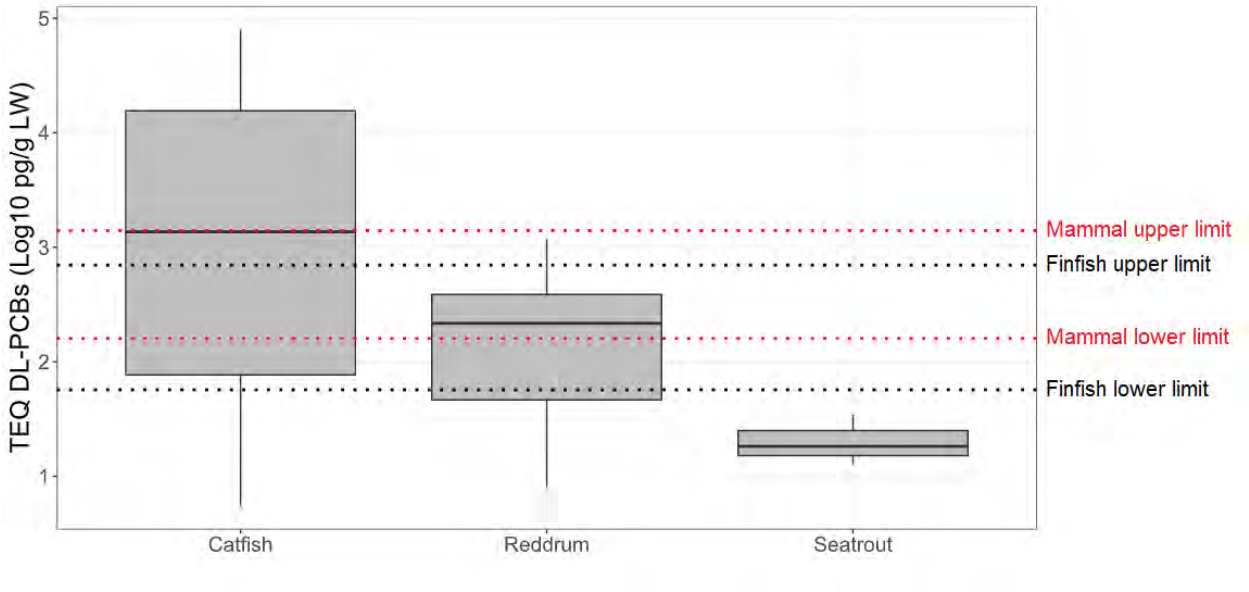

Figure 6. TEQ assessment for DL-PCBs in fish livers displayed with the upper and lower limit of adverse effects for finfish (black dotted lines) and aquatic mammals (red dotted lines) reported in Log_{10} transformed pg g^{-1} lipid weight (or pg g^{-1} LW TEQ).

3.3.4. Average yearly intake of NMPs through seafood consumption: Based on the sum of total NMPs quantified in fish muscle and in the gill/mantle tissue of oysters (**Table 2(c)**), the average

Texas A&M University at Galveston
1001 Texas Clipper Road
Galveston, TX 77554

adult yearly intake was estimated for the biota (**Table 4**). Oysters exhibited the highest ADI values which were 3x higher than catfish, 5x higher than seatrout, and 14x higher than the red drum (**Table 4**).

Table 4. The estimated Average daily intake (ADI) of NMPs in an adult human represented as mg NMPs Kg^{-1} of body weight day^{-1}. The ADI data is shown per species with the minimum (min) and maximum (max) daily intakes also shown. Each ADI value was also converted to a yearly intake to assess the likely annual exposure of a person to NMPs.

	ADI (min - max) (**mg NMPs Kg^{-1} body weight day^{-1}**)	**Yearly Intake (min - max)** (**mg NMPs Kg^{-1} body weight $year^{-1}$**)
Oysters	0.46 (0 - 1.47)	167.62 (1.72 – 536.70)
Catfish	0.15 (0 - 0.69)	55.63 (0 – 253.67)
Red drum	0.03 (0 - 0.13)	12.08 (0 – 46.95)
Seatrout	0.09 (0.02 - 0.18)	32.85 (7.80 – 65.74)

4. Discussion

4.1. Morphometric parameters

Amongst the fish species sampled, only gafftopsail catfish were within the adult size range, whereas red drum and spotted sea trout were categorized as juveniles. For example, in the wild adult gafftopsail catfish typically measure between 30 - 40 cm in length and between weigh 450 - 910 g (TPWD, 2024). In our study, the gafftopsail catfish sampled from Matagorda Bay weighed 415.80 ± 73.92 g and exhibited a total length of 35.2 ± 2.48 cm, therefore placing them within

Texas A&M University at Galveston
1001 Texas Clipper Road
Galveston, TX 77554

range of adult catfish. Adult red drum in the wild can range from 28 - 33 inches (71 - 84 cm) and weigh between 3.4 - 4 Kg (Wenner, 1996). However, the red drum sampled from Matagorda Bay weighed 620.71 ± 138.90 g and had a total length of 37 ± 3.17 cm, indicating a juvenile size range. In turn adult spotted seatrout can average ≥48 cm in total length and weigh ≥1 Kg (TPWD, 2023). In our study, the spotted seatrout sampled from Matagorda Bay had an average weight of 297.78 ± 53.53 g and total length of 33.46 ± 2.24 cm, also placing them within a juvenile age class. Finally, mature eastern oysters typically weigh between 20 - 70 g (Grizzle et al., 2017). The eastern oysters sampled from Matagorda Bay exhibited an average weight of 41.60 ± 6.52 g, placing them within range of fully grown and adult oysters (**Table 1**).

4.2. PAH body-burdens, sources, and toxicity risk assessment

4.2.1. PAH body-burdens: Eastern oysters exhibited the highest concentration of PAHs (**Table 2 (a)**), with levels 2x higher than those found in catfish, and 1.2x those in seatrout and red drum (although not statistically significant). The elevated PAH levels in shellfish vs. fish reported in our study are overall consistent with observations from other aquatic ecosystems. For example, Rowe et al., (2020) measured sum of total PAH levels in shellfish (eastern oysters) and finfish (spotted seatrout) from a neighboring bay system, the Galveston Bay. Oysters were reported to exhibit sum of total PAHs levels 14x (203 ± 68 ng g^{-1} WW, mean ± standard error) higher than those reported in finfish (14.35 ± 7.88 ng g^{-1} WW) sampled from the bay (Rowe et al., 2020). Such a trend is also evident in other aquatic ecosystems, for example, Olayinka et al., (2019) reported pink shrimp and blue marine crabs to have 2x higher (50.65 ± 21.88 and 60.30 ± 15.66 mg Kg^{-1}) sum of total PAH levels relative to that in fish (spadefish: 33.97 ± 9.19 mg Kg^{-1}, grunter: 35.02 ± 12.20 mg Kg^{-1}) sampled ftom Atlast Cove, Nigeria (Olayinka et al., 2019).

Texas A&M University at Galveston
1001 Texas Clipper Road
Galveston, TX 77554

Kanhai et al., (2015) report sum of total PAH levels in Mangrove oysters (*Crassostrea rhizophorae*) to be 10x higher (109 ± 18.4 to 362 ± 63.0 ng g^{-1} DW) than those measured in sea catfish (*Cathorops spixii*) (7.5 ± 0.9 to 43.5 ± 25.5 ng g^{-1} DW) sampled from Caroni Swamp, Trinidad, West Indies (Kanhai et al., 2015). Finally, a comprehensive review by Honda and Suzuki (2020) comparing PAH body-burdens in shellfish and fish from various aquatic ecosystems also reported overall higher concentrations in invertebrates vs. vertebrates (fish), with sum of total PAHs concentration in invertebrates ranging from 8.7 – 7000 ng g^{-1} WW (median concentration of 475 ng g^{-1} WW in Zebra mussels and amphipods), and in fish ranging from 1.52 - 1064 ng g^{-1} WW (median concentration of 120 ng g^{-1} WW in crayfish) (Honda and Suzuki, 2020).

The higher body burden of pollutants in eastern oysters reported in our study is a likely reflection of their filter feeding capacity, overall lipophilicity of PAHs, and lower metabolic biotransformation capacity of invertebrates (relative to finfish) to metabolize and excrete PAHs. Which can all contribute to a higher bioaccumulation of PAHs in oysters. Oysters exhibit a massive capacity to filter ~25 - 50 gallons of sea water per day (Ehrich and Harris, 2015; NOAA, 2020), which can increase their exposure to various contaminants including PAHs (Fisher et al., 2000; Bustamante et al., 2012; Trevisan et al., 2017; Wang et al., 2020). Invertebrates tend to have a lower biotransformation capacity for pollutants in comparison to fish, and therefore are less efficient at metabolizing and depurating contaminants (Neff et al., 1976; Vidal-Liñán et al., 2016; Honda and Suzuki, 2020). The species-specific accumulation (from difference in diet, habitat, ability to expel pollutants) of various PAH congeners has been noted by Neff et al. (1976), where the uptake and depuration of various oil derived PAHs (NAP, FLU, PHE etc.),

Texas A&M University at Galveston
1001 Texas Clipper Road
Galveston, TX 77554

across mollusk, shrimps and fish was studied. The authors reported that shrimp (*Penaeus aztecus)* and fish (*Fundulus similis)* were quick to accumulate as well as depurate PAHs, while oysters (*Crassostrea virginica)* and clams (*Rangia cuneata*) were slow to depurate, which resulted in higher body burdens in oysters and clams vs. shrimp and fish (Neff et al., 1976).

In contrast to the muscle tissue in fish, their livers exhibited sum of total PAH levels that were 5x to 14x higher (**Table 3(a)**). This is likely due to the lipophilic nature of PAHs (Sverdrup et al., 2002) and the higher lipid content in fish livers in comparison to muscle (Ando et al., 1993; Arrington et al., 2006). For example, in our study the gravimetrically determined lipid weight in livers was 4x higher than in muscle for catfish, 11x higher for seatrout, and 12x higher for red drum (data not shown). PAHs are hydrophobic (Log K_{ow} = 3.37 - 6.75) and highly lipophilic (Choi et al., 2010), therefore contributing to their accumulation in the liver tissue. The propensity of PAHs to preferentially accumulate in lipid rich tissues has also been shown in other studies. For example, Xu et al. (2011) showed a significant positive correlation between tissue lipid content and PAH bioaccumulation, i.e., the brain exhibited greater PAH bioaccumulation vs. muscle (Xu et al., 2011). Similar to our study, Jafarabadi et al., (2019) showed ~1.4x higher PAH bioaccumulation in the livers vs. muscle of fish collected from the Persian Gulf (such as red snapper, bream, and mackerel) (Jafarabadi et al., 2019). And a study from Poyang lake (China) also showed ~1.4x higher PAH levels in the liver vs. muscle of carp (Zhao et al., 2014).

4.2.2. PAH congener profiles, sources, and toxicity: In our study, LMW PAHs predominated with ACE and FLU being the most prominent in the livers of all fish species, and accounting for 25-75% of sum total congeners (**Figure 1(b)**). ACE and FLU both comprise three aromatic rings, and

Texas A&M University at Galveston
1001 Texas Clipper Road
Galveston, TX 77554

have similar Log K_{ow} values (ACE: 3.92 and FLU: 4.18) (Jesus et al., 2022). Previously, Abayi et al. (2021) demostrated the prevalence of LMW PAHs (ACE, FLU, and NAP) in sediments and fish collected from the White Nile river in East Africa. LMW PAHs were reported to contribute up to 98% of total PAHs (Abayi et al., 2021). Xu et al., (2011) also report LMW PAHs to comprise 90% of total PAHs content in fish collected from lake Bai-Yang-Dian, Northern China (Xu et al., 2011). Fish collected from the Persian gulf were also reported to contain ~3x higher LMW PAHs vs. HMW PAHs (Jafarabadi et al., 2019).

The prevalence of LMW PAHs reflects the prominence of oil-derived hydrocarbons (i.e., petrogenic) sources. For example, LMW PAHs primarily originate from petrogenic sources such as crude oil spills, petroleum products, and from the natural seepage of petroleum (Patel et al., 2020). While HMW PAHs are often products of pyrolytic sources, such as from the combustion of petroleum, wood, coal etc. (Budzinski et al., 1997; Wolska et al., 2012; Montuori et al., 2022). PAH ratios have been extensively used to diagnose sources of PAHs (Blumer, 1976; Simoneit, 1985; Lipiatou and Saliot, 1991; Yunker et al., 1996; Budzinski et al., 1997; Yunker et al., 1999). Two key diagnostic ratios used to ascertain PAH sources included: FLT/(FLT+PYR) and ANT/(ANT+PHE) ratios. Where FLT/(FLT+PYR) ratios above 0.4 and ANT/(ANT+PHE) ratios above 0.1 indicate combustion (pyrogenic) processes. As high-temperature combustion conditions favor the increase in proportion of FLT and ANT relative to PYR and PHE (Yunker et al., 1995; Budzinski et al., 1997).

The source ratio graph in **Figure 4** indicates that in both muscle and liver samples, a majority of PAHs are from petroleum or petrogenic sources (55% for muscle, 72% for liver), with a smaller

Texas A&M University at Galveston
1001 Texas Clipper Road
Galveston, TX 77554

proportion from combustion or pyrogenic sources (16% for muscle, 21% for liver). The remainder percent comprises incomplete combustion of petroleum products. The prominent ratios likely reflects the overall increased incidences of oil spills along the GoM (HARC, 2014; Rice, 2019; Trevizo, 2019; Rowe et al., 2021). The Calhoun Port Authority in Matagorda Bay received over 11.8 million tons of cargo in 2015, with its primary shipments consisting of petrochemicals, crude oil, condensate, and aluminum-related materials (bauxite and alumina) (TDT, 2020). The sources of petroleum derived PAHs in Matagorda Bay have been previously attributed to shipping activity in the area (Lloyd et al., 2024). In 2014, a cargo shipped collied with an oil tanker in Galveston Bay, near Texas city, which led to the spillage of 168,000 gallons of fuel oil into lower Galveston Bay (DARRP, 2014), which then dispersed along shorelines of Galveston and Matagorda Bays (Tresaugue, 2014). Furthermore, shelf sediments along Matagorda Bay appear to be dominated by petrogenic LMW PAHs, such as NAP and ACE (Wang et al., 2014).

4.2.3. PAH cancer risk of consumption: A cancer risk assessment was performed to determine whether seafood consumption could cause sufficient exposure to carcinogenic PAHs, such as BaP and BaPE (Collins et al., 1991; Lee and Shim, 2007; FDA, 2010; EPA, 2017; ATSDR, 2022). The BaP and BaPE levels were below the minimum threshold for concern as established by the FDA after the Deepwater Horizon (DH) oil spill (FDA, 2010) (**Figure 5**). Although widely adopted, a criticism of the FDA LOC approach is that it significantly underestimate risks to sensitive populations, including pregnant women, and children, by failing to account for increased vulnerability, appropriate consumption rates, relevant health endpoints, and health-protective exposure durations (Rotkin-Ellman et al., 2012).

Texas A&M University at Galveston
1001 Texas Clipper Road
Galveston, TX 77554

4.3. PCB body-burdens and toxicity

4.3.1. PCB body-burdens: Similar to the trend observed for PAHs, our study also showed eastern oysters to exhibit significantly higher levels of total PCBs compared to the muscle tissue of fish. Specifically, PCB levels in oysters were 11x higher than in catfish (statistically significant), 6x higher than redrum (not significant) and 2.5x higher than seatrout (not significant) (**Table 2(b)**). Such a trend is also evident in other aquatic ecosystems. For example, in Todos os Santos Bay (Brazil), oysters exhibited ~10x higher PCB concentrations (<0.08 - 50 ng g DW^{-1}) vs. the fish sampled from the bay (0.23 to 4.55 ng g^{-1} DW) (Santos et al., 2020). Similarly, fish (*Plastycephalus bassensis)* and oysters *(Crassostrea gigas)* sampled from Tasmanian estuarine and coastal waters revealed oysters to exhibit 5x higher total PCBs levels than the fish. Similar to PAHs, the higher body-burdens of PCBs in oysters is likely a reflection of their filter feeding capacity (Ehrich and Harris, 2015; NOAA, 2020), overall higher lipophilicity of PCBs (Safe and Hutzinger, 1984; Bourez et al., 2013), and lower metabolic biotransformation capacity of invertebrates (relative to finfish) to metabolize and excrete PCBs (Bright et al., 1995; Vidal-Liñán et al., 2016).

In contrast to muscle tissue, the livers of fish exhibited 11-15x higher PCB levels (**Table 3(b)**). The higher levels in livers reflect the lipophilic nature of PCBs (Safe and Hutzinger, 1984; Bourez et al., 2013) and the higher lipid content of the livers vs. muscle (as previously discussed for PAHs) (Ando et al., 1993; Arrington et al., 2006). PCBs are highly lipophilic (Log K_{ow}= 4.43 – 5.02) (Ballschmiter et al., 2005). Bodin et al., (2014) have shown hepatic PCB levels to be 10x higher than the muscle tissue of fish sampled from the Gironde estuary in southwest France (Bodin et al., 2014). Monosson et al. (2003) collected muscle, liver and gonad tissue from

Texas A&M University at Galveston
1001 Texas Clipper Road
Galveston, TX 77554

mummichog fish (*Fundulus heteroclitus*) from Hudson river and Newark bay and found total PCB levels in the gonads and livers (1265 - 3453 ng g^{-1} WW total PCBs) to be ~6-13x higher than levels measured in muscle tissue (209 - 263 ng g^{-1} WW). They attributed the tissue specific differences to be due to the high lipophilicty of PCBs and higher lipid content of livers (Monosson et al., 2003). Similarly, the analysis of fish muscle, liver, kindey and brain from a heavily polluted water resevoir in Slovakia (Zemplinska sirava) found total PCB concentrations in the liver to be 2x higher than in muscle, and 15x higher than in the brain and kidneys (Brázová et al., 2012). Morever, PCBs measured in the muscle, and liver of Red mullet, mackerel, anchovy and blue whiting along the Catalan coast of the Mediterraininian sea, reported livers to exhibit 10x higher concentrations of total PCBs than muscle (Albaiges et al., 1987).

4.3.2. PCB congener profiles: PCBs are exclusively of anthropogenic origin and were widely used in heat absorbing or electrical/insulating materials such as electrical equipment, capacitors, and transformers (Delzell et al., 1994). Despite their ban in the 1970's, they continue to persist in the environment due to their resistance to biodegradation (Boyle and Highland, 1979). The high chlorination of PCBs results in chemical and structural properties that collectively reduce the susceptibility of PCBs to chemical, biological, and photolytic degradation pathways, thus increasing their environmental persistence, which explains their prevalence and designation as a persistent pollutant (Delzell et al., 1994; Elangovan et al., 2019; Xiang et al., 2020).

In our study, in the muscle tissue of fish (or gill/mantle for oysters), 44% of sum of total PCBs in oysters, 85% in catfish, 28% in redrum, 33% in seatrout were attributed to DL-PCBs (the rest were NDL-PCBs) (**Table 2(b)**). Similarly for the livers from fish, the DL-PCBs were widely

Texas A&M University at Galveston
1001 Texas Clipper Road
Galveston, TX 77554

detected with 67% of sum of total PCBs in catfish, 26% in redrum, and 51% in seatrout attributed to DL-PCBs (**Table 2(b)**). DL- PCBs are those with chlorine atoms at the *para* position (opposite sides of the benzene ring) and two or more at the *meta* positions (adjacent but not next to on the benzene ring) (Safe et al., 1985; ATSDR, 2023). Chlorine atom substitutions in these position results in a coplanar structure similar to that of 2,3,7,8-TCDD (2,3,7,8-tetrachlorodibenzodioxin), and thus exhibit its high toxicity (Safe et al., 1985). These include non-ortho dioxin like PCBs such as, 3,4,4',5-tetra- (PCB 81), 3,3',4,4'-tetra- (PCB 77), 3,3',4,4',5-penta- (PCB 126), and 3,3',4,4',5,5'-hexachlorobiphenyl (PCB 169) and mono-ortho dioxin-like PCBs such as PCBs 105, 114, 118, 123, 156, 167 and 189 (Giesy and Kannan, 1998). In oysters, PCB 77 dominated constituting 49% of total DL-PCBs (**Table 2(b)**). For the fish, catfish showed a similar prominence of PCB 126 in both muscle and liver tissue, at ~60% of total DL-PCBs (**Table 2(b)** and **3(b)**). The livers of red drum and seatrout showed a prominence of PCB 114 in each species (36% and 49% respectively) (**Table 3(b)**). Whereas PCB 156 dominated in red drum muscle (26% of total DL-PCBs) and PCB 105 dominated in seatrout muscle (35% of total DL-PCBs) (**Table 2(b)**).

The prominence of DL-PCBs is typical of industrialized aquatic ecosystems. For example, Carro et al. (2018) report in DL-PCBs in bivalve mollusks collected from estuaries along Galician Rias in Northwestern Spain to comprise 72% of the total PCBs. Among the DL-PCB congeners, 93% were contributed by PCB 126 (Carro et al., 2018). In another study, DL-PCBs were also detected at higher concentrations than NDL-PCBs in commercially available finfish and shellfish, accounting for up to 96% of the PCBs in tuna and 90% in oysters (Gómara et al., 2005). Gómara et al., (2005), also reported PCB 126 to be the most prominent congener in finfish and shellfish. A

Texas A&M University at Galveston
1001 Texas Clipper Road
Galveston, TX 77554

study from coastal Korea (Busan, Incheon, Pohang, Ulsan) focusing on the PCB content of fish and bivalves found that up to 60% of the dietary intake of PCBs to the Korean population from seafood was from DL-PCBs, and of which PCB-126 was also the most prominent congener (Moon and Ok, 2006).

Amongst the NDL-PCBs in the muscle tissue of fish (or gill/mantle for oysters), we find PCB 18 to be the most commonly (and prominently) detected PCB congener, ranging from 60% to 76% of the total NDL-PCBs (**Table 3(b)**). For the NDL-PCBs in the livers of fish, we also find PCB 1 to dominate in catfish (31% of the total NDL-PCBs), PCB 18 was the most abundant in red drum livers (83% of total), and PCB 128 dominated in seatrout livers (57% of total). The varying ratios of NDL-PCBs may reflect varying extents of microbial anaerobic degradation of highly chlorinated PCBs, resulting in the removal of chlorines from the *meta* and *para* positions. This results in an increase in lower chlorinated *ortho*-substituted PCB congeners such as PCBs 18, 52, and 128 (Tiedje et al., 1993; Abramowicz, 1995). Therefore, the prevalence of PCB 18 and PCB 128 in biota may reflect biodegradation of dioxin like PCBs via anaerobic bacteria. The analysis of PCB congeners in the muscle and liver tissues of sharks sampled from Galveston Bay (TX, USA) have reported PCB 128 body-burdens to range from 4 – 28% (Cullen et al., 2019). And Hernout et al., (2020) has shown a prevalence of PCB 18 in the livers of fish (~20 - 65%) sampled from Sabine Lake (TX, USA) (Hernout et al., 2020). Finally, Finklea et al. (2000) analyzed PCBs in the blubber of stranded bottlenose dolphins from Matagorda Bay (TX, USA). Their analysis revealed the prevalence of PCB 128 ($\leq$1400 ng g^{-1} LW). All these studies demonstrate the prevalence of select PCB congeners in biota sampled along the Gulf of Mexico.

Texas A&M University at Galveston
1001 Texas Clipper Road
Galveston, TX 77554

4.3.3. TEQ assessment of DL-PCBs: The Toxicity equivalent (TEQ) analysis showed red drum to be within the range of the upper and lower limits for adverse effects in finfish, suggesting a propensity of the DL-PCBs body-burdens to cause adverse effects (**Figure 6**). For the seatrout, the TEQ was 1.4x lower than the low limit for adverse effects in finfish, indicating a significantly lower risk of adverse effects (i.e., protective of ≥99% of fish). And for catfish, the TEQ levels were 1.11x higher than the upper limit for adverse effects set for finfish, indicating a potential health risk (such as immunosuppression effects) (i.e., ≥10% may show adverse effects) (Kannan et al., 2000). The high TEQ values in catfish are likely representative of the high PCB 126 body-burdens in livers (65% of total DL-PCBs) (**Table 3(b)**). Not all the congeners in the TEQ calculation have equal TEF values due to their relative toxicity and therefore are "weighed" differently. Of the DL-PCBs, PCB 126 exhibits the highest TEF value at 10 – 1000x higher than the others, therefore contributing to the high TEQ values observed in catfish. A caveat is that TEF standards for DL-PCBs are derived from studies on early life stage fish with mortality as an endpoint (Vandermeulen, 1987). Therefore, the derived TEQ values may not be directly applicable towards explaining sub-lethal toxicity effects in older finfish (as is this case in our study).

4.4. NMP body-burdens and average human daily intake risk assessment

4.4.1. NMP body-burdens: Eastern oysters exhibited significantly higher body-burdens of NMPs vs. fish (**Table 2(c)**). Specifically, the NMP levels in oysters were 5x higher than in catfish, 9x higher than in seatrout, and 25x higher than in red drum (**Table 2(c)**). The higher body burden of NMPs in oysters is likely a direct reflection of their filter feeding capacity (Ehrich and Harris, 2015; NOAA, 2020). For example, in Sanggou Bay, China, Pacific oysters exhibited 4x higher

Texas A&M University at Galveston
1001 Texas Clipper Road
Galveston, TX 77554

concentrations of NMPs than those detected in greenling and sea squirt fish (Sui et al., 2024). In fish livers, the concentration of NMPs was 51x higher in redrum and 7x higher in seatrout in comparison to levels in muscle tissue of each species respectively (**Table 2(c)** and **Table 3(c)**). These differences in NMPs body-burdens between liver (i.e., higher levels) vs. muscle may be due to the liver's rich blood supply and its primary role in filtering (and detoxifying) exogenous substances from the blood (Wisse et al., 1985; Wood, 2014; Zhao et al., 2014; Ozougwu, 2017). As a result, causing a higher exposure and bioaccumulation of NMPs in the liver. A toxicological study exposing European seabass (*Dicentrarchus labrax*) to NMPs (≤3 μm particle size) for ≤5 days showed approximately 4x and 3x higher microplastics accumulation in the liver vs. the gut and gills respectively (Zitouni et al., 2021). Similarly, goldfish exposed to NMPs (for 30 days) and exhibited a ~14x higher bioaccumulation in the liver vs. muscle tissue (Brandts et al., 2022). Additionally, various fish species sampled from the Pearl river in China (such as carp, bream, catfish, tilapia) were found to contain ~2x higher levels of plastics additives in their livers vs. muscle (Peng et al., 2021).

PP was the most prominently detected NMP in the gill/mantle tissues oysters, at 60% of total NMPs (**Table 2(c)**). In fish muscle, N66 was the most prominent NMP detected in red drum (100% of total NMPs) and seatrout (97%) (**Table 2(c)**). Similarly, in the livers of red drum and seatrout, N66 accounted for 89% and 100% of the total NMPs quantified (**Table 3(c)**). Overall, the most prominently detected NMPs in the biota were PP > N66 > SBR > PE. PP is commonly used in packaging materials like bottles and containers, automotive parts such as bumpers and battery cases, textiles for items like diapers and filters, and household goods including reusable containers and furniture (Guidetti et al., 1996; Maddah, 2016; Hossain et al., 2024). Whereas N66

Texas A&M University at Galveston
1001 Texas Clipper Road
Galveston, TX 77554

is primarily used in textiles and fabrics, including carpets, clothing, and upholstery, due to its durability and resistance to wear and tear. It is also used in engineering plastics for automotive and industrial components like gears, bushings, and bearings, as well as in consumer goods like ropes, cords, fishing gear, nets and toothbrush bristles (Stafford et al., 1986; Zhang et al., 2010; Shakiba et al., 2021). SBR is a tire-derived NMP which accumulates on road surfaces through vehicular activity and is a major source of microplastics pollution into the environment (Hägg et al., 2023). Therefore, the overall abundance of these plastics in industrial and consumer products is likely to explain their prevalence in the biota. Finally, the prominence of PE highlights the presence of general plastics degradation products, including those from plastic pellets such as nurdles (OSPAR, 2018).

The prevalence of PP and PE in aquatic biota has been previously reported by Ribeiro et al. (2020). The authors measured the presence of plastics in various shellfish and fish from Australia and detected PE to be the most prevalently detected plastic in the biota ($\leq$2,400 μg g^{-1} tissue), and PP detected at $\leq$60 μg g^{-1} tissue (Ribeiro et al., 2020). A meta-analysis on the extent of microplastics ingested by fish worldwide conducted by Lim et al. (2022), found that majority ingested were fibrous microplastics (70%), of which 16% were PE (Lim et al., 2022).

Finally, PP and PE, which were commonly detected in the biota from Matagorda Bay, were also some of the most widely produced plastics by the Formosa Plastics Corporation chemical plant located in Point Comfort, along Matagorda Bay (Detore, 2018; Hays, 2019). The Formosa Plastics Corporation (headquartered in Taiwan) is a major producer of plastic resins and petrochemicals, including PP, PE, and PVC. Their Point Comfort facility is significant for their

Texas A&M University at Galveston
1001 Texas Clipper Road
Galveston, TX 77554

operations in the United States (Conkle, 2018). In 2016, a substantial spill of plastic pellets and powder from this facility contaminated Matagorda Bay, leading to a lawsuit by environmental activist Ms. Diane Wilson (Wilson, 2018). In 2019, Formosa was found liable for illegal discharges, resulting in a $50 million settlement for environmental cleanup (Conkle, 2018; Wilson, 2018). Additionally, Formosa Plastics has been involved in other serious incidents. In 2005, an explosion at their Illinois plant producing PVC caused five fatalities (OSHA, 2005). In 2013, a fire at the Point Comfort facility resulted in injuries and environmental harm (CSB, 2006). The company has also faced scrutiny for air pollution violations, leading to fines and mandated corrective actions (EPA, 2012).

4.4.2. Average Daily Intake (ADI) of NMPs: The ADIs calculated for likely human exposures to microplastics through seafood consumption simply maps the NMPs body-burdens to an estimated daily intake of seafood (DSHS, 2011). As a result, the estimated ADIs for the NMPs varies from 0.03 – 0.46 mg NMPs Kg^{-1} body weight day^{-1} for the consumption of red drum to oysters (**Table 4**). Converted to an estimated annual exposure, we estimated an average level of ≤167.62 mg NMPs Kg^{-1} body weight $year^{-1}$ (**Table 4**). The levels computed in this manuscript are relatively modest as compared to another study that estimated plastics ingestion rates by humans of ≤5 grams of microplastics/week (or ≤260 grams of microplastics $year^{-1}$) (Senathirajah et al., 2021). We are however within range of a study by Ribeiro et al. (2021), who deployed oysters (*Saccostrea glomerata*) at the mouth of Brisbane River (Australia) for 14 days and quantified a body-burden of ≤38.8 mg g^{-1} microplastics in the oysters and using an analytical method similar to the one in our study, i.e., Py-GCMS. The microplastics accumulated in oysters over 14 days can be approximated to a daily body burden of ≤2.8 mg $gram^{-1}$ oyster (by dividing 38.8 mg g^{-1} by

14). Implementing a similar ADI approach to the one taken in our study yields an average daily intake of 1.2 mg NMPs Kg^{-1} body weight day^{-1}, and annual intake of 434 mg NMPs Kg^{-1} body weight $year^{-1}$. These values are only 3x higher than the ones computed for the oysters sampled from Matagorda Bay in this study (**Table 4**).

A caveat to these estimates is that they appear to far exceed levels detected in the body-burdens of humans. For example, Leslie et al., (2022a) used Py-GCMS to quantify NMPs in human blood and reported total levels of 1.6 µg mL^{-1}. While NMPs measurements in blood are not equatable to tissue body-burdens in wildlife biota as measured in our study, nevertheless the levels measured by Leslie et al., (2022a) are ~200x lower than the lowest NMP body burden measured for red drum muscle in our study (i.e., 355.42 $\pm$ 183.75 µg g^{-1} DW, **Table 2(c)**). In another study, the quantification of microplastics in infant and adult human feces reported concentrations ranging from 3 – 36 µg g^{-1} (Zhang et al., 2021). Once again, comparing these levels to the lowest NMP body-burden quantified for red drum muscle yields levels in humans that are ~10x – 100x lower than those measured in fish. The differences in NMPs body-burdens between the aquatic wildlife (as measured in our study) and humans may indicate a trophic dilution of NMPs in an ecosystem. For example, we report that oysters exhibit ~5x – 25x higher body-burdens than fish (i.e., catfish, red drum, and seatrout), whereas fish (red drum) exhibits a ~10x – 200x higher body-burden than humans. Further studies applying the Py-GCMS analytical method to quantify NMPs across food webs which include wildlife biota and humans, will provide a more comprehensive assessment of the fate and distribution of these emerging pollutants in ecosystems.

Texas A&M University at Galveston
1001 Texas Clipper Road
Galveston, TX 77554

Objective 3: Single or Mixtures Toxicity of Persistent or Microplastics Pollutants in Embryo-larval Zebrafish

Texas A&M University at Galveston
1001 Texas Clipper Road
Galveston, TX 77554

1. Introduction

There are increasing concerns for the adverse health effects of microplastics exposure in wildlife and humans (Kannan and Vimalkumar, 2021; Jeong et al., 2024). Research indicates that 60% of marine mammals, 50% of sea birds, and 42% of fish are affected by plastic exposure in the environment, highlighting a widespread issue across various marine species (Ugwu et al., 2021). Marine animals often mistake plastic debris for food, leading to ingestion and potential internal injuries (Sigler, 2014). Sea turtles, seabirds, fish, and marine mammals are particularly vulnerable to this threat. The ingestion of plastic can block digestive tracts, cause malnutrition, and lead to starvation and death (Tong et al., 2023). Additionally, marine animals can become entangled in discarded fishing gear, plastic bags, and other debris, causing physical harm, and hindering their ability to swim and forage (Gregory, 2009).

In **Figure 1** we summarize the effects of plastic pollution across trophic levels with likely detrimental effects indicated. The trophic transfer and retention of plastics are likely to occur in smaller species but may be limited for top predators in some food webs due to the size mismatch between the predators and the prevalent plastic particles in the environment, a process known as trophic dilution (Provencher et al., 2018). Consequently, if biomagnification happens, the patterns might differ from those observed with chemical contaminants in the same ecosystem. The physical properties of plastics could lead to trophic dilution, where lower concentrations are found in top predators (as we report it is likely based on our results shown for ***Objective 2***).

Texas A&M University at Galveston
1001 Texas Clipper Road
Galveston, TX 77554

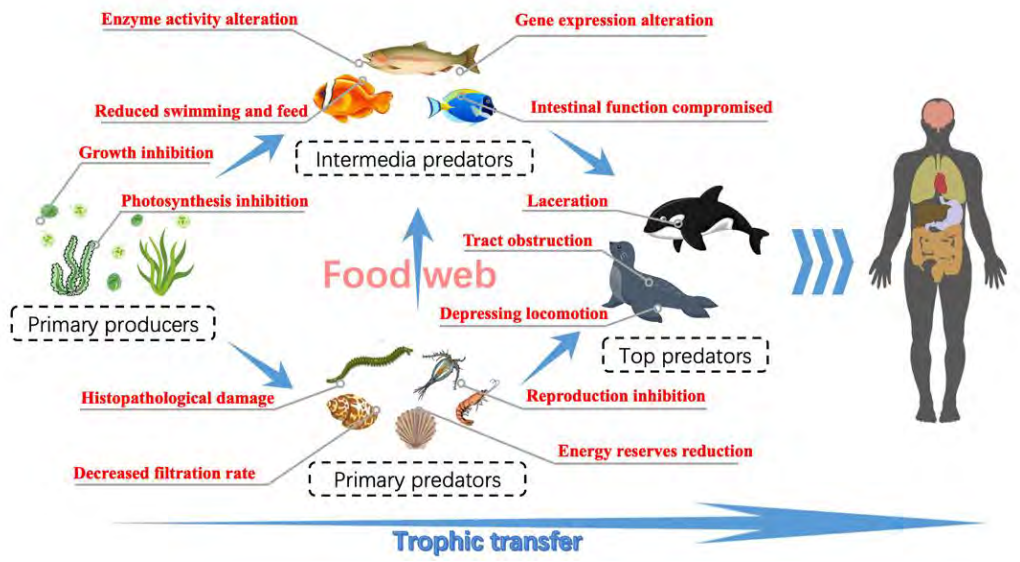

Figure 1. Potential pathways for the bioaccumulation and biomagnification of microplastics across food webs and trophic levels (Tong et al., 2023).

In this objective we tested select single PAHs or PCBs, and their mixtures with a surrogate microplastics particles, polystyrene (PS) latex beads (0.1 µm). The toxicity of these pollutants was tested by using embryo-larval life stages of zebrafish (*Danio rerio*) as a model organism exposed from 2 – 5 days post fertilization or dpf (i.e., exposed for 72 hours). And the effects of exposure were tested on the sub-lethal endpoints of metabolic rate, pollutant biotransformation enzyme activity (ethoxyresorufin-O-deethylase or EROD activity), and cardiac morphology and functions in embryo-larval life stages of zebrafish. Importantly, the levels of PAHs and PCBs tested were environmentally relevant and reflected the most prominent body-burdens detected in the biota of Matagorda Bay. We hypothesized that the mixtures exposure of select PAHs/PCBs with microplastics will increase or enhance the toxicity of the single PAHs or PCBs.

Texas A&M University at Galveston
1001 Texas Clipper Road
Galveston, TX 77554

2. Methods

2.1. Embryo-larval zebrafish (Danio rerio) as a model organism for toxicity assessments

Newly fertilized embryo-larval Zebrafish (*Danio rerio*) were used as a model organism to study the toxicity single or mixtures PAHs, PCBs and/or microplastic particles. Embryo-larval Zebrafish (wild type, strain: AB) were purchased from the Zebrafish International Resource Center (ZIRC) (Eugene, OR), and all animal procedures were conducted according to an approved IACUC protocol. Embryo-larval life stages of Zebrafish (i.e., 48 hours post fertilization) were exposed to various environmentally relevant mixtures of PAHs, PCBs and Polystyrene (PS) particles.

2.2. Toxicity exposures study design

The toxicological study design involved exposing two days post fertilized (dpf) zebrafish (*Danio rerio*) embryos to select pollutants or their mixtures for up to 3 days (72 hours) or up to 5 dpf. Fish were exposed under a semi-static renewal exposure design which involved replacing 50% of the exposure aquaria for each treatment group for each day of the trial. The fish were kept in 28 ± 1 ºC by keeping the beakers in temperature-controlled water baths. Up to 25 embryo/larval fish were exposed to each test chemical. At test termination, n=10 fish/treatment were placed in a multi-well micro-respirometer plate to measure oxygen consumption (or metabolic rate) over a duration of several hours ($\leq$6 hours). Another subset of n=5 fish were observed under a microscope to quantify key morphological features, such as fish size, shape, presence of anomalous features (including cardiac morphology and function). The final sub-set of n=10 fish were placed on a solution containing a chromogenic substrate that changes color to reflect the

Texas A&M University at Galveston
1001 Texas Clipper Road
Galveston, TX 77554

metabolic biotransformation capacity of the fish using the ethoxyresorufin-O-deethylase or EROD activity assay.

The single compound toxicity trials included exposure to select PAHs and PCBs, which were chosen based upon their abundance and detection frequency in the biota sampled from Matagorda Bay. For example, the selection criteria for PAHs and PCBs for single or mixtures toxicity studies involved selecting only those chemicals that represented ≥20% of the sum total body-burdens for ≥20% of the fish species tested. The shortlisted PAHs (and their concentrations) to be tested as single compounds included (summarized in **Table 1**): phenanthrene (0.2 µM), pyrene (0.1 µM), Benzo(a)anthracene (0.6 µM), and indeno[1,2,3-cd]pyrene (0.1 µM). And the shortlisted PCBs (and their concentrations) to be tested as single compounds included: PCBs 18 (0.1 µM), 81 (0.02 µM), 105 (0.04 µM), and 0.02 (µM). We chose polystyrene (PS) latex beads (0.1 µm) as a representative microplastic at a final concentration of 10 µg L^{-1}. Polystyrene was chosen as a commonly used plastic that is abundantly found in fish tissue (Ding et al., 2018; Assas et al., 2020; Wang et al., 2021; Leslie et al., 2022b). The microplastic concentration was based on the findings of Umamaheswari et al. (2021) where 10 µg L^{-1} concentration of aqueous suspension PS (0.1 µm) was found to induce reactive oxygen species (ROS) mediated apoptotic responses in Zebrafish. The particle size (0.1 µm) of PS chosen have been demonstrated to be taken up by zebrafish into the tissue (Umamaheswari et al., 2021). The aqueous suspension of PS plastics coupled with semi static renewal of water ensured that the plastics were dispersed through the aquaria (**Figure 2**).

Texas A&M University at Galveston
1001 Texas Clipper Road
Galveston, TX 77554

Table 1. A list of the chemical compounds and their respective concentrations tested as single compounds.

(a) Solvent control (0.1% DMSO)
(b) PAHs
Phenanthrene (0.2 µM)
Pyrene (0.1 µM)
Benzo[a]anthracene (BaA, 0.6 µM)
Indeno[123-cd]pyrene (IcdP, 0.1 µM)
(c) PCBs
PCB 18 (0.1 µM)
PCB 81 (0.02 µM)
PCB 105 (0.04 µM)
(d) Plastic - PS (polystyrene, 10 µg L^{-1})

We also performed a series of mixtures toxicity trials in which each single compound (i.e., PAH or PCB) was combined with the PS microplastic (10 µg L^{-1}). In addition to these tests, the PAHs or PCBs were also combined as separate PAHs only or PCBs only mixtures, PAHs only mixture + PS, PCBs only mixture + PS, or PAHs + PCBs + PS mixture (summarized in **Table 2**).

Texas A&M University at Galveston
1001 Texas Clipper Road
Galveston, TX 77554

Table 2. A summary of the chemical compounds used to compose mixtures toxicity studies (PS = Polystyrene, 10 μg L^{-1}).

(a) PAH mixtures
Phenanthrene (0.2 μM) + PS
Pyrene (0.1 μM) + PS
Benzo[a]anthracene (BaA, 0.6 μM) + PS
Indeno[123-cd]pyrene (IcdP, 0.1 μM) + PS
(b) PCB mixtures
PCB 18 (0.1 μM) + PS
PCB 81 (0.02 μM) + PS
PCB 105 (0.04 μM) + PS
(c) Complete mixtures
All PAHs
All PCBs
All PAHs + PCBs
All PAHs + PS
All PCBs + PS
All PAHs + PCBs + PS

Texas A&M University at Galveston
1001 Texas Clipper Road
Galveston, TX 77554

The single or mixtures exposure levels tabulated in **Tables 1** and **2** are graphically summarized in **Figure 2** below.

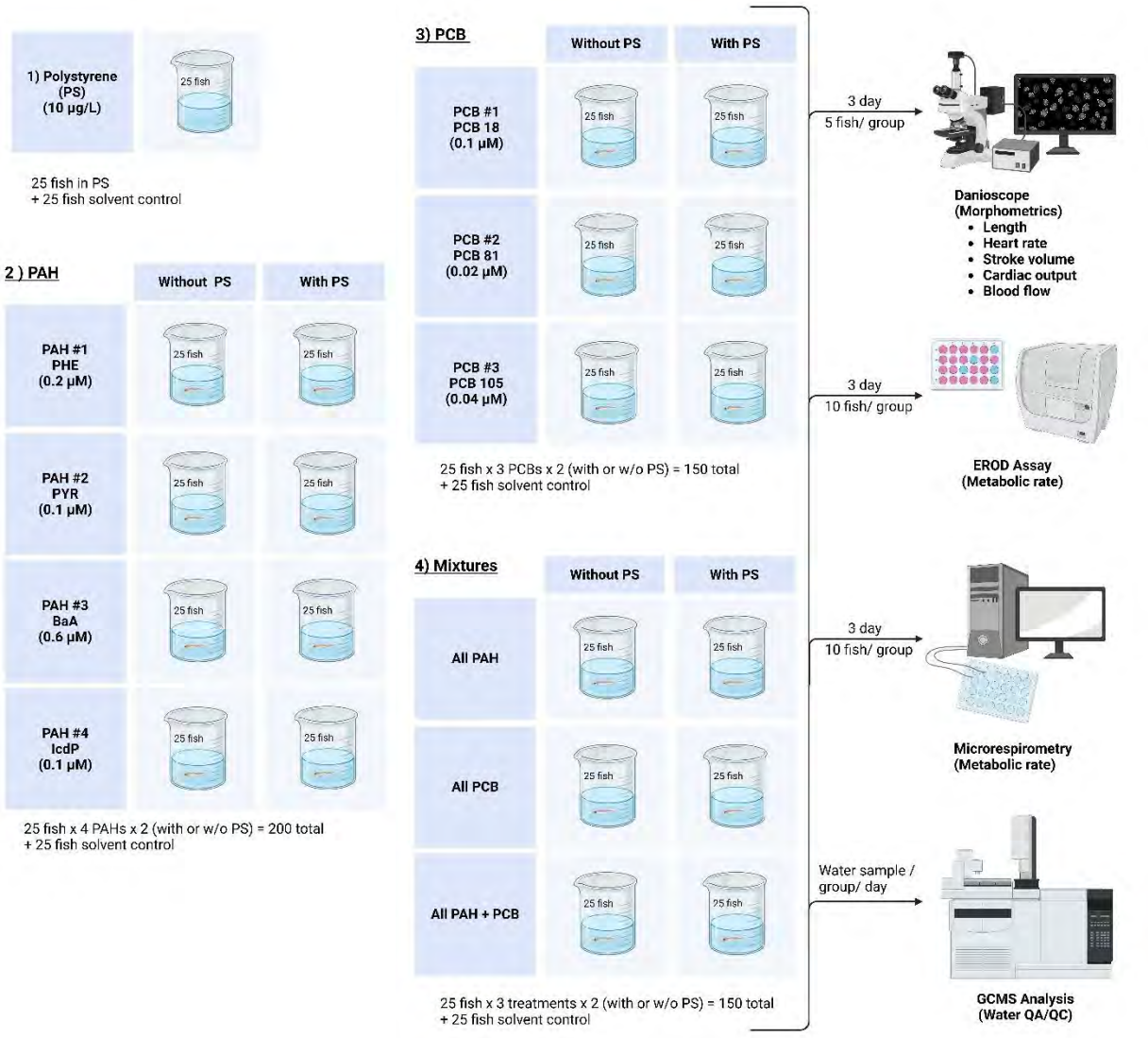

Figure 2. A schematic summary of the major treatment groups tested to determine the single or mixtures toxicity of select PAHs, PCBs and/or the microplastic beads of polystyrene (PS). The panel to the right indicates the various analyses conducted to determine the toxicity effects of exposure and confirm pollutant levels in the exposure aquaria.

Texas A&M University at Galveston
1001 Texas Clipper Road
Galveston, TX 77554

2.3. Analytical analysis of PAHs and PCBs in the exposure aquaria

Water samples were collected each day from each of the treatment groups before and after the semi-static renewal. Briefly, 1 ml of water samples were collected before and after the semi-static renewal and dried with a LABCONCO freeze dryer. The samples were then spiked with PAH and PCB internal standards (2.5 µg mL^{-1} final concentration BaP-d_{12} and PCB 65-d_5) and reconstituted in dichloromethane (DCM) to a 40x concentration factor. Blanks were also run and subtracted for any background contamination. GCMS analysis of the water samples was conducted to measure PAHs and PCBs levels, whereas Py-GCMS/MS was used to measure microplastic (PS) levels using the previously established protocol described in ***Objective 2***. The actual concentrations of the pollutants were quantified and compared with the theoretical nominal exposure concentrations set for each treatment.

2.4. Zebrafish body morphometry and cardiac physiology assessment using Danioscope

A subset from each of the treatments (n = 5) was used to measure morphometrics parameters of the fish (**Figure 2**). An electric stereo microscope camera (ZEISS steREO Discovery V8, Germany) was used in conjunction with pylon viewer (version 7.4.0.14900) by Basler (Ahrensberg, Germany) to capture images and videos of each of the embryos after toxicity test termination. At the end of the experiment, all fish were humanely euthanized using cold stunning in an ice bath (4 °C) followed by cervical severing as per the approved IACUC protocol. The DanioScope software (version 1.2.206) developed by Noldus (Netherlands) was used to analyze the captured images to measure length, heart rate (beats/min), and flow activity (% blood flow),

Texas A&M University at Galveston
1001 Texas Clipper Road
Galveston, TX 77554

along with any visible deformities such as dorsal/ventral spinal bend, underdeveloped jaw, few/no chromatophores, or dorsal fin aberrations. Heart Rate was measured by drawing a circle around the heart using the DanioScope software, which then measures the change in pixels to measure the beat of the heart. Similarly, the arterial Flow Rate was measured using the DanioScope software which measures the percent change in pixels (of the circled area) of the artery exiting the heart, which is proportional to the rate of blood flow.

To calculate the Stroke Volume (volume of blood pumped from the ventricle per beat), first the Heart Volume was calculated using the video captured images of systole (i.e., contraction of heart muscles) and diastole (i.e., relaxation of heart muscles) which was subsequently used to measure their volume (at systole and diastole) using the following formula (where: HV = heart volume, L= longitudinal length, W= latitudinal width) (Hoage et al., 2012; Naderi et al., 2024):

$$Heart\ Volume\ (HV) = \frac{\pi}{6} \times L \times W^2$$

Finally, the cardiac volume at systole (i.e., ventricle contraction) and diastole (i.e., ventricle relaxation) was used to measure the Stroke Volume (in µL) using the following formula (SV= stroke volume, EDV= end diastolic volume, ESV= end systolic volume) (Hu et al., 2001; Bruss and Raja, 2019):

$$Stroke\ Volume\ (SV) = EDV - ESV$$

Texas A&M University at Galveston
1001 Texas Clipper Road
Galveston, TX 77554

2.5. Pollutant biotransformation and metabolic rate assessment

2.5.1. Ethoxyresorufin-O-deethylase (EROD) assay: A subset of the fish from each of the treatment groups (n = 10) were used to measure pollutant metabolism (or biotransformation) activity using the EROD assay (**Figure 2**). The EROD assay allows for the assessment of the Phase I xenobiotic metabolizing enzyme, CYP1A1, which is involved in the breakdown of pollutants such as PAHs and PCBs (Nilsen et al., 1998). The experiment was conducted following the EROD assay protocol outlined in Noury et al. (2006). Briefly, n = 10 individual embryo-larval zebrafish from each treatment group were placed into each well of a 24 well plate. Each well contained 200 µL of 1.5 µM of 7-ethoxyresorufin or ER (i.e., the substrate for the EROD assay). The biotransformation of ER to the product resorufin, via the catalytic activity of CYP1A1, was measured after 4 hours using a fluorescence plate reader to quantify the resorufin produced. The resorufin was detected at 587 nm with a 545 nm excitation wavelength (Noury et al., 2006). All quantification of the resorufin produced was against a 12-point calibration curve from 2 µM to 0.001 µM. Each 24 well plate was maintained at 28 ± 1 °C throughout the experiment. At test termination, all fish were humanely euthanized using cold stunning in an ice bath (4 °C) followed by cervical severing as per the approved IACUC protocol.

2.5.2. Metabolic rate assessment using micro-respirometry

The oxygen consumption rate of 5 dpf embryo-larval Zebrafish (at test termination) was measured using a 24 well micro-respirometry system designed by Loligo® Systems for use with embryo-larval Zebrafish. The microrespirometer uses optical fluorescence to measure the

Texas A&M University at Galveston
1001 Texas Clipper Road
Galveston, TX 77554

dissolved oxygen in the water in gas tight 1.7 mL wells. Individual fish were placed into each of the wells to measure changes in their oxygen consumption rate. Each of the wells contained an oxygen sensor that was calibrated with 10% sodium sulfite in deionized water (0% oxygen saturation) and in fully aerated water (100% oxygen saturation) before use. From each of the treatments, n=10 embryo-larval zebrafish were placed in individual wells. Four wells were left without zebrafish (only water) to measure the baseline oxygen level (blank to be subtracted). The fish were allowed to acclimate for 30 mins before measuring the change in oxygen levels per well in the presence of the fish. Once started, the fish were monitored in the microrespirometer for 3 hours (or before the well conditions get hypoxic) to determine the metabolic rate of the fish exposed to different treatments. At termination, the fish were humanely euthanized using cold stunning in an ice bath (4 °C) as per an approved IACUC protocol. Finally, the euthanized zebrafish were frozen and later dried (in pre-weighed weigh boats) for 24 hours at 0.20 mBar vacuum and -80 ºC using a LABCONCO freeze dryer. The embryo larval zebrafish were then weighed (with the weigh boat) using a Sartorius Cubis microbalance (model: CPA2P) to measure their dry weight to calculate mass-specific metabolic rate (MO_2).

The measurement of oxygen consumption rate allows for the determination of whole organism bioenergetics or metabolic rate (Fry, 1971; Lapointe et al., 2014). This measurement can inform the ability of an organism to invest energy into survival, growth and movement, and therefore allows the assessment of physical fitness (Brett, 1964; Priede, 1985; Reidy et al., 2000; Pettersen et al., 2016; Somero et al., 2017; Pettersen et al., 2018). The mass-specific metabolic rate (MO_2) was calculated using the equation adapted from Petersen and Gamperl (2010):

Texas A&M University at Galveston
1001 Texas Clipper Road
Galveston, TX 77554

$$MO_2 = [((C_i - C_f) \times V_c) \times 60] \times (m \times t)^{-1}$$

Where C_i is the initial oxygen concentration measurement (mg O_2 L^{-1}); C_f is the final oxygen concentration (mg O_2 L^{-1}); V_c is the respirometer volume (liters); m is the mass of fish in Kg, and t is the time (minutes) of measurement. The resulting MO_2 measurements reported in mg O_2 Kg^{-1} fish min^{-1} were converted to µg O_2 Kg^{-1} fish hr^{-1} for allow convenient comparison with other studies that involve embryo-larval Zebrafish (Barrionuevo and Burggren, 1999; Bagatto et al., 2001; Barrionuevo et al., 2010).

2.6. Statistical analysis

Statistical analysis was conducted using R (v4.1.3) and associated packages, tidyr and ggplot2 (for visualization) with significance at $\alpha = 0.05$. The normality of data was tested using Shapiro-Wilk's test followed by Levene's test for homogeneity of variance. For pairwise comparisons, either a parametric t-test or non-parametric Mann-Whitney U test was conducted. For multiple variable correlational analysis, the non-parametric Spearman rank correlation was conducted. The statistical analysis of data comprising a main effects variable, and a covariate involved use of a two-way ANOVA test, followed by Tukey's post hoc analysis. PCA analysis was performed using the prcomp function and visualized using the ggplot function.

Texas A&M University at Galveston
1001 Texas Clipper Road
Galveston, TX 77554

3. Results

3.1. Exposure aquaria water concentrations

The actual concentrations of PAHs and PCBs measured in the exposure aquaria of the various treatment groups is shown in **Table 3**. The overall actual values reported for each chemical across the various treatment groups varies from 0.4 μM (for PCB 18) to 20.3% (for BaA) (**Table 3**). The overall variable and low recoveries may reflect loss of chemicals due to uptake or bioaccumulation into the exposed animals (i.e., embryo-larval zebrafish) or loss to the surfaces of the test vessels (beakers). As the exposure study design constituted a semi-static renewal every 24 hours, it is likely that these mechanisms were consequential towards influencing the overall low recovery. Despite the low actual concentrations, the ng mL^{-1} equivalent concentrations for each compound were: 0.89 ng mL^{-1} for PHE, 0.81 ng mL^{-1} for PYR, 27.85 ng mL^{-1} for BaA, 3.04 ng mL^{-1} for IcdP, 0.10 ng mL^{-1} for PCB 18, 0.15 ng mL^{-1} for PCB 81, and 0.88 ng mL^{-1} for PCB 105. These exposure levels are still within the environmentally realistic range. The maximum muscle body-burdens (as measured in ***Objective 2***) for the compounds tested in the exposure studies, were 4x - 839x higher than the actual concentrations measured in the exposure aquaria. And the maximum liver body-burdens were 4x - 12,000x higher than the levels measured in the exposure aquaria. Furthermore, the min-max PAH levels tested in our exposure studies, i.e., 0.81 - 27.85 ng mL^{-1} (**Table 3**), were within range of dissolved total PAH levels measured in the surface waters of various global coastal and estuarine ecosystems, i.e., 0.01 - 17.05 ng mL^{-1} (Bacosa et al., 2020). Therefore, the PAHs and PCBs were tested at levels within their respective environmentally relevant concentration ranges.

Texas A&M University at Galveston
1001 Texas Clipper Road
Galveston, TX 77554

Table 3. The actual concentrations of the select PAHs and PCBs (as mean ± standard error) measured in the exposure aquaria during the *in vivo* toxicological studies with single or mixtures pollutants. (PHE = phenanthrene, PYR = pyrene, BaA = Benzo[a]anthracene, IcdP = indeno[1,2,3-cd]pyrene, PS = polystyrene beads).

Treatment Groups	PHE (0.2 µM)	PYR (0.1 µM)	BaA (0.6 µM)	IcdP (0.1 µM)	PCB 18 (0.1 µM)	PCB 81 (0.02 µM)	PCB 105 (0.04 µM)
Single compound (n = 6-8)	0.020 ± 0.010	0.002 ± 0.001	0.133 ± 0.012	0.019 ± 0.002	0.0004 ± 0.0003	0.001 ± 0.0002	0.004 ± 0.001
Single compound + PS (n = 6-8)	0.000 ± 0.000	0.001 ± 0.001	0.246 ± 0.033	0.020 ± 0.002	0.0004 ± 0.0002	0.001 ± 0.0001	0.004 ± 0.001
All PAHs/PCBs (n = 7-8)	0.005 ± 0.004	0.008 ± 0.005	0.001 ± 0.0002	0.009 ± 0.003	0.0003 ± 0.0002	0.001 ± 0.0002	0.002 ± 0.001
All PAHs/PCBs+PS (n = 8)	0.0004 ± 0.0003	0.002 ± 0.001	0.0005 ± 0.0002	0.009 ± 0.004	0.0003 ± 0.0001	0.0005 ± 0.0001	0.002 ± 0.001
All PAHs+PCBs (n = 8)	0.0003 ± 0.0001	0.004 ± 0.001	0.110 ± 0.027	0.006 ± 0.001	0.0003 ± 0.0001	0.0004 ± 0.0003	0.002 ± 0.001

Texas A&M University at Galveston
1001 Texas Clipper Road
Galveston, TX 77554

All PAHs+PCBs+PS (n = 8)	0.001 ± 0.001	0.005 ± 0.002	0.274 ± 0.062	0.009 ± 0.002	0.0004 ± 0.0002	0.0005 ± 0.0001	0.002 ± 0.001
Average % of Nominal	**2.3 ± 1.1**	**3.7 ± 1.0**	**20.3 ± 3.3**	**11.3 ± 1.3**	**0.4 ± 0.1**	**2.7 ± 0.4**	**6.9 ± 0.8**

Texas A&M University at Galveston
1001 Texas Clipper Road
Galveston, TX 77554

3.2. Effects of exposure on morphometric parameters

3.2.1. Effects of exposure on the total length of embryo-larval zebrafish: The exposure of embryo-larval zebrafish to the select pollutants only exhibited a statistically significant decrease in total length for the mixture exposure to BaA + PS ($p = 0.01$) (**Figure 3(a)**). The total length of fish in the solvent control group (0.1% DMSO) was a marginal 5% longer than the BaA + PS exposure group. The lengths of the fish in the solvent control group (3.9 $\pm$ 0.03 mm) are within range for ~ 5 dpf embryo-larval life stages zebrafish ($\leq$5 mm) (Singleman and Holtzman, 2014).

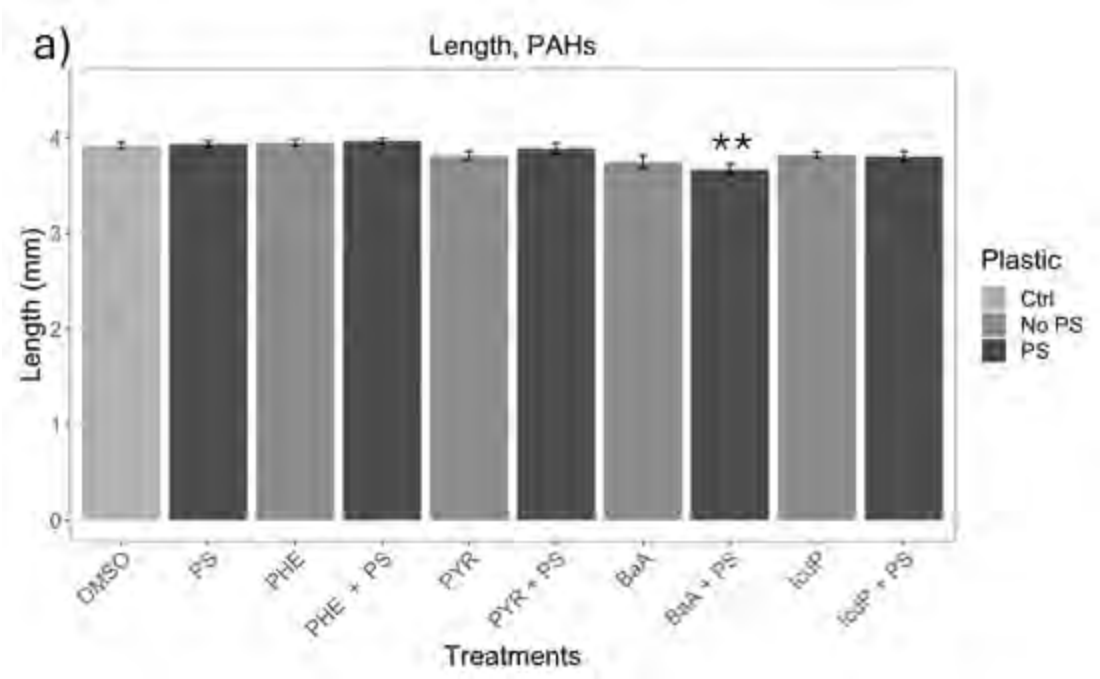

Texas A&M University at Galveston
1001 Texas Clipper Road
Galveston, TX 77554

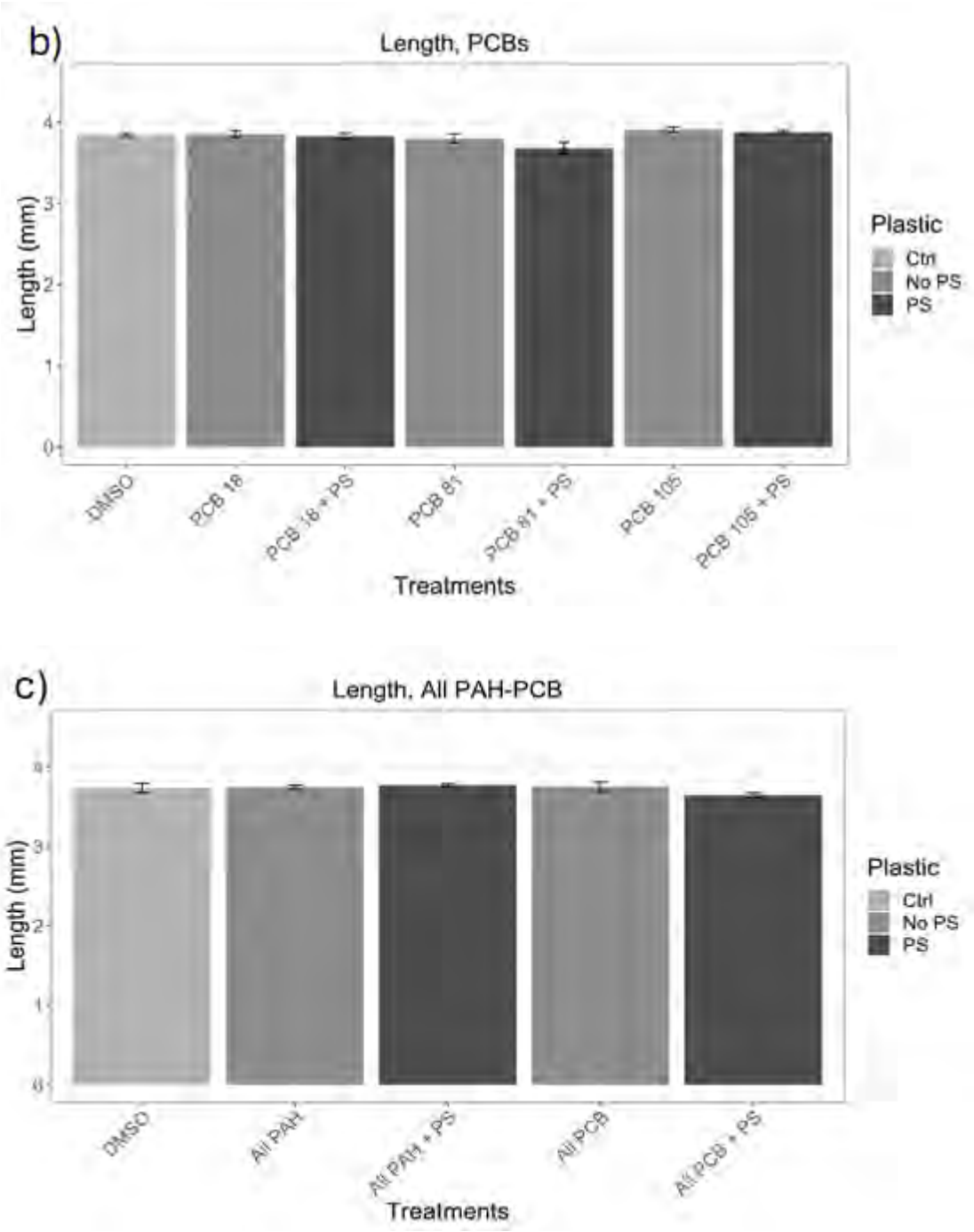

Figure 3. Effects of single compound and/or mixtures exposures to **a)** PAHs (+ PS), **b)** PCBs (+ PS), and **c)** combined PAHs, PCBs and PS on the total lengths of zebrafish. (** $p \leq 0.01$).

Texas A&M University at Galveston
1001 Texas Clipper Road
Galveston, TX 77554

3.2.2. Effects of exposure on the dry weight of embryo-larval zebrafish: Exposure to select single PAHs and a PAH + PS mixture showed a significant increase in dry weights. For example, exposure to BaA caused a statistically significant 58% increase in body weight relative to the solvent control group (0.1% DMSO). Whereas exposure to IcdP or IcdP + PS significantly increased body weight by 59% and 53% respectively (**Figure 4(a)**). The exposure of fish to PCBs showed exposure to PCB 105 only to significantly increase body weight by 31%. While in contrast, exposure to the mixture of PCB 81 + PS significantly decreased body weight by 43% (**Figure 4(b)**). Finally, exposure to the PAHs only mixture caused a 63% significantly lower body weight relative to the solvent control group (0.1% DMSO) (**Figure 4(c)**).

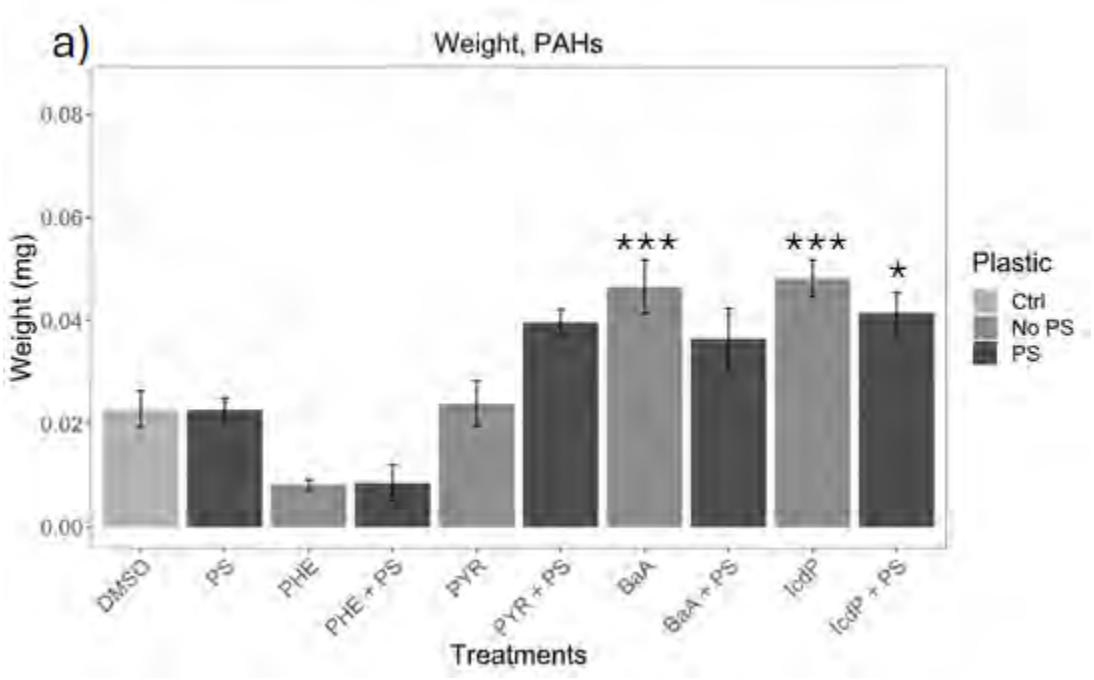

Texas A&M University at Galveston
1001 Texas Clipper Road
Galveston, TX 77554

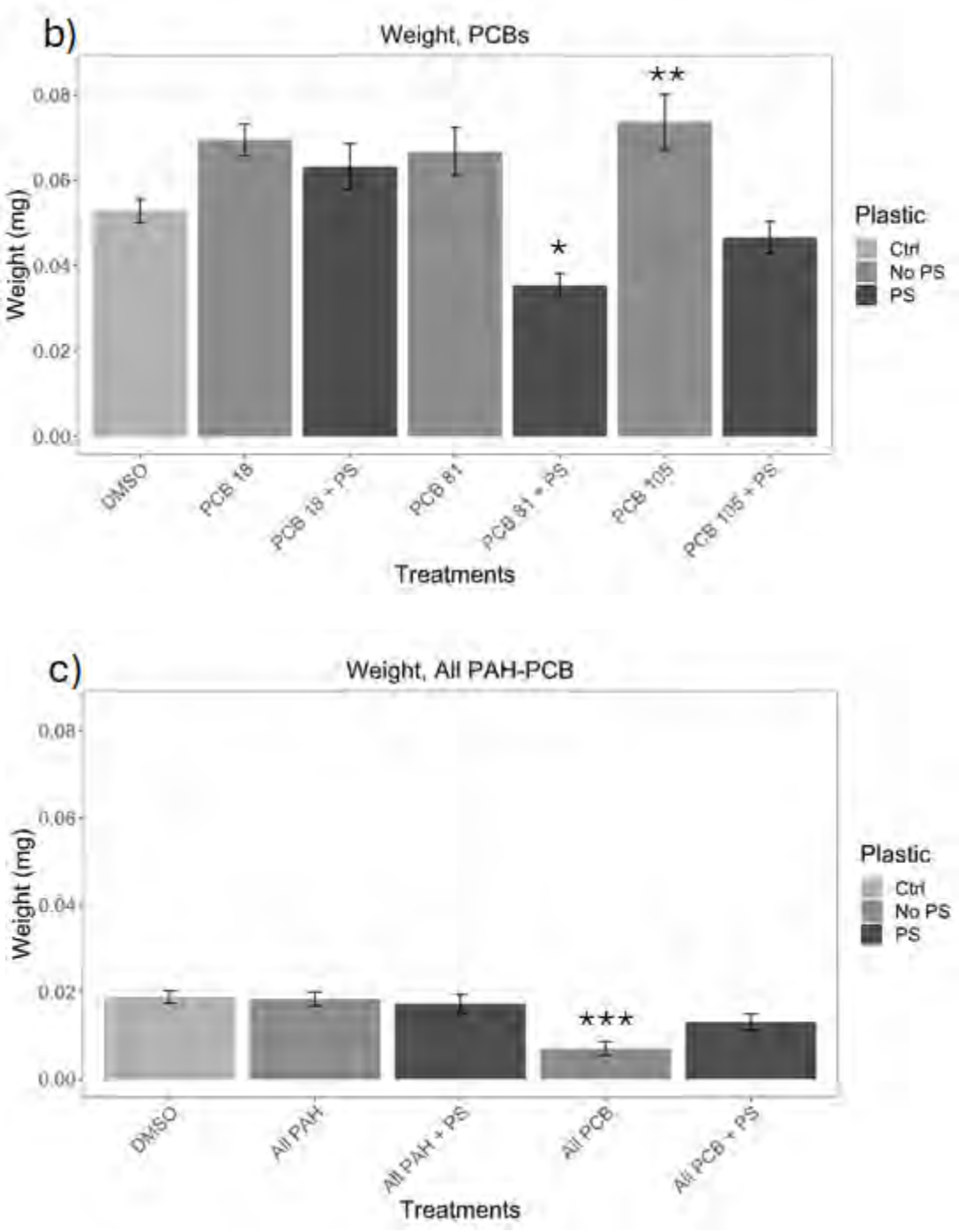

Figure 4. Effects of single compound and/or mixtures exposures to **a)** PAHs (+ PS), **b)** PCBs (+ PS), and **c)** combined PAHs, PCBs and PS on the dry weights of zebrafish. (* $p \leq 0.05$, ** $p \leq 0.01$, *** $p \leq 0.001$).

Texas A&M University at Galveston
1001 Texas Clipper Road
Galveston, TX 77554

3.2.3. Effects of exposure on the mass specific EROD activity of embryo-larval zebrafish: The EROD activity data precluded statistical analysis as it comprised pseudo-replication and a single mean value was calculated for each treatment group. Therefore, the EROD datasets are qualitatively analyzed using multivariate PCA analysis as shown in *sub-section 3.2.8*. However, general trends in the datasets can be observed and commented upon. For example, for the PAHs we see PHE and PHE + PS to exhibit EROD activities 59% and 57% greater than that measured for the solvent control group (0.1% DMSO) (**Figure 5(a)**). Whereas an average of the remainder PAH treatment groups constituted 99% of the solvent control activity (0.1% DMSO). The mixtures exposure to PCB 81 + PS exhibited a 51% increase in EROD activity relative to the solvent control. Whereas the remaining groups averaged 91% of the activity in the solvent control group (**Figure 5(b)**). Finally, for the All PAHs and PCBs mixtures groups we see elevated EROD activities for all groups relative to the solvent control. The All PCBs group exhibited an EROD activity level that was 80% higher than the solvent control group (0.1% DMSO), whereas the All PAHs treatment group was 48% higher than the solvent group, the All PAHs + PS group was 52% higher, and the All PCBs + PS group was 44% higher than the solvent control group (**Figure 5(c)**).

Texas A&M University at Galveston
1001 Texas Clipper Road
Galveston, TX 77554

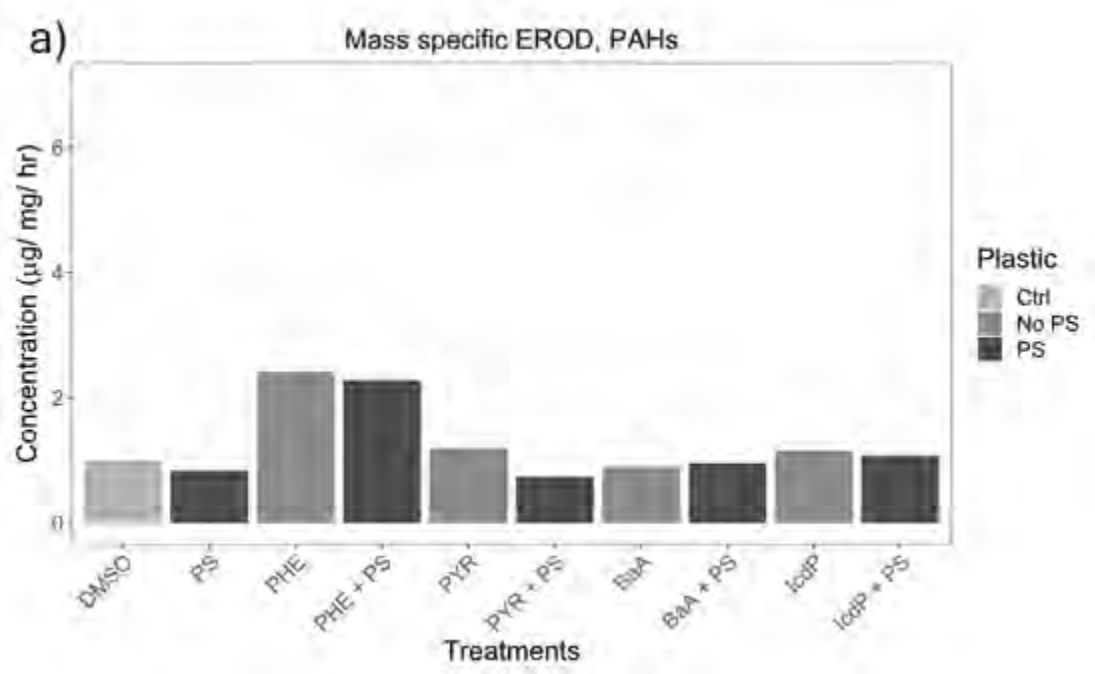

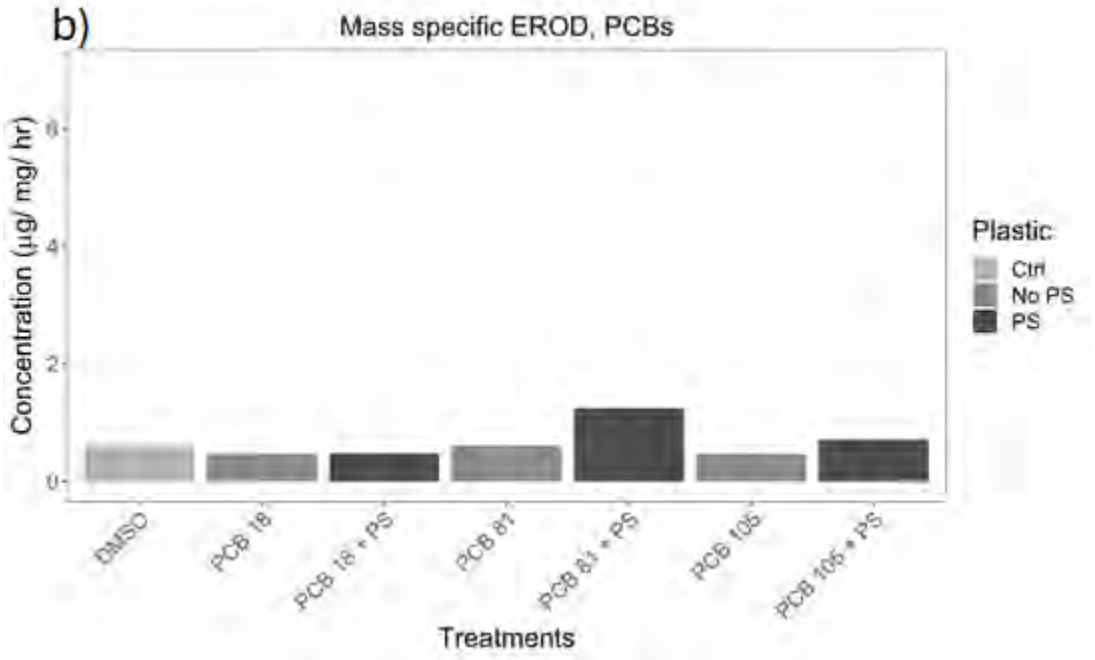

Texas A&M University at Galveston
1001 Texas Clipper Road
Galveston, TX 77554

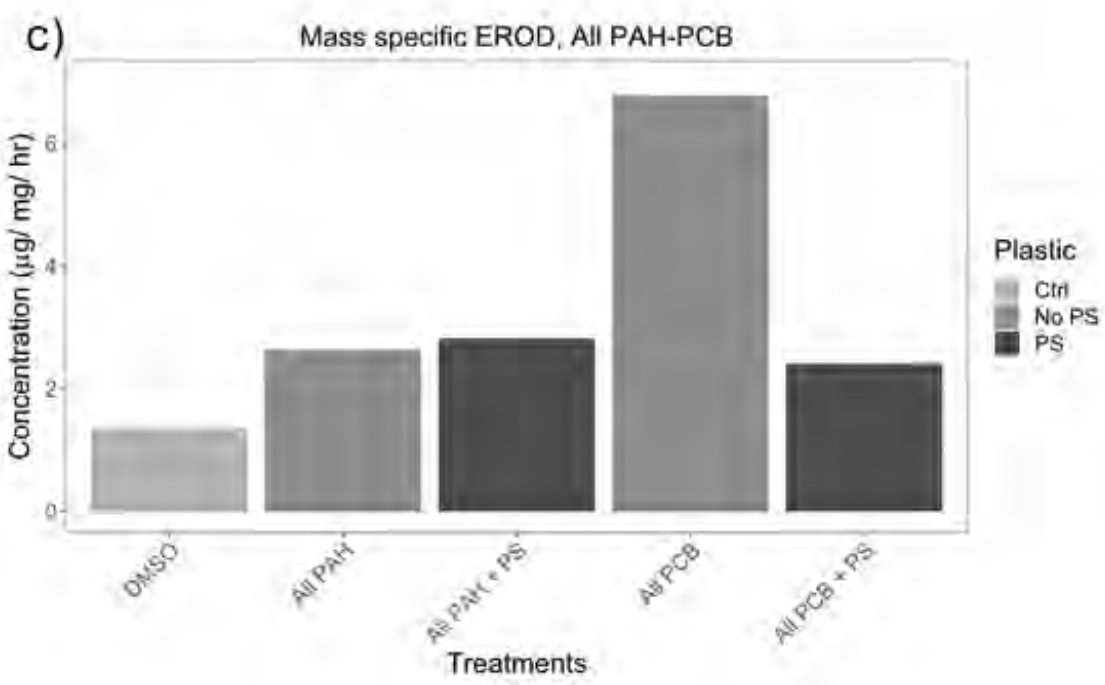

Figure 5. Effects of single compound and/or mixtures exposures to **a)** PAHs (+ PS), **b)** PCBs (+ PS), and **c)** combined PAHs, PCBs and PS on the *in vivo* EROD activities of zebrafish.

3.2.4. Effects of exposure on the mass specific metabolic rate (MO_2) of embryo-larval zebrafish:

We find the MO_2 values for the zebrafish exposed to single or mixtures compounds to approximately reflect the trends previously seen for the mass specific EROD activity assessments (shown in *section 3.2.3.*). For exposure to PAHs, we see the PHE and PHE + PS exposed groups increase metabolic rate relative to the solvent control group by 46% (statistically significant) and 70% respectively (**Figure 6(a)**). The absence of statistical significance for the PHE + PS treatment group, despite a 70% elevated activity relative to the solvent control group, is a likely reflection of the greater variability in its MO_2 response (98% coefficient of variation) vs. that of

Texas A&M University at Galveston
1001 Texas Clipper Road
Galveston, TX 77554

the PHE only group (50% coefficient of variation). Like the EROD assessment for exposure to PCBs, we see the PCB 81 + PS group to increase MO_2 by 57% relative to the solvent control group. However, this elevation was not statistically significant given a ~78% coefficient of variation (**Figure 6(b)**). Finally, and like the EROD assessment for the All PCBs exposure group, we see a statistically significant increase in MO_2 activity at a level 84% higher than the solvent control group (0.1% DMSO) (**Figure 6(c)**).

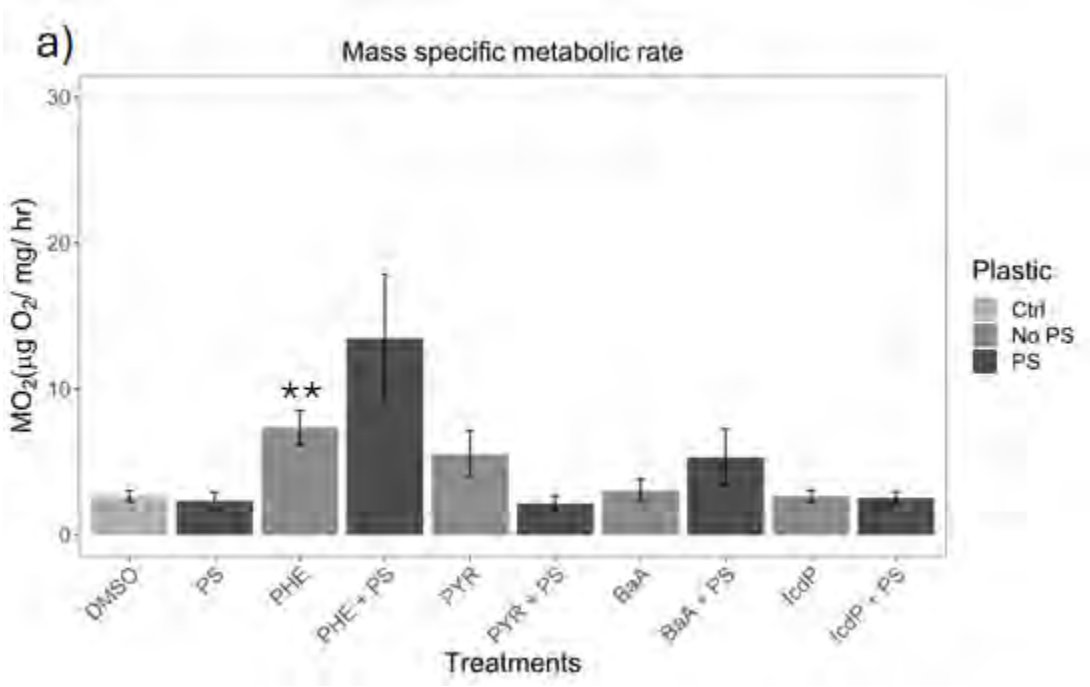

Texas A&M University at Galveston
1001 Texas Clipper Road
Galveston, TX 77554

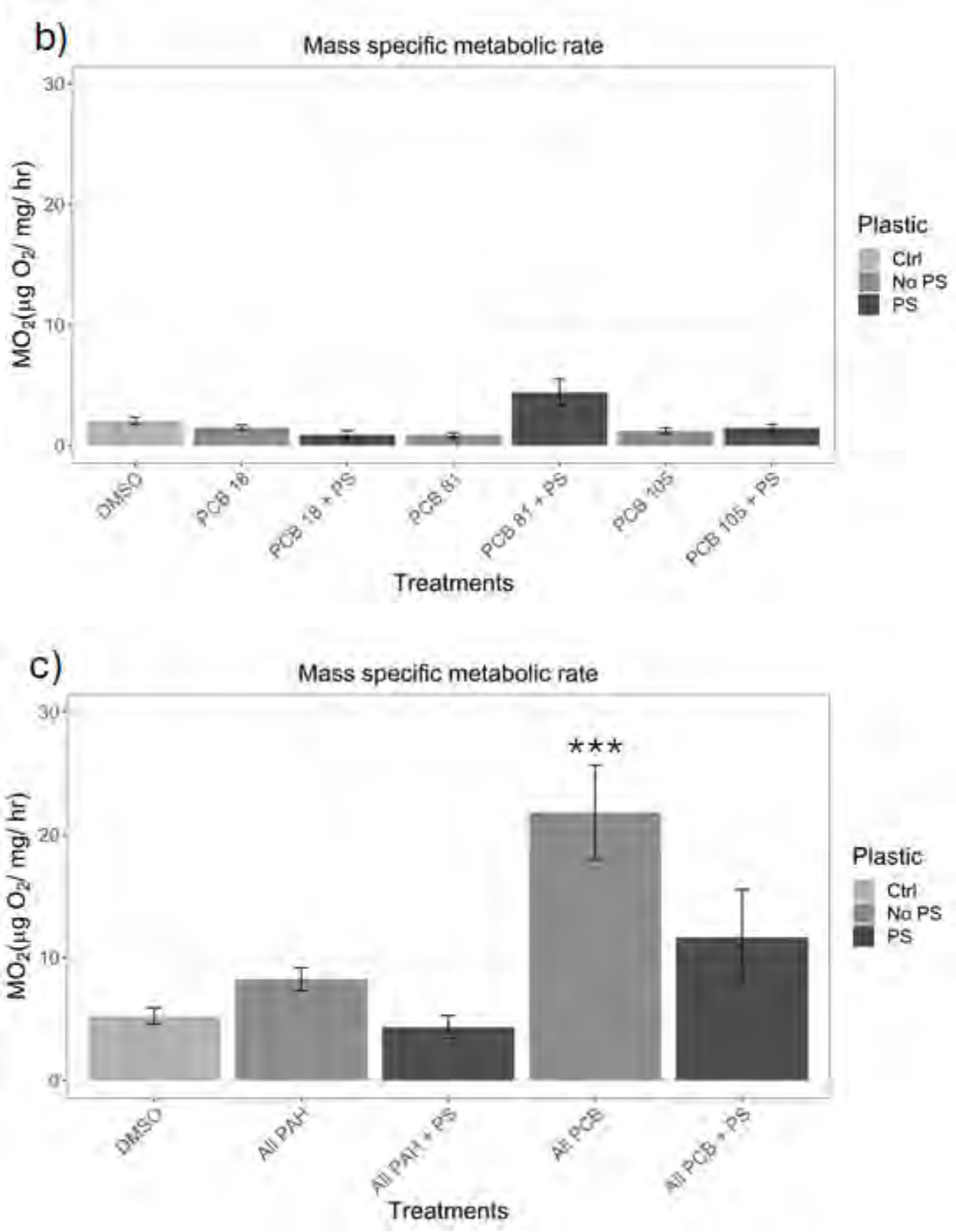

Figure 6. Effects of single compound and/or mixtures exposures to **a)** PAHs (+ PS), **b)** PCBs (+ PS), and **c)** combined PAHs, PCBs and PS on the mass specific metabolic rate (or MO_2) of zebrafish. (** $p \leq 0.01$, *** $p \leq 0.001$).

Texas A&M University at Galveston
1001 Texas Clipper Road
Galveston, TX 77554

3.2.5. Effects of exposure on the heart rate of embryo-larval zebrafish: The analysis of heart rate across all treatment groups showed no statistically significant effects of exposure (**Figure 7**). The mixture exposure group of BaA + PS was the only treatment to exhibit a heart rate that was the highest (23%) relative to the solvent control group (**Figure 7(a)**). However, this elevated heart rate was not statistically significant.

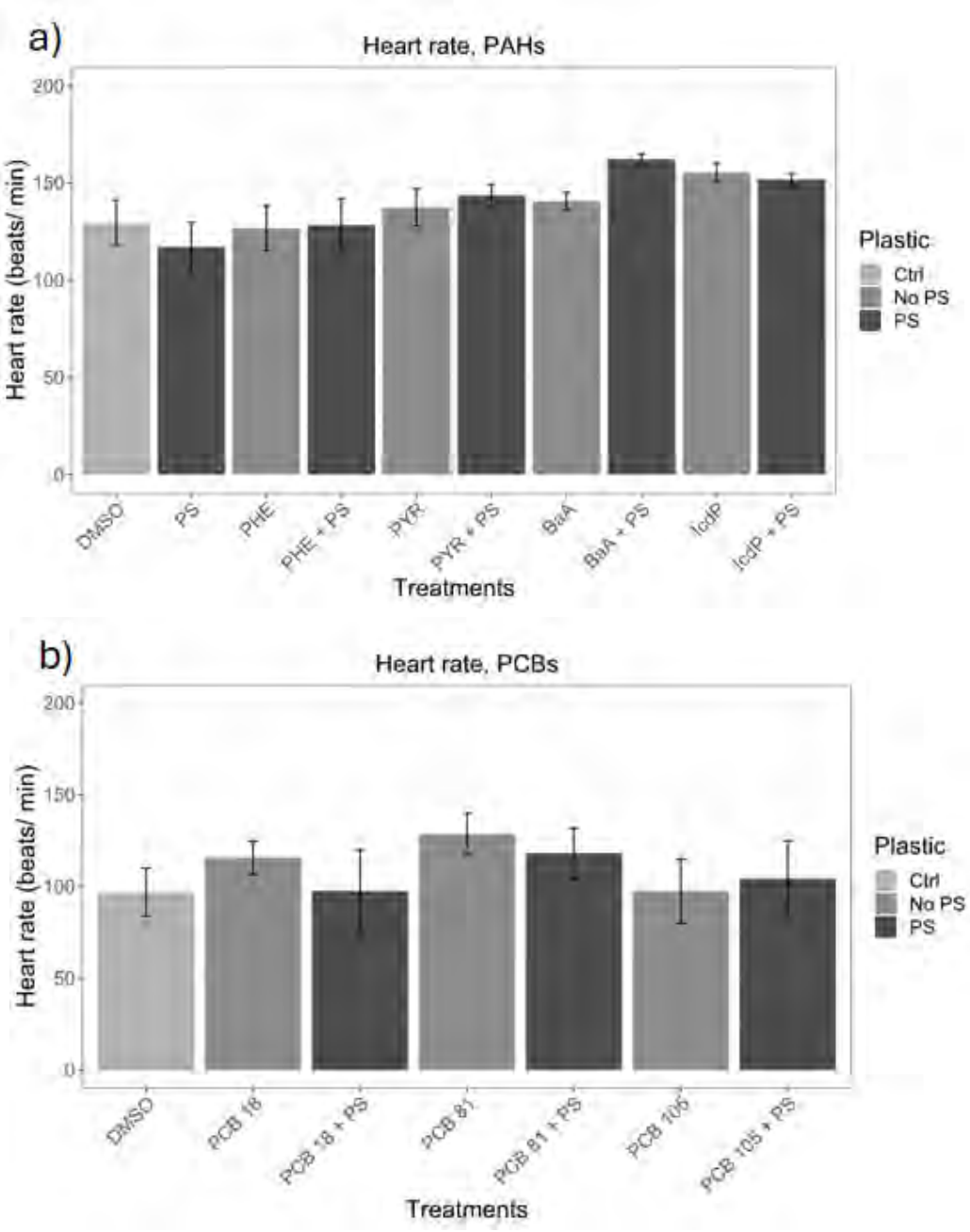

Texas A&M University at Galveston
1001 Texas Clipper Road
Galveston, TX 77554

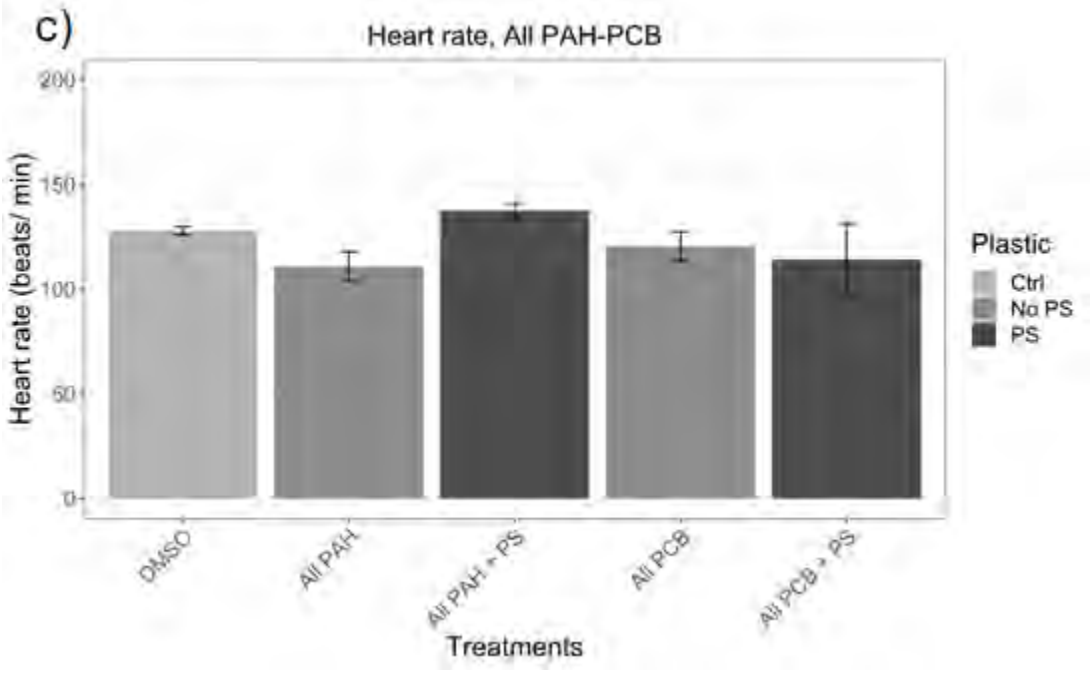

Figure 7. Effects of single compound and/or mixtures exposures to **a)** PAHs (+ PS), **b)** PCBs (+ PS), and **c)** combined PAHs, PCBs and PS on the heart rate of zebrafish.

3.2.6. Effects of exposure on the cardiac stroke volume of embryo-larval zebrafish: The analysis of cardiac stroke volume showed no statistically significant effects of exposure (**Figure 8**). However, despite its lack of significance, the mixtures exposure to All PCBs resulted in a 63% increase in the stroke volume (**Figure 8(c)**).

Texas A&M University at Galveston
1001 Texas Clipper Road
Galveston, TX 77554

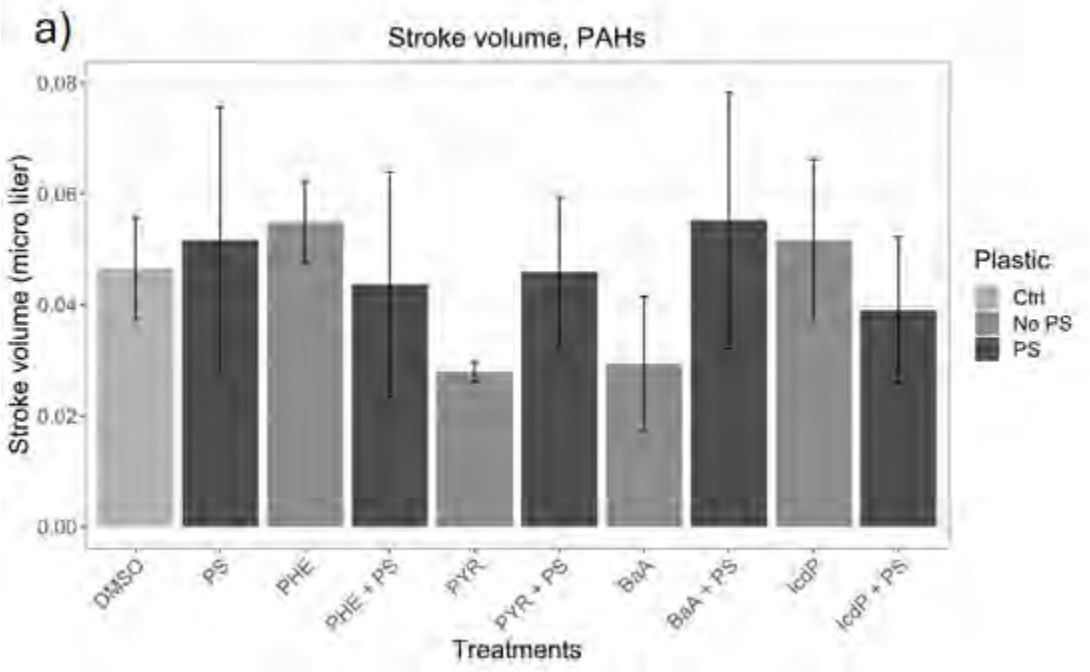

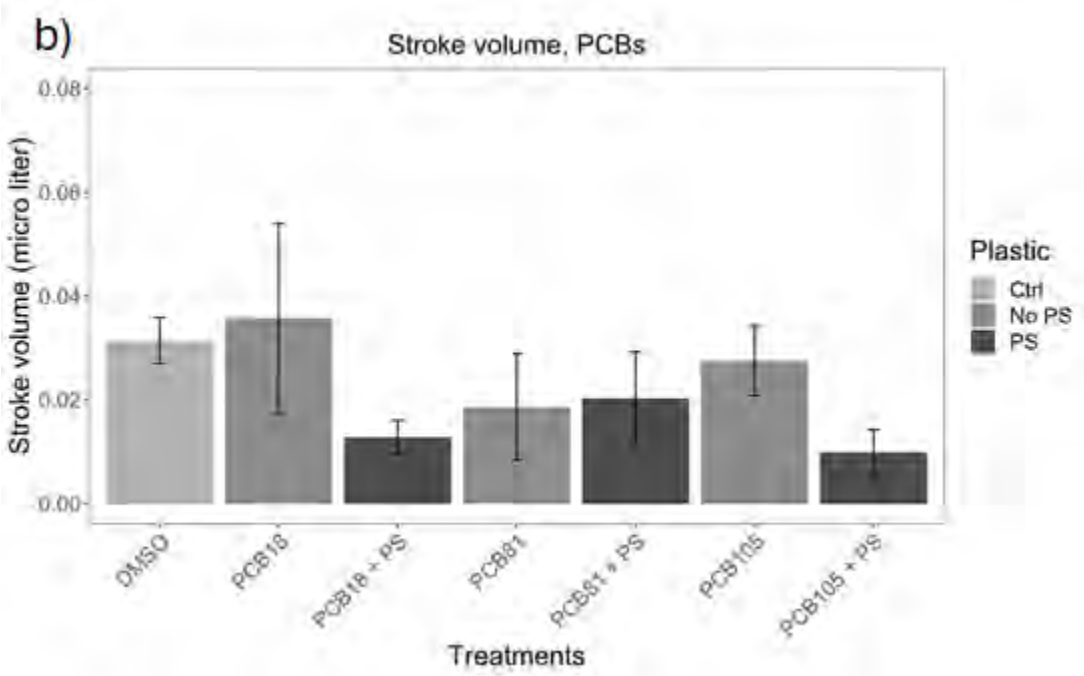

Texas A&M University at Galveston
1001 Texas Clipper Road
Galveston, TX 77554

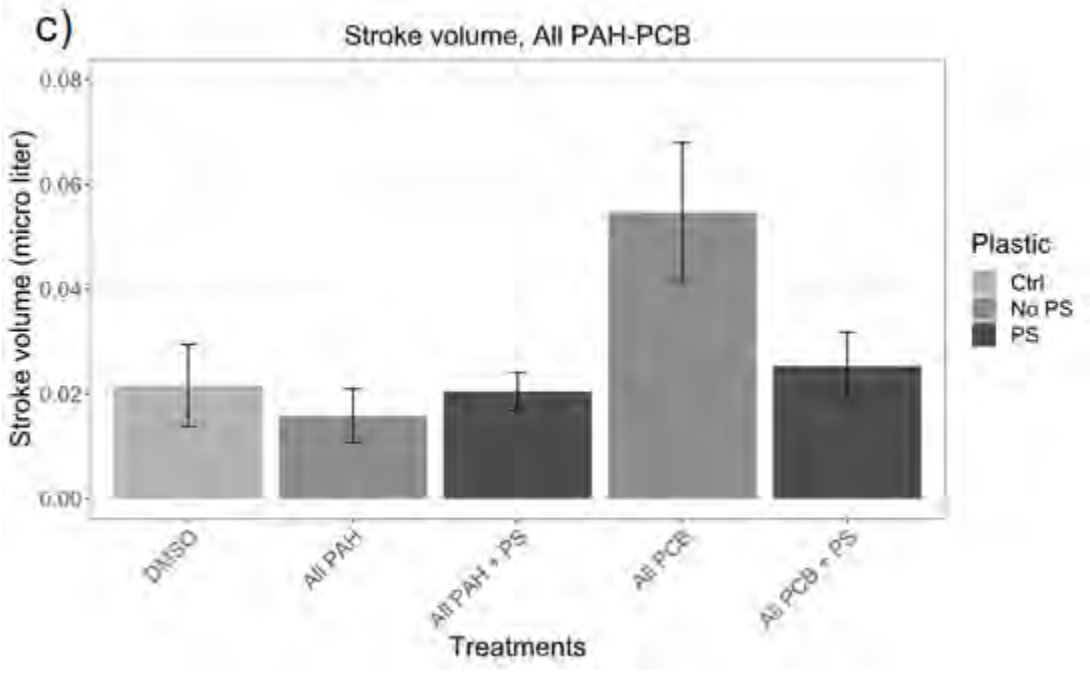

Figure 8. Effects of single compound and/or mixtures exposures to **a)** PAHs (+ PS), **b)** PCBs (+ PS), and **c)** combined PAHs, PCBs and PS on the stroke volume of zebrafish.

3.2.7. Effects of exposure on the cardiac (arterial) flow activity of embryo-larval zebrafish: The analysis cardiac flow activity shows its lowering only for exposure to single PCBs or PCBs + PS mixtures (**Figure 9(b)**). Specifically, we see PCB 18 and PCB 18 + PS (significant reduction for PCB 18 + PS only); and PCB 105 and PCB 105 + PS, to all be decreased by ≤50% relative to the solvent control group (0.1% DMSO). Whereas, the arterial flow activity for PCB 81 and PCB 81 + PS exposure decreasd by 99% realtive to the solvent control group (**Figure 9(b)**). These results implicate a strong inhibitory effect of PCBs on cardiac activity. And while not statistically significant, exposure of zebrafish to All PCBs showed a 90% decrease in cardiac flow activity (**Figure 9(c)**).

Texas A&M University at Galveston
1001 Texas Clipper Road
Galveston, TX 77554

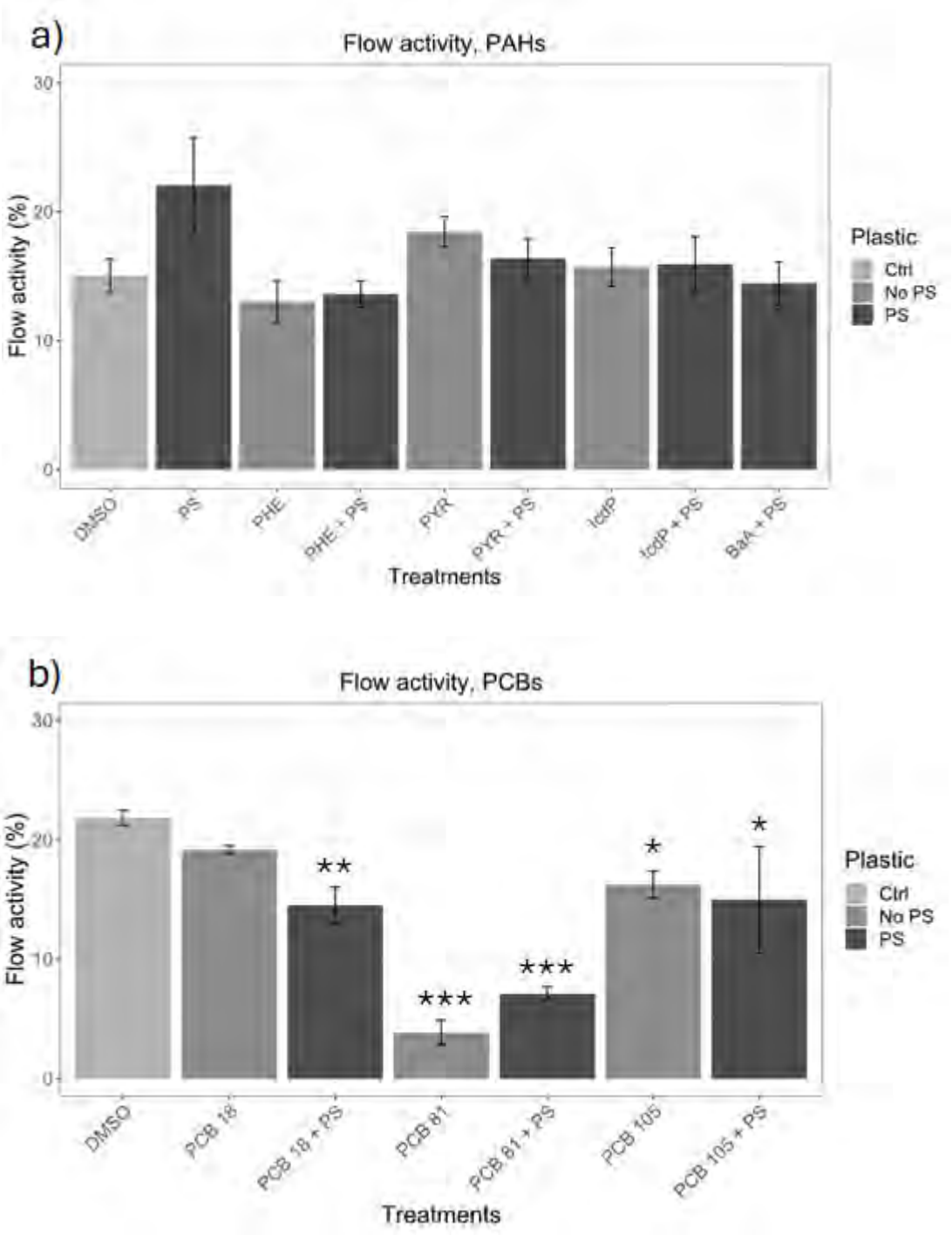

Texas A&M University at Galveston
1001 Texas Clipper Road
Galveston, TX 77554

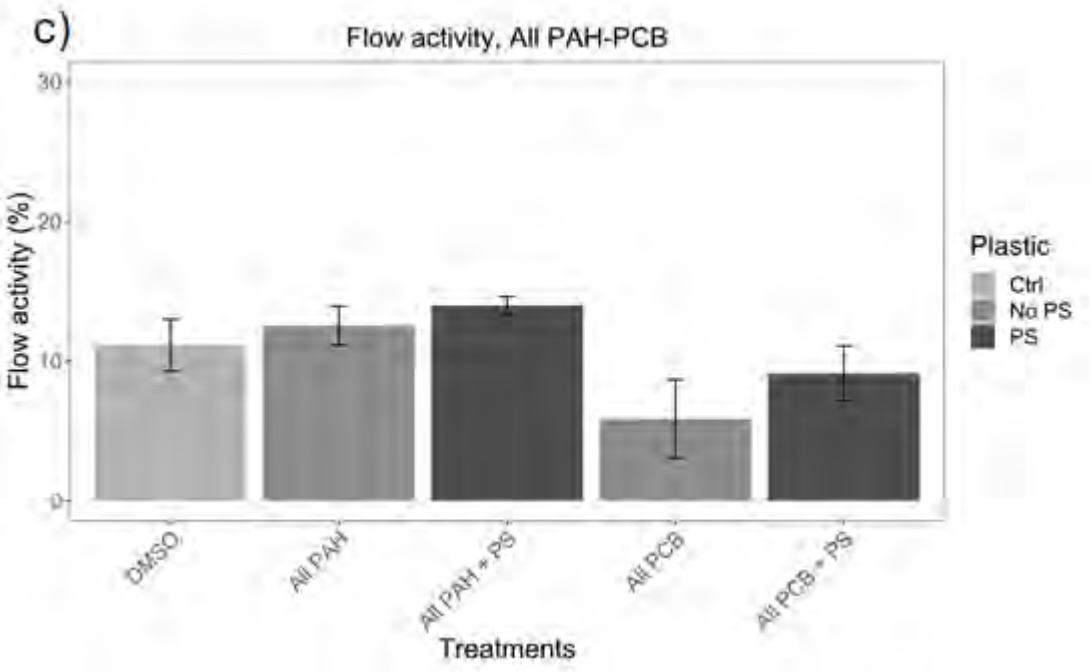

Figure 9. Effects of single compound and/or mixtures exposures to **a)** PAHs (+ PS), **b)** PCBs (+ PS), and **c)** combined PAHs, PCBs and PS on the arterial cardiac blood flow of zebrafish. (* $p \leq 0.05$, ** $p \leq 0.01$, *** $p \leq 0.001$).

3.2.8. Multivariate principal component analysis (PCA) of exposure effects on all biological response variables: The overall effects of exposure on the various biomarkers was assessed using a PCA plot. This analysis shows some charactertistic correspondences in the datasets (**Figure 10**). For example, we see single PAHs and PAHs + PS mixtures effects to be orthogonal to those caused by single PCBs and PCBs + PS. While exposure to single PCBs and PCBs + PS exposure appear to be most correlative with effects on body weight and length, we see single PAHs and PAHs + PS to correlate mainly with effects on cardiac performance such as flow activity, heart rate, and stroke volume. Finally, we see mixtures exposures to All PAHs and All PCBs to be

Texas A&M University at Galveston
1001 Texas Clipper Road
Galveston, TX 77554

strongly correlative with mass specific metabolic rate (MO_2) and EROD activity (**Figure 10**). Furthermore, MO_2 and EROD activity are strongly correlated with one another (**Figure 11**), indicating a close correspondence between the induction of the monooxygenase metabolic activity of CYP1A1 (as measured by the EROD activity assay) and overall increase in organismal metabolic (or O_2) consumption rate (**Figure 10**).

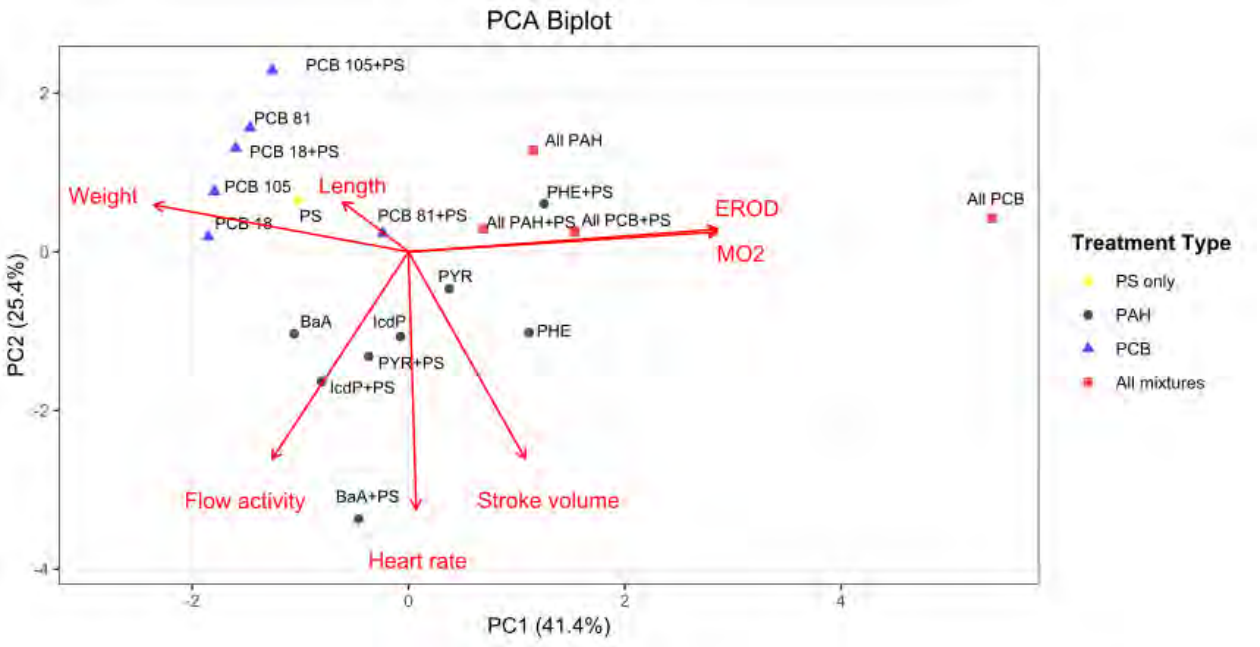

Figure 10. PCA plot showing the overall correspondences between the single and/or mixtures PAHs, PCBs, and PS treatment levels, and the various effects biomarkers measured in the exposed zebrafish.

Texas A&M University at Galveston
1001 Texas Clipper Road
Galveston, TX 77554

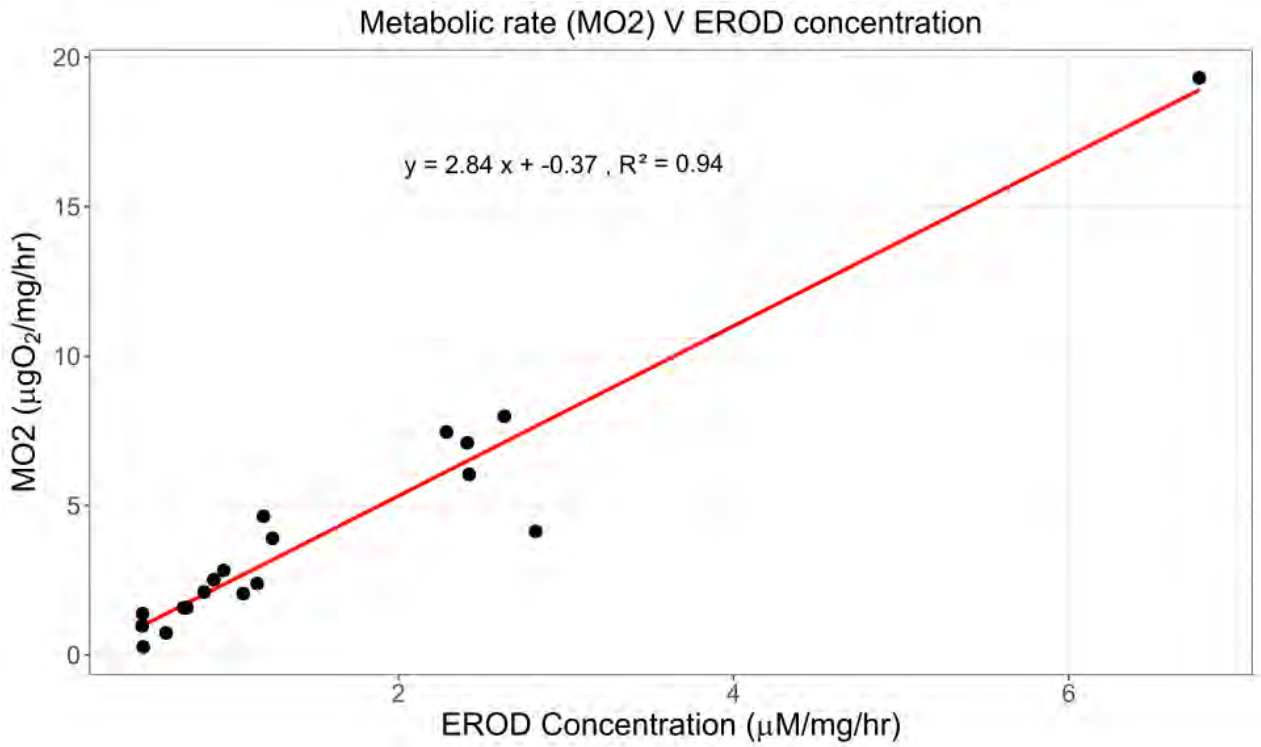

Figure 11. Correlational analysis of the relationship between mass specific metabolic rate (MO_2) and EROD actvity in embryo larval zebrafish exposed to PAHs, PCBs, and/or PS.

4. Discussion

In this objective, we stuided the effects of exposure of embryo-larval life stages of zebrafish to single or mixtures PAHs, PCBs, and PS microplastics. The exposure studies tested selected compounds based upon their overall abundance and prominence in the body-burdens of fish collected from Matagorda Bay (as described in ***Objective 2***). In agreement with other published studies, we see that exposure to both PAHs and PCBs (single compounds or as mixtures) causes adverse effects on cardiac functions (Incardona et al., 2004; Incardona et al., 2006; Singleman and Holtzman, 2021; Green et al., 2025). These effects are mainly due to induction or interaction with

Texas A&M University at Galveston
1001 Texas Clipper Road
Galveston, TX 77554

CYP1A1's catalytic response, which results in an uncoupling of the electron transfer needed to complete its monoxygenation catalytic cycle. Therefore, resulting in oxidative stress and the associated cellular dysregulations, such as structural damage to cellular organelles and/or DNA strand breaks (Wassenberg and Di Giulio, 2004; Green et al., 2008).

Almost all invertebrate and vertebrate taxa (including fish and humans) metabolize or detoxify planar aromatic compounds (such as PAHs and PCBs) using a superfamily of enzymes that include the cytochrome P450 (CYP450) mixed function mono-oxygenases (Safe et al., 1985; Moorthy et al., 2015). The specificity of CYP450 induction, in particular the CYP1A1 isoform, is controlled by a cell receptor signaling pathway called the aryl hydrocarbon receptor (AhR) signaling system (Lo and Matthews, 2012). Much like CYP450 enzymes, the AhR signaling system is also highly conserved (or shared) amongst invertebrate and vertebrate taxa (Beischlag et al., 2008). AhR is activated by planar aromatic compounds, such as PAHs and PCBs, and the biological consequences of exposures to these compounds is in large part AhR-mediated (Safe et al., 1985; Denison et al., 2002). Once activated, AhR regulates various detoxification enzyme genes, some of which include CYP450s (Rowlands et al., 1996; Beischlag et al., 2008). Therefore, aberrant AhR signaling and CYP1A1 catalytic induction, under PAHs and PCBs exposures, are amongst the common causal factors responsible for adverse effects on organismal development and cardiac functions (Incardona et al., 2014; Cherr et al., 2017; Takeshita et al., 2021).

Within this context, the close correlation between MO_2 and EROD activity indicates a functional relationship (**Figure 11**). As discussed, CYP450 reactions catalyze a mono-oxygenation reaction

Texas A&M University at Galveston
1001 Texas Clipper Road
Galveston, TX 77554

in which one atom of molecular oxygen (O_2) is incorporated into the substrate, and the other reduced to H_2O, with help from reducing equivalents derived from NADPH as cofactor (Miller, 2005; Guengerich, 2018). The use of O_2 in such oxidoreductase reactions yields large catabolic power to CYP450 mediated reactions (Jabłońska and Tawfik, 2022), and also underscores the requirement of this catalytic ability on the availability of O_2. Therefore, as we see in the PCA plot in **Figure 10**, exposure to mixtures of PAHs and PCBs (All PAHs or All PCBs) cause EROD activity to strongly correlate with MO_2 (or the oxygen consumption rate). This interesting result indicates that the measurement of *in vivo* EROD activity may be a good proxy for measuring metabolic (or oxygen consumption) rate. However, this may only be the case where the structural similarity of pollutants, i.e., comprising planar or co-planar polycyclic aromatic rings such as for PAHs and PCBs, mediates additive or synergistic toxicity effects through shared pathways, such as AhR signaling and CYP450 inductions (Birnbaum and DeVito, 1995; Berg et al., 2006).

Finally, our experimental design allowed us to test whether exposure to microplastics particles, PS (0.1 μm particle size) or PS mixtures with single or mixed PAHs or PCBs attenuated or exacerbated toxicity effects. A key finding of our exposure studies was that exposure to PS only (at 10 μg L^{-1} final concentration) caused no statistically significant effect on any of the biomarkers measured. However, PS appeared to cause additive or synergistic effects on MO_2 when co-exposed with PAHs. Although not statistically significant, MO_2 increased when co-exposed with PHE (i.e., PHE + PS), or PCB-81 (PCB-81 + PS) (**Figure 6(a)** and **(b)**). In contrast, only the All PCBs treatment group was able to statistically significantly increase MO_2 relative to the solvent control group (**Figure 6(c)**). Overall, the greatest effect on cardiac function was seen

Texas A&M University at Galveston
1001 Texas Clipper Road
Galveston, TX 77554

for effects on cardiac (arterial) flow activity on exposures to the single PCBs: 81 or 105, and the PCB + PS mixtures for: PCB 18 + PS, PCB 81 + PS, and PCB 105 + PS (**Figure 9(b)**).

Exposure to microplastics can cause cardiotoxic effects (Persiani et al., 2023). A study by Sun et al., (2021) has shown exposure of embryo-larval zebrafish (up to 4 days post hatch) to 200 µg L^{-1} of 0.1 µm polyethylene (PE) nanoplastics beads to cause increased pericardial edema and lowered blood flow (and with no effects on heart rate). The authors suggest the likely damage of vascular endothelia (i.e., cells that form the inner layer of blood vessels) may causes blood vessels to vasodilate, hence causing decreased blood flow while not affecting the heart rate (Sun et al., 2021). Similarly, in our study we see a decrease in cardiac flow activity for the PCB 18 + PS, PCB 81 + PS, and PCB 105 + PS treatment groups (**Figure 9(b)**). However, we tested microplastics at levels 20x lower those used by Sun et al., (2021). At an equivalent concentration in the Sun et al., (2021) study, the PE microplastics caused no effects on blood flow in the embryo-larval zebrafish. Therefore, it is likely that the lower blood flow rate also seen in our study indicates effects mainly caused by exposure to the PCBs, and not the co-exposure with PS (as exposure to PS only did not cause a statistically significant effect on cardiac flow rate). PCB body-burdens in humans are typically correlated with hypertension or high blood pressure (Goncharov et al., 2011; Perkins et al., 2016). It is therefore unclear whether the lowered blood flow observed in our study (**Figure 9(b)**) indicates initial vascular damage, which may later manifest as hypertension. Therefore, the inclusion of cardiac morphology and functions as biomarkers may allude to common mechanisms of adverse effects between wildlife and humans exposed to persistent (PAHs, PCBs) and/or emerging (microplastics) pollutants.

Texas A&M University at Galveston
1001 Texas Clipper Road
Galveston, TX 77554

5. Conclusions

In this study we showed that exposures to mixtures of PAHs or PCBs strongly induced a CYP450 biotransformation response (i.e., EROD activity), which also corresponded with an elevated metabolic rate (i.e., MO_2). The elevated metabolic rate likely reflects the increased metabolic demand for molecular oxygen (O_2), which in turn satisfies the increased catalytic mono-oxygenation reactions that are catalyzed by CYP450s. Exposure of fish to only polystyrene (PS) microplastics particles in suspension caused no statistically significant effect on any of the biomarkers measured. However, co-exposure of the fish to PHE + PS or PCB 81 + PS induced MO_2 activity by 70% and 57% respectively relative to their respective solvent control group (0.1% DMSO). Although these increases were not statistically significant. Finally, we observed a statistically significant decrease in cardiac blood flow activity in fish exposed to PCB 18, 81, and 105; and co-exposed to PCB 18 + PS, PCB 81 + PS, and PCB 105 + PS. We postulate this effect to be more potently caused by exposure to the PCBs, as exposure to PS microplastics only showed no effects on blood flow. Our studies show the utility of using *in vivo* EROD activity as a likely proxy for MO_2 measurements for exposure assessments to PAHs and PCBs. And the importance of including cardiac function biomarkers in the toxicity assessments of persistent (PAHs, PCBs) and/or emerging (microplastics) pollutants.

Texas A&M University at Galveston
1001 Texas Clipper Road
Galveston, TX 77554

Objective 4: Promote Educational Outreach on the Science of Ecosystem Health Monitoring

Texas A&M University at Galveston
1001 Texas Clipper Road
Galveston, TX 77554

1. Summary of Educational Outreach Activities

Public educational outreach was engaged with on July 27th, 2022. Twenty-four high school senior students attending the summer TAMUG Sea Camp program participated in a hands-on Toxicology laboratory experiment led by Dr. David Hala and Mr. Asif Mortuza (graduate student recruited on the MBMT project) (**Figure 1**). The lab involved generating a dose-response curve of daphnia (*Daphnia magna*) immobility versus increasing saline concentrations. The purpose of this lab was to demonstrate how to experimentally determine safe versus adverse levels of a chemical, given its exposure effects on an observable biological endpoint (such as mobility in daphnia).

Three additional outreach activities were also performed on the nature of plastics pollution in coastal and marine environments as part of the TAMUG Sea Camp program. These activities were led by Dr. Karl Kaiser, and his graduate students: Marcus Wharton, Emily Summers, and Katie Miller. The Dates of the activities were:

Ocean Conservation Camp: June 14th, 2022

Ocean Careers Awareness: June 27th, 2022

Marine Science Research: July 27th, 2022

All activities were structured to give students an overview of current issues related to plastics and microplastics pollution in coastal and marine environments and demonstrate collection and analysis of microplastics in various samples collected along Galveston beaches. Students learned to use analytical techniques to identify plastics such as infrared spectroscopy. At the end of the

Texas A&M University at Galveston
1001 Texas Clipper Road
Galveston, TX 77554

class, students visited Dr. Kaiser's research lab, and were given a short introduction on the state-of-the-art analysis of microplastics in biological tissues using Py-GCMS/MS.

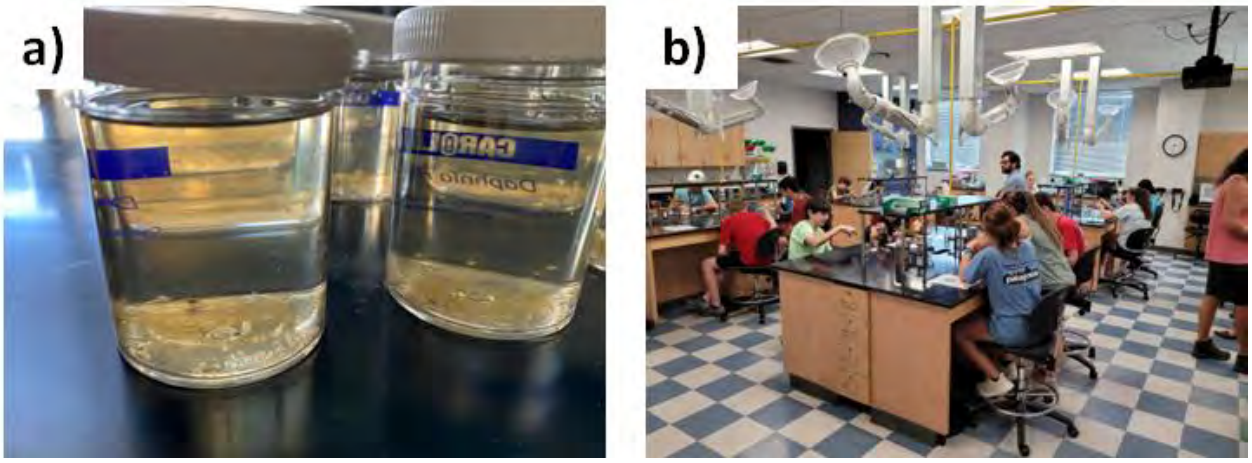

Figure 1. Images showing the Toxicology lab performed as part of educational outreach on July 27th, 2022. Senior high school students (from various regional schools) participated in a hands-on lab to study how dose-response assessments are used to assess the safety of chemicals. The lab utilized live daphnia **(a)** and involved twenty-four students in a hands-on lab **(b)**.

2. TAMUG Sea Camp Toxicology Lab Protocol

Acute Toxicity Test using *Daphnia* sp.

1. Objectives

After completing this experiment, you should be able to:

- Explain the principle of dose-response toxicity testing.
- Record observations associated with an *in vivo* toxicity test.

Texas A&M University at Galveston
1001 Texas Clipper Road
Galveston, TX 77554

2. Introduction

Pharmaceutical and agrochemicals for personal and commercial use have to undergo extensive regulatory testing using 'sentinel' wildlife species for both environmental risk assessment and hazard classification. The toxicity data generated from such tests (i.e., effects on organism health, survival etc.) are used by regulatory agencies to decide on hazard classification and risk assessment (such as the calculation of Predicted No Effect Concentration – PNEC) of the substance.

In this practical we will use a modified OECD 202 test guideline to perform an acute toxicity test using *Daphnia magna* (**Fig. 1**). The original 24 hours duration of the OECD 202 guideline has been shortened to ~0.5 hours. This class practical aims to demonstrate a key aspect of toxicity testing, i.e., the generation of concentration-response data to help determine a harmful and/or safe level of a chemical.

Fig. 1. Photo of *Daphnia magna* (from: https://it.wikipedia.org/wiki/Daphnia_magna).

3. Summary of Lab Experiment

Toxicity tests using *Daphnia magna* aim to estimate a test chemical concentration required to immobilize 50% of the *Daphnia* after exposure. Herein, immobilization defines those organisms not able to swim within a few seconds (~15 seconds) after gentle agitation to the test container. Toxicity testing requires the use of a geometric concentration series. The highest concentration tested is expected to result in 100% immobilization and should not exceed 1 gram/Liter concentration. In contrast, the lowest concentration tested should (preferably) give no observable adverse effect.

4. Materials

- Graduated medicine cups.
- Measuring cylinder.
- One *Daphnia* culture per team (~30-40 organisms per culture).
- Plastic transfer pipettes.
- 2% Sodium Chloride (NaCl) solution.
- Culture water (0% salt).

Texas A&M University at Galveston
1001 Texas Clipper Road
Galveston, TX 77554

5. Experimental Procedure

(a) Salt Solution Preparation

- A 2% concentrated salt solution will be prepared for you.
- Prepare a dilution series of salt solutions using a measuring cylinder and graduated medicine cups.
- A simple and quick way to prepare the dilution series is as follows:
    - Pour ~30 mL of 2% salt solution into the first medicine cup. From this solution, use a plastic transfer pipette to aliquot ~15 mL into a new graduated medicine cup already containing 15 mL of culture water (i.e., fill up to the 30 mL mark) to make the 1% salt solution.
    - Once again, transfer ~15 mL of the 1% salt solution into a new medicine cup already containing 15 mL of culture water to make the 0.5 % salt solution.
    - Repeat until the 0.25% salt solution (you can discard 15 mL of volume from this last salt solution to ensure that all medicine cups have the same volume.
    - The 0% salt solution will simply be 15 mL of culture water only.
    - The proposed dilution series are summarized in **Table 1.**

Table 1. Summary of the dilutions needed to prepare the various salt solutions.

Salt Solution Concentration	Amount of Salt Stock Solution	Amount of Culture Water
2%	30 mL	--
1.0%	15 mL of 2% Salt Solution	15 mL
0.5%	15 mL of 1% Salt Solution	15 mL
0.25%	15 mL of 0.5% Salt Solution	15 mL
0%	0 mL	15 mL

(b) Effects of Salinity Exposure on Daphnia mobility

- Using one *Daphnia* culture per group, transfer between 6 organisms (using small plastic graduated transfer pipettes) to each cup and observe the daphnids. Note the time the daphnids were introduced: _____.
- After 5, 10 and 20 minutes, count the number of *Daphnia* that are immobile and observe the behavior of the living *Daphnia*.
- Record your observations in **Table 2**.

Texas A&M University at Galveston
1001 Texas Clipper Road
Galveston, TX 77554

Table 2. Record of toxicity effect data, such as numbers of immobile *Daphnia* and accompanying observations. An example calculation to calculate % immobility is shown if n=6 daphnia are used per cup.

Salt Concentration (%)	Number of Immobile *Daphnia*			Example Calculation for Total Numbers Immobile (or % Immobile)
	5 min	10 min	20 min	
2%				**6 ((6/6)*100 = 100% immobile)**
1.0%				**5 ((5/6)*100 = 83% immobile)**
0.5%				**2 ((2/6)*100 = 33% immobile)**
0.25%				**0 (0% immobile)**
0%				**1 ((1/6)*100 = 17% immobile)**

6. Data Analysis and Interpretation

- Graph the % salt concentration (independent variable) versus total % immobility data (dependent variable) on the chart grid provided in **Fig 2**.
- Using your graph, approximately estimate the EC_{50} and NOEC concentrations (if relevant).

Texas A&M University at Galveston
1001 Texas Clipper Road
Galveston, TX 77554

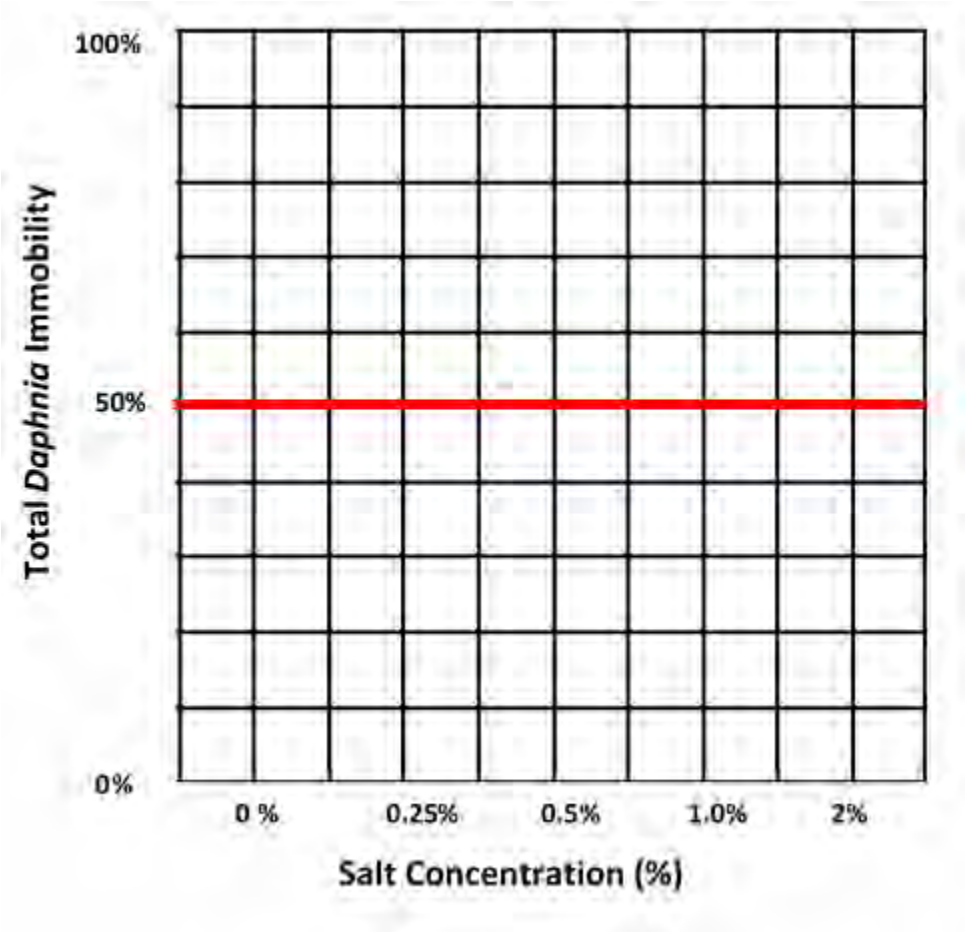

Fig. 2. Graph the effect of increasing salinity exposure on *Daphnia* immobility.

Estimated EC_{50}: _____.

Estimated NOEC: _____.

References

ATSDR, 2022. Guidance for Calculating Benzo(a)pyrene Equivalents for Cancer Evaluations of Polycyclic Aromatic Hydrocarbons. Agency for Toxic Substances and Disease Registry.

ATSDR, 2023. What Are Polychlorinated Biphenyls (PCBs)? Case Studies, Vol. 2023. Center for Disease Control.

Abayi, J. J. M., Gore, C. T., Nagawa, C., Bandowe, B. A. M., Matovu, H., Mubiru, E., Ngeno, E. C., Odongo, S., Sillanpää, M., Ssebugere, P., 2021. Polycyclic aromatic hydrocarbons in sediments and fish species from the White Nile, East Africa: Bioaccumulation potential, source apportionment, ecological and health risk assessment. Environmental Pollution 278, 116855.

Abramowicz, D. A., 1995. Aerobic and anaerobic PCB biodegradation in the environment. Environmental health perspectives 103, 97-99.

Albaiges, J., Farran, A., Soler, M., Gallifa, A., Martin, P., 1987. Accumulation and distribution of biogenic and pollutant hydrocarbons, PCBs and DDT in tissues of western Mediterranean fishes. Marine Environmental Research 22, 1-18.

Alpizar, F., Carlsson, F., Lanza, G., Carney, B., Daniels, R. C., Jaime, M., Ho, T., Nie, Z., Salazar, C., Tibesigwa, B., Wahdera, S., 2020. A framework for selecting and designing policies

to reduce marine plastic pollution in developing countries. Environmental Science & Policy 109, 25-35, doi:https://doi.org/10.1016/j.envsci.2020.04.007.

Anchondo, C., 2019. Environmentalists take petrochemical giant Formosa to court over plastics pollution. The Texas Tribune.

Ando, S., Mori, Y., Nakamura, K., Sugawara, A., 1993. Characteristics of Lipid Accumulation Types in Five Species of Fish. Nippon Suisan Gakkaishi 59, 1559-1564.

Andrady, A. L., 2011. Microplastics in the marine environment. Marine pollution bulletin 62, 1596-1605.

Andrady, A. L., Neal, M. A., 2009. Applications and societal benefits of plastics. Philos Trans R Soc Lond B Biol Sci 364, 1977-84, doi:10.1098/rstb.2008.0304.

Arman, N. Z., Salmiati, S., Aris, A., Salim, M. R., Nazifa, T. H., Muhamad, M. S., Marpongahtun, M., 2021. A review on emerging pollutants in the water environment: Existences, health effects and treatment processes. Water 13, 3258.

Arrington, D. A., Davidson, B. K., Winemiller, K. O., Layman, C. A., 2006. Influence of life history and seasonal hydrology on lipid storage in three neotropical fish species. Journal of Fish Biology 68, 1347-1361.

Texas A&M University at Galveston
1001 Texas Clipper Road
Galveston, TX 77554

Assas, M., Qiu, X., Chen, K., Ogawa, H., Xu, H., Shimasaki, Y., Oshima, Y., 2020. Bioaccumulation and reproductive effects of fluorescent microplastics in medaka fish. Marine Pollution Bulletin 158, 111446, doi:https://doi.org/10.1016/j.marpolbul.2020.111446.

Bacosa, H. P., Steichen, J., Kamalanathan, M., Windham, R., Lubguban, A., Labonté, J. M., Kaiser, K., Hala, D., Santschi, P. H., Quigg, A., 2020. Polycyclic aromatic hydrocarbons (PAHs) and putative PAH-degrading bacteria in Galveston Bay, TX (USA), following Hurricane Harvey (2017). Environ Sci Pollut Res Int 27, 34987-34999, doi:10.1007/s11356-020-09754-5.

Bagatto, B., Pelster, B., Burggren, W., 2001. Growth and metabolism of larval zebrafish: effects of swim training. Journal of Experimental Biology 204, 4335-4343.

Ballschmiter, K., Klingler, D., Ellinger, S., Hackenberg, R., 2005. High-resolution gas chromatography retention data as a basis for estimation of the octanol–water distribution coefficients (Kow) of PCB: the effect of experimental conditions. Analytical and bioanalytical chemistry 382, 1859-1870.

Barboza, L. G. A., Vieira, L. R., Branco, V., Figueiredo, N., Carvalho, F., Carvalho, C., Guilhermino, L., 2018. Microplastics cause neurotoxicity, oxidative damage and energy-related changes and interact with the bioaccumulation of mercury in the European seabass, Dicentrarchus labrax (Linnaeus, 1758). Aquatic toxicology 195, 49-57.

Texas A&M University at Galveston
1001 Texas Clipper Road
Galveston, TX 77554

Barrionuevo, W., Burggren, W., 1999. O2 consumption and heart rate in developing zebrafish (Danio rerio): influence of temperature and ambient O2. American Journal of Physiology-Regulatory, Integrative and Comparative Physiology 276, R505-R513.

Barrionuevo, W., Fernandes, M., Rocha, O., 2010. Aerobic and anaerobic metabolism for the zebrafish, Danio rerio, reared under normoxic and hypoxic conditions and exposed to acute hypoxia during development. Brazilian journal of biology 70, 425-434.

Barron, M. G., Heintz, R., Rice, S. D., 2004. Relative potency of PAHs and heterocycles as aryl hydrocarbon receptor agonists in fish. Marine Environmental Research 58, 95-100, doi:https://doi.org/10.1016/j.marenvres.2004.03.001.

Beischlag, T. V., Luis Morales, J., Hollingshead, B. D., Perdew, G. H., 2008. The aryl hydrocarbon receptor complex and the control of gene expression. Critical reviews in eukaryotic gene expression 18, 207-250.

Berdutina, A., Neklyudov, A., Ivankin, A., Karpo, B., Mitaleva, S., 2000. Comparison of proteolytic activities of the enzyme complex from mammalian pancreas and pancreatin. Applied Biochemistry and Microbiology 36, 363-367.

Berg, M., Birnbaum, L., Denison, M., De, M., Farland, W., Feeley, M., Fiedler, H., Håkansson, H., Hanberg, A., Haws, L., Rose, M., Safe, S., Schrenk, D., Tohyama, C., Tritscher, A., Tuomisto, J., Tysklind, M., Walker, N., Peterson, R., 2006. REVIEW The 2005 World Health Organization

Reevaluation of Human and Mammalian Toxic Equivalency Factors for Dioxins and Dioxin-Like Compounds. Toxicological Sciences 93, 223-241.

Bhattacharya, A., Khare, S., 2022. Ecological and toxicological manifestations of microplastics: current scenario, research gaps, and possible alleviation measures. Journal of Environmental Science and Health, Part C 38, 1-20.

Birnbaum, L. S., DeVito, M. J., 1995. Use of toxic equivalency factors for risk assessment for dioxins and related compounds. Toxicology 105, 391-401, doi:10.1016/0300-483x(95)03237-a.

Black, J. A., Birge, W. J., Westerman, A. G., Francis, P. C., 1983. Comparative aquatic toxicology of aromatic hydrocarbons. Fundamental and Applied Toxicology 3, 353-358.

Blumer, M., 1976. Polycyclic aromatic compounds in nature. Scientific American 234, 34-45.

Bodin, N., Tapie, N., Le Ménach, K., Chassot, E., Elie, P., Rochard, E., Budzinski, H., 2014. PCB contamination in fish community from the Gironde Estuary (France): Blast from the past. Chemosphere 98, 66-72.

Bour, A., Haarr, A., Keiter, S., Hylland, K., 2018. Environmentally relevant microplastic exposure affects sediment-dwelling bivalves. Environmental pollution 236, 652-660.

Bourez, S., Van den Daelen, C., Le Lay, S., Poupaert, J., Larondelle, Y., Thomé, J.-P., Schneider, Y.-J., Dugail, I., Debier, C., 2013. The dynamics of accumulation of PCBs in cultured adipocytes vary with the cell lipid content and the lipophilicity of the congener. Toxicology letters 216, 40-46.

Boyle, R. H., Highland, J. H., 1979. The persistence of PCBs. Environment: Science and Policy for Sustainable Development 21, 6-37.

Brandts, I., Cánovas, M., Tvarijonaviciute, A., Llorca, M., Vega, A., Farré, M., Pastor, J., Roher, N., Teles, M., 2022. Nanoplastics are bioaccumulated in fish liver and muscle and cause DNA damage after a chronic exposure. Environmental research 212, 113433.

Brandts, I., Teles, M., Gonçalves, A., Barreto, A., Franco-Martinez, L., Tvarijonaviciute, A., Martins, M., Soares, A., Tort, L., Oliveira, M., 2018. Effects of nanoplastics on Mytilus galloprovincialis after individual and combined exposure with carbamazepine. Science of the total environment 643, 775-784.

Brennecke, D., Duarte, B., Paiva, F., Caçador, I., Canning-Clode, J., 2016. Microplastics as vector for heavy metal contamination from the marine environment. Estuarine, Coastal and Shelf Science 178, 189-195.

Brett, J. R., 1964. The respiratory metabolism and swimming performance of young sockeye salmon. Journal of the Fisheries Board of Canada 21, 1183-1226.

Bright, D. A., Grundy, S. L., Reimer, K. J., 1995. Differential bioaccumulation of non-ortho-substituted and other PCB congeners in coastal Arctic invertebrates and fish. Environmental science & technology 29, 2504-2512.

Browne, M. A., Dissanayake, A., Galloway, T. S., Lowe, D. M., Thompson, R. C., 2008. Ingested microscopic plastic translocates to the circulatory system of the mussel, Mytilus edulis (L.). Environmental science & technology 42, 5026-5031.

Bruss, Z. S., Raja, A., 2019. Physiology, stroke volume.

Brázová, T., Hanzelová, V., Miklisová, D., Šalgovičová, D., Turčeková, Ľ., 2012. Biomonitoring of polychlorinated biphenyls (PCBs) in heavily polluted aquatic environment in different fish species. Environmental Monitoring and Assessment 184, 6553-6561.

Budzinski, H., Jones, I., Bellocq, J., Pierard, C., Garrigues, P., 1997. Evaluation of sediment contamination by polycyclic aromatic hydrocarbons in the Gironde estuary. Marine chemistry 58, 85-97.

Burns, E. E., Boxall, A. B. A., 2018. Microplastics in the aquatic environment: Evidence for or against adverse impacts and major knowledge gaps. Environmental Toxicology and Chemistry 37, 2776-2796, doi:https://doi.org/10.1002/etc.4268.

Bustamante, J., Arana, G., de Diego, A., Madariaga, J. M., 2012. The use of SPMDs and implanted oysters for monitoring PAHs and PCBs in an aquatic environment in the estuary of Urdaibai (Western Pyrenees). Environ. Eng. Manag. J 11, 1707-1714.

CSB, 2006. Chemical Safety Board (CSB): CSB Issues Case Study of Formosa Plastics Point Comfort, Texas, Fire and Explosions: Unprotected Piping, Non-Fireproofed Structures, Lack of Automatic Shutoff Valves Noted as Causes; Flame-Resistant Clothing Recommended. Accessed on-line (1/20/2025): https://www.csb.gov/csb-issues-case-study-of-formosa-plastics-point-comfort-texas-fire-and-explosions-unprotected-piping-non-fireproofed-structures-lack-of-automatic-shutoff-valves-noted-as-causes-flame-resistant-clothing-recommended/.

Carpenter, D. O., 1998. Polychlorinated biphenyls and human health. International journal of occupational medicine and environmental health 11, 291-303.

Carro, N., García, I., Ignacio, M., Mouteira, A., 2018. Polychlorinated dibenzo-P-dioxins and dibenzofurans (PCDD/Fs) and dioxin-like polychlorinated biphenyls (dl-PCBS) in bivalve mollusk from Galician Rías (NW, SPAIN). Chemosphere 197, 782-792.

census.gov, 2019. Coastline America, Accessed on-line on 1/5/2023: https://www.census.gov/content/dam/Census/library/visualizations/2019/demo/coastline-america.pdf.

comptroller.texas.gov, 2020. Manufacturing in the Gulf Coast Region, Accessed on-line 1/5/2024: https://comptroller.texas.gov/economy/economic-data/manufacturing/2020/gulf-coast.php.

Cherr, G. N., Fairbairn, E. A., Whitehead, A., 2017. Impacts of Petroleum-Derived Pollutants on Fish Development. Annual review of animal biosciences 5, 185-203.

Choi, H., Harrison, R., Komulainen, H., Saborit, J. M. D., 2010. Polycyclic aromatic hydrocarbons. WHO guidelines for indoor air quality: selected pollutants. World Health Organization.

Cole, M., Lindeque, P., Halsband, C., Galloway, T. S., 2011. Microplastics as contaminants in the marine environment: a review. Marine pollution bulletin 62, 2588-2597.

Collins, J., Brown, J., Dawson, S., Marty, M., 1991. Risk assessment for benzo [a] pyrene. Regulatory toxicology and pharmacology 13, 170-184.

Conkle, J. L., 2018. San Antonio Bay Estuarine Waterkeeper and S. Diane Wilson vs. Formosa Plastics Corp.

Cullen, J. A., Marshall, C. D., Hala, D., 2019. Integration of multi-tissue PAH and PCB burdens with biomarker activity in three coastal shark species from the northwestern Gulf of Mexico. Sci Total Environ 650, 1158-1172, doi:10.1016/j.scitotenv.2018.09.128.

Texas A&M University at Galveston
1001 Texas Clipper Road
Galveston, TX 77554

DARRP, 2014. Texas City Y | Oil Spills | Damage Assessment, Remediation, and Restoration Program. NOAA.

DSHS, 2011. Characterization of Potential Adverse Health Effects Associated with Consuming Fish from Sabine Lake, Texas, 1 - 42.

Dawson, A., Huston, W., Kawaguchi, S., King, C., Cropp, R., Wild, S., Eisenmann, P., Townsend, K., Bengtson Nash, S., 2018. Uptake and depuration kinetics influence microplastic bioaccumulation and toxicity in Antarctic krill (Euphausia superba). Environmental science & technology 52, 3195-3201.

Deblonde, T., Cossu-Leguille, C., Hartemann, P., 2011. Emerging pollutants in wastewater: A review of the literature. International Journal of Hygiene and Environmental Health 214, 442-448, doi:https://doi.org/10.1016/j.ijheh.2011.08.002.

Delzell, E., Doull, J., Giesy, J., Mackay, D., Munro, I., Williams, G., 1994. Polychlorinated Biphenyls. Regulatory Toxicology and Pharmacology 20, S187-S307.

Deng, Y., Zhang, Y., Lemos, B., Ren, H., 2017. Tissue accumulation of microplastics in mice and biomarker responses suggest widespread health risks of exposure. Scientific reports 7, 1-10.

Denison, M. S., Pandini, A., Nagy, S. R., Baldwin, E. P., Bonati, L., 2002. Ligand binding and activation of the Ah receptor. Chem Biol Interact 141, 3-24.

Detore, D., 2018. Formosa: PE, PP capacity expansions underway in Texas. Plastics News.

Ding, J., Zhang, S., Razanajatovo, R. M., Zou, H., Zhu, W., 2018. Accumulation, tissue distribution, and biochemical effects of polystyrene microplastics in the freshwater fish red tilapia (Oreochromis niloticus). Environmental pollution 238, 1-9.

Duis, K., Coors, A., 2016. Microplastics in the aquatic and terrestrial environment: sources (with a specific focus on personal care products), fate and effects. Environmental Sciences Europe 28, 1-25.

EPA, 2012. Case Summary: Settlement with Formosa Plastics Corporation for Site-Wide Corrective Actions at Point Comfort, Texas Facility. United States Environmental Protection Agency.

EPA, 2017. IRIS Toxicological Review of Benzo[A]Pyrene (Final Report) | IRIS | US EPA.

Ehrich, M. K., Harris, L. A., 2015. A review of existing eastern oyster filtration rate models. Ecological Modelling 297, 201-212.

Eisler, R., & Belisle, A. A., 1996. Planar PCB hazards to fish, wildlife, and invertebrates: a synoptic review. US Department of the Interior, National Biological Service.

Elangovan, S., Pandian, S. B. S., SJ, G., Joshi, S. J., 2019. Polychlorinated biphenyls (PCBs): Environmental fate, challenges and bioremediation. Microbial metabolism of xenobiotic compounds, 165-188.

Eneh, O. C., 2011. A review on petroleum: source, uses, processing, products, and the environment. Journal of Applied Sciences 11, 2084-2091.

FDA, 2010. Protocol for Interpretation and Use of Sensory Testing and Analytical Chemistry Results for Re-Opening Oil-Impacted Areas Closed to Seafood Harvesting Due to The Deepwater Horizon Oil Spill. Vol. 2023. FDA, fda.gov.

Finklea, B., Miller, G., Busbee, D., 2000. Polychlorinated biphenyl residues in blubber of male Atlantic bottlenose dolphins (Tursiops truncatus) that stranded and died at Matagorda Bay. Bulletin of environmental contamination and toxicology 64, 323-332.

Fisher, M., 2016. Recreational Fishery Landings of the Matagorda/Lavaca Bay System from 1981-2016

Fisher, W. S., Oliver, L. M., Winstead, J. T., Long, E. R., 2000. A survey of oysters Crassostrea virginica from Tampa Bay, Florida: associations of internal defense measurements with contaminant burdens. Aquatic Toxicology 51, 115-138.

Frank, D. S., Mora, M. A., Sericano, J. L., Blankenship, A. L., Kannan, K., Giesy, J. P., 2001. Persistent organochlorine pollutants in eggs of colonial waterbirds from Galveston Bay and East Texas, USA. Environmental Toxicology and Chemistry: An International Journal 20, 608-617.

Fry, F., 1971. The effect of environmental factors on the physiology of fish. Fish physiology, Vol. 6. Elsevier, pp. 1-98.

Gall, S. C., Thompson, R. C., 2015. The impact of debris on marine life. Marine pollution bulletin 92, 170-179.

Gavrilescu, M., Demnerová, K., Aamand, J., Agathos, S., Fava, F., 2015. Emerging pollutants in the environment: present and future challenges in biomonitoring, ecological risks and bioremediation. New Biotechnology 32, 147-156, doi:https://doi.org/10.1016/j.nbt.2014.01.001.

Geissen, V., Mol, H., Klumpp, E., Umlauf, G., Nadal, M., van der Ploeg, M., van de Zee, S. E. A. T. M., Ritsema, C. J., 2015. Emerging pollutants in the environment: A challenge for water resource management. International Soil and Water Conservation Research 3, 57-65, doi:https://doi.org/10.1016/j.iswcr.2015.03.002.

Giesy, J. P., Kannan, K., 1998. Dioxin-like and non-dioxin-like toxic effects of polychlorinated biphenyls (PCBs): implications for risk assessment. Critical reviews in toxicology 28, 511-569.

Goncharov, A., Pavuk, M., Foushee, H. R., Carpenter, D. O., 2011. Blood pressure in relation to concentrations of PCB congeners and chlorinated pesticides. Environ Health Perspect 119, 319-25, doi:10.1289/ehp.1002830.

Green, C. S., Morris, J. M., Magnuson, J. T., Leads, R. R., Lay, C. R., Gielazyn, M., Rosman, L., Schlenk, D., Roberts, A. P., 2025. Exposure to the Polychlorinated biphenyl mixture Aroclor 1254 elicits neurological and cardiac developmental effects in early life stage zebrafish (Danio rerio). Chemosphere 371, 144023, doi:https://doi.org/10.1016/j.chemosphere.2024.144023.

Green, R. M., Hodges, N. J., Chipman, J. K., O'Donovan, M. R., Graham, M., 2008. Reactive oxygen species from the uncoupling of human cytochrome P450 1B1 may contribute to the carcinogenicity of dioxin-like polychlorinated biphenyls. Mutagenesis 23, 457-63, doi:10.1093/mutage/gen035.

Gregory, M. R., 2009. Environmental implications of plastic debris in marine settings--entanglement, ingestion, smothering, hangers-on, hitch-hiking and alien invasions. Philos Trans R Soc Lond B Biol Sci 364, 2013-25, doi:10.1098/rstb.2008.0265.

Grizzle, R. E., Ward, K. M., Peter, C. R., Cantwell, M., Katz, D., Sullivan, J., 2017. Growth, morphometrics, and nutrient content of farmed eastern oysters, Crassostrea virginica (Gmelin), in New Hampshire, USA. Aquac Res 48, 1525-1537, doi:10.1111/are.12988.

Guengerich, F. P., 2018. Mechanisms of Cytochrome P450-Catalyzed Oxidations. ACS Catal 8, 10964-10976, doi:10.1021/acscatal.8b03401.

Guidetti, G. P., Rigosi, G. L., Marzola, R., 1996. The use of polypropylene in pipeline coatings. Progress in Organic Coatings 27, 79-85, doi:https://doi.org/10.1016/0300-9440(95)00523-4.

Gómara, B., Bordajandi, L. R., Fernández, M. A., Herrero, L., Abad, E., Ábalos, M., Rivera, J., González, M. J. é., 2005. Levels and trends of polychlorinated dibenzo-p-dioxins/Furans (PCDD/Fs) and Dioxin-like Polychlorinated Biphenyls (PCBs) in Spanish commercial fish and shellfish products, 1995− 2003. Journal of agricultural and food chemistry 53, 8406-8413.

HARC, 2014. Oil spills - a continual risk for Galveston Bay. Houston Advanced Research Center (HARC).

Hays, K., 2019. Formosa Plastics' Texas polyethylene plant operational, second plant to come online in December. S&P Global.

Hernout, B., Leleux, J., Lynch, J., Ramaswamy, K., Faulkner, P., Matich, P., Hala, D., 2020. The integration of fatty acid biomarkers of trophic ecology with pollutant body-burdens of PAHs and PCBs in four species of fish from Sabine Lake, Texas. Environmental Advances 1, 100001, doi:https://doi.org/10.1016/j.envadv.2020.100001.

Texas A&M University at Galveston
1001 Texas Clipper Road
Galveston, TX 77554

Hill, L. K., Sollers, I., & Thayer, J., 2011. Evaluation of a simple estimation method for the derivation of cardiac output from arterial blood pressure and heart rate. Biomed Sciences Instrumentation, 48, 165-170.

Hoage, T., Ding, Y., Xu, X., 2012. Quantifying cardiac functions in embryonic and adult zebrafish. Cardiovascular development: methods and protocols, 11-20.

Honda, M., Suzuki, N., 2020. Toxicities of polycyclic aromatic hydrocarbons for aquatic animals. International journal of environmental research and public health 17, 1363.

Hong, J., Kima, H. Y., Kim, D. G., Seo, J., Kimb, K. J., 2004. Rapid determination of chlorinated pesticides in fish by freezing-lipid filtration, solid-phase extraction and gas chromatography-mass spectrometry. J Chromatogr A 1038, 27-35, doi:10.1016/j.chroma.2004.03.003.

Horton, A. A., Walton, A., Spurgeon, D. J., Lahive, E., Svendsen, C., 2017. Microplastics in freshwater and terrestrial environments: Evaluating the current understanding to identify the knowledge gaps and future research priorities. Science of The Total Environment 586, 127-141, doi:https://doi.org/10.1016/j.scitotenv.2017.01.190.

Hossain, M. T., Shahid, M. A., Mahmud, N., Habib, A., Rana, M. M., Khan, S. A., Hossain, M. D., 2024. Research and application of polypropylene: a review. Discover Nano 19, 2.

Hu, N., Yost, H. J., Clark, E. B., 2001. Cardiac morphology and blood pressure in the adult zebrafish. The Anatomical Record: An Official Publication of the American Association of Anatomists 264, 1-12.

Hylland, K., 2006. Polycyclic aromatic hydrocarbon (PAH) ecotoxicology in marine ecosystems. Journal of Toxicology and Environmental Health, Part A 69, 109-123.

Hägg, F., Herzke, D., Nikiforov, V. A., Booth, A. M., Sperre, K. H., Sørensen, L., Creese, M. E., Halsband, C., 2023. Ingestion of car tire crumb rubber and uptake of associated chemicals by lumpfish (Cyclopterus lumpus). Frontiers in Environmental Science 11, doi:10.3389/fenvs.2023.1219248.

Incardona, J. P., Collier, T. K., Scholz, N. L., 2004. Defects in cardiac function precede morphological abnormalities in fish embryos exposed to polycyclic aromatic hydrocarbons. Toxicology and Applied Pharmacology 196, 191-205, doi:https://doi.org/10.1016/j.taap.2003.11.026.

Incardona, J. P., Day, H. L., Collier, T. K., Scholz, N. L., 2006. Developmental toxicity of 4-ring polycyclic aromatic hydrocarbons in zebrafish is differentially dependent on AH receptor isoforms and hepatic cytochrome P4501A metabolism. Toxicol Appl Pharmacol 217, 308-21, doi:10.1016/j.taap.2006.09.018.

Incardona, J. P., Gardner, L. D., Linbo, T. L., Brown, T. L., Esbaugh, A. J., Mager, E. M., Stieglitz, J. D., French, B. L., Labenia, J. S., Laetz, C. A., Tagal, M., Sloan, C. A., Elizur, A., Benetti, D. D., Grosell, M., Block, B. A., Scholz, N. L., 2014. Deepwater Horizon crude oil impacts the developing hearts of large predatory pelagic fish. Proc Natl Acad Sci U S A 111, E1510-8, doi:10.1073/pnas.1320950111.

Jabłońska, J., Tawfik, D. S., 2022. Innovation and tinkering in the evolution of oxidases. Protein Sci 31, e4310, doi:10.1002/pro.4310.

Jafarabadi, A. R., Bakhtiari, A. R., Yaghoobi, Z., Yap, C. K., Maisano, M., Cappello, T., 2019. Distributions and compositional patterns of polycyclic aromatic hydrocarbons (PAHs) and their derivatives in three edible fishes from Kharg coral Island, Persian Gulf, Iran. Chemosphere 215, 835-845.

Jeong, E., Lee, J.-Y., Redwan, M., 2024. Animal exposure to microplastics and health effects: A review. Emerging Contaminants 10, 100369, doi:https://doi.org/10.1016/j.emcon.2024.100369.

Jesus, F., Pereira, J. L., Campos, I., Santos, M., Ré, A., Keizer, J., Nogueira, A., Gonçalves, F. J., Abrantes, N., Serpa, D., 2022. A review on polycyclic aromatic hydrocarbons distribution in freshwater ecosystems and their toxicity to benthic fauna. Science of the Total Environment 820, 153282.

Kannan, K., Blankenship, A., Jones, P., Giesy, J., 2000. Toxicity reference values for the toxic effects of polychlorinated biphenyls to aquatic mammals. Human and Ecological Risk Assessment 6, 181-201.

Kannan, K., Vimalkumar, K., 2021. A Review of Human Exposure to Microplastics and Insights Into Microplastics as Obesogens. Frontiers in Endocrinology 12, doi:10.3389/fendo.2021.724989.

Kennicutt, M. C., 2017. Sediment Contaminants of the Gulf of Mexico. In: Ward, C. H., (Ed.), Habitats and Biota of the Gulf of Mexico: Before the Deepwater Horizon Oil Spill: Volume 1: Water Quality, Sediments, Sediment Contaminants, Oil and Gas Seeps, Coastal Habitats, Offshore Plankton and Benthos, and Shellfish. Springer New York, New York, NY, pp. 217-273.

Lapointe, D., Vogelbein, W. K., Fabrizio, M. C., Gauthier, D. T., Brill, R. W., 2014. Temperature, hypoxia, and mycobacteriosis: effects on adult striped bass Morone saxatilis metabolic performance. Diseases of aquatic organisms 108, 113-127.

LeMoine, C. M., Kelleher, B. M., Lagarde, R., Northam, C., Elebute, O. O., Cassone, B. J., 2018. Transcriptional effects of polyethylene microplastics ingestion in developing zebrafish (Danio rerio). Environmental pollution 243, 591-600.

Lebreton, L., Egger, M., Slat, B., 2019. A global mass budget for positively buoyant macroplastic debris in the ocean. Scientific Reports 9, 12922, doi:10.1038/s41598-019-49413-5.

Lebreton, L., Slat, B., Ferrari, F., Sainte-Rose, B., Aitken, J., Marthouse, R., Hajbane, S., Cunsolo, S., Schwarz, A., Levivier, A., Noble, K., Debeljak, P., Maral, H., Schoeneich-Argent, R., Brambini, R., Reisser, J., 2018. Evidence that the Great Pacific Garbage Patch is rapidly accumulating plastic. Sci Rep 8, 4666, doi:10.1038/s41598-018-22939-w.

Lee, B. M., Shim, G. A., 2007. Dietary exposure estimation of benzo [a] pyrene and cancer risk assessment. Journal of Toxicology and Environmental Health, Part A 70, 1391-1394.

Leslie, H. A., van Velzen, M. J. M., Brandsma, S. H., Vethaak, A. D., Garcia-Vallejo, J. J., Lamoree, M. H., 2022. Discovery and quantification of plastic particle pollution in human blood. Environ Int 163, 107199, doi:10.1016/j.envint.2022.107199.

Lim, K. P., Lim, P. E., Yusoff, S., Sun, C., Ding, J., Loh, K. H., 2022. A meta-analysis of the characterisations of plastic ingested by fish globally. Toxics 10, 186.

Lipiatou, E., Saliot, A., 1991. Fluxes and transport of anthropogenic and natural polycyclic aromatic hydrocarbons in the western Mediterranean Sea. Marine chemistry 32, 51-71.

Liu, Z., Yu, P., Cai, M., Wu, D., Zhang, M., Huang, Y., Zhao, Y., 2019. Polystyrene nanoplastic exposure induces immobilization, reproduction, and stress defense in the freshwater cladoceran Daphnia pulex. Chemosphere 215, 74-81.

Lloyd, J., Lu, K., Liu, Z., 2024. Investigating concentrations and sources of polycyclic aromatic hydrocarbons in South and Central Texas bays and estuaries along the Gulf of Mexico, USA. Frontiers in Marine Science 11, 1456717.

Lo, R., Matthews, J., 2012. High-resolution genome-wide mapping of AHR and ARNT binding sites by ChIP-Seq. Toxicol Sci 130, 349-61.

Maddah, H. A., 2016. Polypropylene as a promising plastic: A review. Am. J. Polym. Sci 6, 1-11.

Markic, A., Gaertner, J.-C., Gaertner-Mazouni, N., Koelmans, A. A., 2020. Plastic ingestion by marine fish in the wild. Critical Reviews in Environmental Science and Technology 50, 657-697, doi:10.1080/10643389.2019.1631990.

Mattsson, K., Ekvall, M. T., Hansson, L. A., Linse, S., Malmendal, A., Cedervall, T., 2015. Altered behavior, physiology, and metabolism in fish exposed to polystyrene nanoparticles. Environ Sci Technol 49, 553-61, doi:10.1021/es5053655.

Miller, W. L., 2005. Minireview: regulation of steroidogenesis by electron transfer. Endocrinology 146, 2544-50, doi:10.1210/en.2005-0096.

Mintenig, S., Bäuerlein, P. S., Koelmans, A. A., Dekker, S. C., Van Wezel, A., 2018. Closing the gap between small and smaller: towards a framework to analyse nano-and microplastics in aqueous environmental samples. Environmental Science: Nano 5, 1640-1649.

Monosson, E., Ashley, J., McElroy, A., Woltering, D., Elskus, A., 2003. PCB congener distributions in muscle, liver and gonad of Fundulus heteroclitus from the lower Hudson River Estuary and Newark Bay. Chemosphere 52, 777-787.

Montuori, P., De Rosa, E., Di Duca, F., De Simone, B., Scippa, S., Russo, I., Sarnacchiaro, P., Triassi, M., 2022. Polycyclic Aromatic Hydrocarbons (PAHs) in the dissolved phase, particulate matter, and sediment of the Sele River, Southern Italy: a focus on distribution, risk assessment, and sources. Toxics 10, 401.

Moon, H.-B., Ok, G., 2006. Dietary intake of PCDDs, PCDFs and dioxin-like PCBs, due to the consumption of various marine organisms from Korea. Chemosphere 62, 1142-1152.

Moore-Eissenberg, L., 2019. No More Nurdles? Formosa's Agreement to Stop Pumping Plastics Into Lavaca Bay Is Historic. Texas Monthly.

Moorthy, B., Chu, C., Carlin, D. J., 2015. Polycyclic aromatic hydrocarbons: from metabolism to lung cancer. Toxicol Sci 145, 5-15.

NOAA, 2020. Water Cleaning Capacity of Oysters Could Mean Extra Income for Chesapeake Bay Growers. NCCOS Coastal Science Website.

NOAA, 2024. Gulf of Mexico Data Atlas - Oil and Gas Structures, accessed on-line 1/17/2024: https://www.ncei.noaa.gov/maps/gulf-data-atlas/atlas.htm?plate=Offshore%20Structures.

Naderi, A. M., Casey, J. G., Huang, M.-H., Victorio, R., Chiang, D. Y., MacRae, C., Cao, H., Gupta, V. A., 2024. Towards Precision Cardiovascular Analysis in Zebrafish: The ZACAF Paradigm. arXiv preprint arXiv:2402.09658.

Neff, J., Cox, B. A., Dixit, D., Anderson, J., 1976. Accumulation and release of petroleum-derived aromatic hydrocarbons by four species of marine animals. Marine Biology 38, 279-289.

Nilsen, B. M., Berg, K., Goksøyr, A., 1998. Induction of cytochrome P450 1A (CYP1A) in fish. A biomarker for environmental pollution. Methods Mol Biol 107, 423-38, doi:10.1385/0-89603-519-0:423.

Nolen, R. M., Faulkner, P., Ross, A. D., Kaiser, K., Quigg, A., Hala, D., 2022. PFASs pollution in Galveston Bay surface waters and biota (shellfish and fish) following AFFFs use during the ITC fire at Deer Park (March 17th–20th 2019), Houston, TX. Science of The Total Environment 805, 150361.

Noury, P., Geffard, O., Tutundjian, R., Garric, J., 2006. Non destructive in vivo measurement of ethoxyresorufin biotransformation by zebrafish prolarva: development and application. Environmental Toxicology: An International Journal 21, 324-331.

OSHA, 2005. Five employees killed in explosion; four injured. Accident Report Detail.

OSPAR, 2018. OSPAR Background document on pre-production Plastic Pellets. Accessed on-line (1/13/2025): https://www.ospar.org/documents?v=39764, 1 - 35.

Okoffo, E. D., Chan, C. M., Rauert, C., Kaserzon, S., & Thomas, K. V., 2022. Identification and Quantification of Micro-Bioplastics in Environmental Samples by Pyrolysis–Gas Chromatography–Mass Spectrometry. Environmental science & technology, 56(19), 13774-13785.

Olayinka, O. O., Adewusi, A. A., Olujimi, O. O., Aladesida, A. A., 2019. Polycyclic aromatic hydrocarbons in sediment and health risk of fish, crab and shrimp around Atlas Cove, Nigeria. Journal of Health and Pollution 9, 191204.

Oziolor, E. M., Apell, J. N., Winfield, Z. C., Back, J. A., Usenko, S., Matson, C. W., 2018. Polychlorinated biphenyl (PCB) contamination in Galveston Bay, Texas: Comparing concentrations and profiles in sediments, passive samplers, and fish. Environ Pollut 236, 609-618, doi:10.1016/j.envpol.2018.01.086.

Ozougwu, J. C., 2017. Physiology of the liver. International Journal of Research in Pharmacy and Biosciences 4, 13-24.

Patel, A. B., Shaikh, S., Jain, K. R., Desai, C., Madamwar, D., 2020. Polycyclic aromatic hydrocarbons: sources, toxicity, and remediation approaches. Frontiers in Microbiology 11, 562813.

Peng, X., Chen, G., Fan, Y., Zhu, Z., Guo, S., Zhou, J., Tan, J., 2021. Lifetime bioaccumulation, gender difference, tissue distribution, and parental transfer of organophosphorus plastic additives in freshwater fish. Environmental Pollution 280, 116948, doi:https://doi.org/10.1016/j.envpol.2021.116948.

Perkins, J. T., Petriello, M. C., Newsome, B. J., Hennig, B., 2016. Polychlorinated biphenyls and links to cardiovascular disease. Environ Sci Pollut Res Int 23, 2160-72, doi:10.1007/s11356-015-4479-6.

Persiani, E., Cecchettini, A., Ceccherini, E., Gisone, I., Morales, M. A., Vozzi, F., 2023. Microplastics: A Matter of the Heart (and Vascular System). Biomedicines 11, doi:10.3390/biomedicines11020264.

Petersen, L., Gamperl, A., 2010. Effect of acute and chronic hypoxia on the swimming performance, metabolic capacity and cardiac function of Atlantic cod (Gadus morhua). Journal of Experimental Biology 213, 808-819.

Pettersen, A. K., Marshall, D. J., White, C. R., 2018. Understanding variation in metabolic rate. Journal of Experimental Biology 221, jeb166876.

Pettersen, A. K., White, C. R., Marshall, D. J., 2016. Metabolic rate covaries with fitness and the pace of the life history in the field. Proceedings of the Royal Society B: Biological Sciences 283, 20160323.

Pitt, J. A., Trevisan, R., Massarsky, A., Kozal, J. S., Levin, E. D., Di Giulio, R. T., 2018. Maternal transfer of nanoplastics to offspring in zebrafish (Danio rerio): a case study with nanopolystyrene. Science of the Total Environment 643, 324-334.

Porta, M., Zumeta, E., 2002. Implementing the Stockholm treaty on persistent organic pollutants. Vol. 59. BMJ Publishing Group Ltd, pp. 651-652.

Priede, I. G., 1985. Metabolic scope in fishes. Fish energetics. Springer, pp. 33-64.

Provencher, J. F., Ammendolia, J., Rochman, C. M., Mallory, M. L., 2018. Assessing plastic debris in aquatic food webs: what we know and don't know about uptake and trophic transfer. Environmental Reviews 27, 304-317, doi:https://doi.org/10.1139/er-2018-0079.

Pulster, E. L., Gracia, A., Armenteros, M., Toro-Farmer, G., Snyder, S. M., Carr, B. E., Schwaab, M. R., Nicholson, T. J., Mrowicki, J., Murawski, S. A., 2020. A First Comprehensive Baseline of Hydrocarbon Pollution in Gulf of Mexico Fishes. Scientific Reports 10, 6437, doi:10.1038/s41598-020-62944-6.

Qiao, R., Deng, Y., Zhang, S., Wolosker, M. B., Zhu, Q., Ren, H., Zhang, Y., 2019. Accumulation of different shapes of microplastics initiates intestinal injury and gut microbiota dysbiosis in the gut of zebrafish. Chemosphere 236, 124334.

Qu, M., Xu, K., Li, Y., Wong, G., Wang, D., 2018. Using acs-22 mutant Caenorhabditis elegans to detect the toxicity of nanopolystyrene particles. Science of the Total Environment 643, 119-126.

Quinete, N., Schettgen, T., Bertram, J., Kraus, T., 2014. Occurrence and distribution of PCB metabolites in blood and their potential health effects in humans: a review. Environmental Science and Pollution Research 21, 11951-11972.

Rauert, C., Pan, Y., Okoffo, E. D., O'Brien, J. W., Thomas, K. V., 2022. Extraction and Pyrolysis-GC-MS analysis of polyethylene in samples with medium to high lipid content. Journal of Environmental Exposure Assessment 1, 13.

Reidy, S., Kerr, S., Nelson, J., 2000. Aerobic and anaerobic swimming performance of individual Atlantic cod. Journal of Experimental Biology 203, 347-357.

Ribeiro, F., Okoffo, E. D., O'Brien, J. W., Fraissinet-Tachet, S., O'Brien, S., Gallen, M., Samanipour, S., Kaserzon, S. L., Mueller, J. F., Galloway, T. S., Thomas, K. V., 2020. Quantitative analysis of selected plastics in high commercial value Australian seafood by Pyrolysis Gas Chromatography Mass Spectrometry. Environmental science & technology.

Ribeiro, F., Okoffo, E. D., O'Brien, J. W., O'Brien, S., Harris, J. M., Samanipour, S., Kaserzon, S., Mueller, J. F., Galloway, T., Thomas, K. V., 2021. Out of sight but not out of mind: Size fractionation of plastics bioaccumulated by field deployed oysters. Journal of Hazardous Materials Letters 2, 100021.

Rice, J., 2019. Texas A&M Water Researchers Find Waxy Residue Near Deer Park Disaster. Houston Public Media

Rochman, C. M., Kurobe, T., Flores, I., Teh, S. J., 2014. Early warning signs of endocrine disruption in adult fish from the ingestion of polyethylene with and without sorbed chemical pollutants from the marine environment. Science of the total environment 493, 656-661.

Rotkin-Ellman, M., Wong, K. K., Solomon, G. M., 2012. Seafood contamination after the BP Gulf oil spill and risks to vulnerable populations: a critique of the FDA risk assessment. Environmental health perspectives 120, 157-161.

Rowe, G. T., Fernando, H., Elferink, C., Ansari, G. A. S., Sullivan, J., Heathman, T., Quigg, A., Petronella Croisant, S., Wade, T. L., Santschi, P. H., 2021. Polycyclic aromatic hydrocarbons (PAHs) cycling and fates in Galveston Bay, Texas, USA. PLOS ONE 15, e0243734, doi:10.1371/journal.pone.0243734.

Rowlands, J. C., McEwan, I. J., Gustafsson, J. A., 1996. Trans-activation by the human aryl hydrocarbon receptor and aryl hydrocarbon receptor nuclear translocator proteins: direct interactions with basal transcription factors. Mol Pharmacol 50, 538-48.

Ryan, P. G., Moore, C. J., Van Franeker, J. A., Moloney, C. L., 2009. Monitoring the abundance of plastic debris in the marine environment. Philosophical Transactions of the Royal Society B: Biological Sciences 364, 1999-2012.

Safe, S., Bandiera, S., Sawyer, T., Robertson, L., Safe, L., Parkinson, A., Thomas, P. E., Ryan, D. E., Reik, L. M., Levin, W., et al., 1985. PCBs: structure-function relationships and mechanism of action. Environ Health Perspect 60, 47-56.

Safe, S., Hutzinger, O., 1984. Polychlorinated biphenyls (PCBs) and polybrominated biphenyls (PBBs): biochemistry, toxicology, and mechanism of action. CRC Critical Reviews in Toxicology 13, 319-395.

Salehin, N., Villarreal, C., Teranikar, T., Dubansky, B., Lee, J., & Chuong, C.-J., 2021. Assessing pressure–volume relationship in developing heart of zebrafish in-vivo. Annals of Biomedical Engineering, 1-14.

Santos, L. H. M. L. M., Insa, S., Arxé, M., Buttiglieri, G., Rodríguez-Mozaz, S., Barceló, D., 2023. Analysis of microplastics in the environment: Identification and quantification of trace

levels of common types of plastic polymers using pyrolysis-GC/MS. MethodsX 10, 102143, doi:https://doi.org/10.1016/j.mex.2023.102143.

Santos, L., Miranda, D., Hatje, V., Albergaria-Barbosa, A., Leonel, J., 2020. PCBs occurrence in marine bivalves and fish from Todos os Santos Bay, Bahia, Brazil. Marine Pollution Bulletin 154, 111070.

Senathirajah, K., Attwood, S., Bhagwat, G., Carbery, M., Wilson, S., Palanisami, T., 2021. Estimation of the mass of microplastics ingested–A pivotal first step towards human health risk assessment. Journal of Hazardous Materials 404, 124004.

Shakiba, M., Rezvani Ghomi, E., Khosravi, F., Jouybar, S., Bigham, A., Zare, M., Abdouss, M., Moaref, R., Ramakrishna, S., 2021. Nylon—A material introduction and overview for biomedical applications. Polymers for advanced technologies 32, 3368-3383.

Sharma, S., Chatterjee, S., 2017. Microplastic pollution, a threat to marine ecosystem and human health: a short review. Environ Sci Pollut Res Int 24, 21530-21547, doi:10.1007/s11356-017-9910-8.

Sigler, M., 2014. The Effects of Plastic Pollution on Aquatic Wildlife: Current Situations and Future Solutions. Water, Air, & Soil Pollution 225, 2184, doi:10.1007/s11270-014-2184-6.

Simoneit, B. R., 1985. Application of molecular marker analysis to vehicular exhaust for source reconciliations. International Journal of Environmental Analytical Chemistry 22, 203-232.

Singleman, C., Holtzman, N. G., 2014. Growth and maturation in the zebrafish, Danio rerio: a staging tool for teaching and research. Zebrafish 11, 396-406, doi:10.1089/zeb.2014.0976.

Singleman, C., Holtzman, N. G., 2021. PCB and TCDD derived embryonic cardiac defects result from a novel AhR pathway. Aquatic Toxicology 233, 105794, doi:https://doi.org/10.1016/j.aquatox.2021.105794.

Sleight, V. A., Bakir, A., Thompson, R. C., Henry, T. B., 2017. Assessment of microplastic-sorbed contaminant bioavailability through analysis of biomarker gene expression in larval zebrafish. Marine pollution bulletin 116, 291-297.

Somero, G. N., Lockwood, B. L., Tomanek, L., 2017. Biochemical adaptation: response to environmental challenges, from life's origins to the Anthropocene. Sinauer Associates, Incorporated Publishers.

Southworth, G., Beauchamp, J., Schmieder, P., 1978. Bioaccumulation potential of polycyclic aromatic hydrocarbons in Daphnia pulex. Water Research 12, 973-977.

Stafford, G. D., Huggett, R., MacGregor, A. R., Graham, J., 1986. The use of nylon as a denture-base material. Journal of Dentistry 14, 18-22, doi:https://doi.org/10.1016/0300-5712(86)90097-7.

Statista, 2025. Value of plastics industry state shipments in the United States in 2021, by select state (in billion U.S. dollars); Acessed on-line (1/28/2025): https://www.statista.com/statistics/1203105/value-of-plastics-industry-shipments-united-states-by-state/.

Steevens, J. A., Reiss, M. R., Pawlisz, A. V., 2005. A methodology for deriving tissue residue benchmarks for aquatic biota: A case study for fish exposed to 2, 3, 7, 8-tetrachlorodibenzo-p-dioxin and equivalents. Integrated Environmental Assessment and Management: An International Journal 1, 142-151.

Sui, Q., Yang, X., Sun, X., Zhu, L., Zhao, X., Feng, Z., Xia, B., Qu, K., 2024. Bioaccumulation of polycyclic aromatic hydrocarbons and their human health risks depend on the characteristics of microplastics in marine organisms of Sanggou Bay, China. Journal of Hazardous Materials 473, 134622.

Sun, M., Ding, R., Ma, Y., Sun, Q., Ren, X., Sun, Z., Duan, J., 2021. Cardiovascular toxicity assessment of polyethylene nanoplastics on developing zebrafish embryos. Chemosphere 282, 131124, doi:https://doi.org/10.1016/j.chemosphere.2021.131124.

Sverdrup, L. E., Nielsen, T., Krogh, P. H., 2002. Soil ecotoxicity of polycyclic aromatic hydrocarbons in relation to soil sorption, lipophilicity, and water solubility. Environmental science & technology 36, 2429-2435.

Texas A&M University at Galveston
1001 Texas Clipper Road
Galveston, TX 77554

TDT, 2020. Texas Port Profiles. Vol. 2024. Texas Department of Transportation.

TPWD, 2023. Spotted Seatrout (Cynoscion nebulosus). Vol. 2023. Texas Parks and Wildlife.

TPWD, 2024. Gafftopsail Catfish (Bagre marinus). Texas.gov.

TSHA, 2023. Handbook of Texas. Vol. 2022, Texas State Historical Association.

Takeshita, R., Bursian, S. J., Colegrove, K. M., Collier, T. K., Deak, K., Dean, K. M., De Guise, S., DiPinto, L. M., Elferink, C. J., Esbaugh, A. J., Griffitt, R. J., Grosell, M., Harr, K. E., Incardona, J. P., Kwok, R. K., Lipton, J., Mitchelmore, C. L., Morris, J. M., Peters, E. S., Roberts, A. P., Rowles, T. K., Rusiecki, J. A., Schwacke, L. H., Smith, C. R., Wetzel, D. L., Ziccardi, M. H., Hall, A. J., 2021. A review of the toxicology of oil in vertebrates: what we have learned following the Deepwater Horizon oil spill. J Toxicol Environ Health B Crit Rev 24, 355-394, doi:10.1080/10937404.2021.1975182.

Tang, J., Ni, X., Zhou, Z., Wang, L., Lin, S., 2018. Acute microplastic exposure raises stress response and suppresses detoxification and immune capacities in the scleractinian coral Pocillopora damicornis. Environmental pollution 243, 66-74.

Tiedje, J. M., Quensen, J. F., Chee-Sanford, J., Schimel, J. P., Boyd, S. A., 1993. Microbial reductive dechlorination of PCBs. Biodegradation 4, 231-240.

Tong, Y., Lin, L., Tao, Y., Huang, Y., Zhu, X., 2023. The occurrence, speciation, and ecological effect of plastic pollution in the bay ecosystems. Sci Total Environ 857, 159601, doi:10.1016/j.scitotenv.2022.159601.

Tresaugue, M., 2014. Oil spill befouls Matagorda Island. Houston Chronicle. Chron.

Trevisan, R., Flores-Nunes, F., Dolores, E. S., Mattos, J. J., Piazza, C. E., Sasaki, S. T., Taniguchi, S., Montone, R. C., Bícego, M. C., Dos Reis, I. M., 2017. Thiol oxidation of hemolymph proteins in oysters Crassostrea brasiliana as markers of oxidative damage induced by urban sewage exposure. Environmental toxicology and chemistry 36, 1833-1845.

Trevizo, P., 2019. Hundreds of dead fish, crabs seen on Kemah property after ship channel spill. Houston Chronicle

Ugwu, K., Herrera, A., Gómez, M., 2021. Microplastics in marine biota: A review. Mar Pollut Bull 169, 112540, doi:10.1016/j.marpolbul.2021.112540.

Umamaheswari, S., Priyadarshinee, S., Kadirvelu, K., Ramesh, M., 2021. Polystyrene microplastics induce apoptosis via ROS-mediated p53 signaling pathway in zebrafish. Chemico-biological interactions 345, 109550.

Van den Berg, M., Birnbaum, L., Bosveld, A., Brunström, B., Cook, P., Feeley, M., Giesy, J. P., Hanberg, A., Hasegawa, R., Kennedy, S. W., 1998. Toxic equivalency factors (TEFs) for PCBs, PCDDs, PCDFs for humans and wildlife. Environmental health perspectives 106, 775-792.

Vandermeulen, J., 1987. Toxicity and sublethal effects of petroleum hydrocarbons in freshwater biota. Oil in Freshwater: Chemistry, Biology, Countermeasure Technology, 267-303.

Verbruggen, E., 2012, Environmental risk limits for polycyclic aromatic hydrocarbons (PAHs): For direct aquatic, benthic, and terrestrial toxicity.

Vidal-Liñán, L., Bellas, J., Soriano, J. A., Concha-Graña, E., Muniategui, S., Beiras, R., 2016. Bioaccumulation of PCB-153 and effects on molecular biomarkers acetylcholinesterase, glutathione-S-transferase and glutathione peroxidase in Mytilus galloprovincialis mussels. Environmental Pollution 214, 885-891, doi:https://doi.org/10.1016/j.envpol.2016.04.083.

von Friesen, L. W., Granberg, M. E., Hassellöv, M., Gabrielsen, G. W., Magnusson, K., 2019. An efficient and gentle enzymatic digestion protocol for the extraction of microplastics from bivalve tissue. Marine pollution bulletin 142, 129-134.

Wang, H., Huang, W., Gong, Y., Chen, C., Zhang, T., Diao, X., 2020. Occurrence and potential health risks assessment of polycyclic aromatic hydrocarbons (PAHs) in different tissues of bivalves from Hainan Island, China. Food and Chemical Toxicology 136, 111108.

Wang, J., Tan, Z., Peng, J., Qiu, Q., Li, M., 2016. The behaviors of microplastics in the marine environment. Marine Environmental Research 113, 7-17.

Wang, L., Wu, W.-M., Bolan, N. S., Tsang, D. C. W., Li, Y., Qin, M., Hou, D., 2021. Environmental fate, toxicity and risk management strategies of nanoplastics in the environment: Current status and future perspectives. Journal of Hazardous Materials 401, 123415, doi:https://doi.org/10.1016/j.jhazmat.2020.123415.

Wang, Z., Liu, Z., Xu, K., Mayer, L. M., Zhang, Z., Kolker, A. S., Wu, W., 2014. Concentrations and sources of polycyclic aromatic hydrocarbons in surface coastal sediments of the northern Gulf of Mexico. Geochemical transactions 15, 1-12.

Wassenberg, D. M., Di Giulio, R. T., 2004. Synergistic embryotoxicity of polycyclic aromatic hydrocarbon aryl hydrocarbon receptor agonists with cytochrome P4501A inhibitors in Fundulus heteroclitus. Environ Health Perspect 112, 1658-64, doi:10.1289/ehp.7168.

Wenner, C. A., 1996. Red drum: natural history and fishing techniques in South Carolina. South Carolina State Documents Depository.

Wilson, D., 2018. Report shows plastic pollution a threat to Texas Gulf Coast, Accessed on-line (1/3/2025): https://waterkeeper.org/news/report-shows-plastic-pollution-a-threat-to-texas-gulf-coast/. Waterkeeper Alliance.

Wisse, E., De Zanger, R., Charels, K., Van Der Smissen, P., McCuskey, R., 1985. The liver sieve: considerations concerning the structure and function of endothelial fenestrae, the sinusoidal wall and the space of Disse. Hepatology 5, 683-692.

Wolska, L., Mechlińska, A., Rogowska, J., Namieśnik, J., 2012. Sources and fate of PAHs and PCBs in the marine environment. Critical reviews in environmental science and technology 42, 1172-1189.

Wood, N. J., 2014. The liver as a firewall—clearance of commensal bacteria that have escaped from the gut. Nature Reviews Gastroenterology & Hepatology 11, 391-391.

Wright, S. L., Thompson, R. C., Galloway, T. S., 2013. The physical impacts of microplastics on marine organisms: a review. Environmental pollution 178, 483-492.

Xiang, Y., Xing, Z., Liu, J., Qin, W., Huang, X., 2020. Recent advances in the biodegradation of polychlorinated biphenyls. World Journal of Microbiology and Biotechnology 36, 1-10.

Xu, F.-L., Wu, W.-J., Wang, J.-J., Qin, N., Wang, Y., He, Q.-S., He, W., Tao, S., 2011. Residual levels and health risk of polycyclic aromatic hydrocarbons in freshwater fishes from Lake Small Bai-Yang-Dian, Northern China. Ecological Modelling 222, 275-286.

Yang, D., Shi, H., Li, L., Li, J., Jabeen, K., Kolandhasamy, P., 2015. Microplastic pollution in table salts from China. Environmental science & technology 49, 13622-13627.

Texas A&M University at Galveston
1001 Texas Clipper Road
Galveston, TX 77554

Yunker, M. B., Macdonald, R. W., Goyette, D., Paton, D. W., Fowler, B. R., Sullivan, D., Boyd, J., 1999. Natural and anthropogenic inputs of hydrocarbons to the Strait of Georgia. Science of The Total Environment 225, 181-209, doi:https://doi.org/10.1016/S0048-9697(98)00362-3.

Yunker, M. B., Macdonald, R. W., Veltkamp, D. J., Cretney, W. J., 1995. Terrestrial and marine biomarkers in a seasonally ice-covered Arctic estuary — integration of multivariate and biomarker approaches. Marine Chemistry 49, 1-50, doi:https://doi.org/10.1016/0304-4203(94)00057-K.

Yunker, M. B., Macdonald, R. W., Vingarzan, R., Mitchell, R. H., Goyette, D., Sylvestre, S., 2002. PAHs in the Fraser River basin: a critical appraisal of PAH ratios as indicators of PAH source and composition. Organic Geochemistry 33, 489-515, doi:https://doi.org/10.1016/S0146-6380(02)00002-5.

Yunker, M. B., Snowdon, L. R., Macdonald, R. W., Smith, J. N., Fowler, M. G., Skibo, D. N., McLaughlin, F. A., Danyushevskaya, A., Petrova, V., Ivanov, G., 1996. Polycyclic aromatic hydrocarbon composition and potential sources for sediment samples from the Beaufort and Barents Seas. Environmental Science & Technology 30, 1310-1320.

Zhang, J., Wang, L., Trasande, L., Kannan, K., 2021. Occurrence of Polyethylene Terephthalate and Polycarbonate Microplastics in Infant and Adult Feces. Environmental Science & Technology Letters 8, 989-994, doi:10.1021/acs.estlett.1c00559.

Zhang, X., Cheng, S., Huang, X., Logan, B. E., 2010. The use of nylon and glass fiber filter separators with different pore sizes in air-cathode single-chamber microbial fuel cells. Energy & Environmental Science 3, 659-664.

Zhao, Z., Zhang, L., Cai, Y., Chen, Y., 2014. Distribution of polycyclic aromatic hydrocarbon (PAH) residues in several tissues of edible fishes from the largest freshwater lake in China, Poyang Lake, and associated human health risk assessment. Ecotoxicol Environ Saf 104, 323-31, doi:10.1016/j.ecoenv.2014.01.037.

Zhu, L., Kang, Y., Ma, M., Wu, Z., Zhang, L., Hu, R., Xu, Q., Zhu, J., Gu, X., An, L., 2024. Tissue accumulation of microplastics and potential health risks in human. Sci Total Environ 915, 170004, doi:10.1016/j.scitotenv.2024.170004.

Zitouni, N., Bousserrhine, N., Missawi, O., Boughattas, I., Chèvre, N., Santos, R., Belbekhouche, S., Alphonse, V., Tisserand, F., Balmassiere, L., 2021. Uptake, tissue distribution and toxicological effects of environmental microplastics in early juvenile fish Dicentrarchus labrax. Journal of Hazardous Materials 403, 124055.

Texas A&M University at Galveston
1001 Texas Clipper Road
Galveston, TX 77554

Reviewed by:

1/30/2025

_____ Date: _____

Dr. David Hala, TAMUG, P.I.

Approved by:

_____ Date: February 1, 2025

Mr. Steven J. Raabe, Trustee

Texas A&M University at Galveston
1001 Texas Clipper Road
Galveston, TX 77554

Image: A pier onlooking Matagorda Bay (photo taken by the P.I. Hala)